INTEGRATING COMPOUND FLOOD CONDITIONS THROUGH 2D HYDRAULIC MODELING FOR SIMULATING FLOOD RISK PROCESSES IN COASTAL CITIES

Dissertation

submitted to the

Department of Earth and Environment

Florida International University

and the

Department of Civil and Environmental Engineering

University of Florence

In candidacy for the degree of

Ph.D. in Earth System Science

Ph.D. in Civil and Environmental Engineering

by

Francisco Peña Guerra
born 30 March 1989
from Monterrey, Mexico

2021

DEDICATION

I dedicate this dissertation to my parents, mentors, family, and friends.

ACKNOWLEDGMENTS

‘You are the architect of your own destiny’ by Bryan Tracy.

I would like to express my sincere appreciation and gratitude to all individuals and institutions that supported my journey to become a flood risk expert. Little I knew that pursuing my passion would take me to unexpected destinations and unforgettable experiences beyond my imagination.

Primero que nada, le doy gracias a Dios por su protección, bendiciones y pruebas durante estos 5 años. A mis padres Gonzalo Peña Ancira✝ y Rosa Alba Guerra Guerra que gracias a su amor, esfuerzo y sacrificios desde pequeño me permitieron acceder a oportunidades únicas que sirvieron para transformar mi vida. A mis hermanos Gonzalo, Nancy, Alejandro y Adrián por sus consejos, apoyo y cuidado de mama desde mi partida. A toda la familia Guerra y Ramones Peña por su cariño, aprecio y palabras de aliento para continuar con mi proyecto de vida. En especial quiero agradecer la familia Peña Lee, tío Fernando✝, tía Phyllis y mis primos Fernando, Vanessa y Kevin por abrirme las puertas de su casa en South Carolina y apoyarme durante mi último año del doctorado. No tengo duda que nuestros padres intercedieron para que pudiéramos fortalecer nuestros lazos familiares.

I am grateful and proud to have Fernando Nardi as my mentor and big brother over the years. Your guidance, support, leadership, and entrepreneurial spirit inspired my scientific growth throughout numerous activities and projects. Thank you for the invaluable lessons and opportunities that helped me become a better version of myself. We will continue to do great things together.

To my committee members Fabio Castelli from University of Florence (Italy), Assefa Melesse, Jayantha Obeysekera, Todd Crowl, and Rene Price from Florida International University (USA). Your interest, supervision, and recommendations helped me expand my technical knowledge and scientific understanding of Miami's complex flood processes to put together this piece of work.

To Todd Crowl, Rita Teutonico, and Maria Donoso for making the Dual degree program a reality. Todd and Rita, thank you for helping me out since my arrival in Miami, the cookouts, and CREST meetings. Thank you, Maria, for involving me with the UNESCO Chair activities and always paying close attention to my progress.

To the University for Foreigners of Perugia and the WARREDOC family Antonio Annis, Andrea Spasiano, Simona Farinelli, Fabrizio Focolari, Paola Tricoli, Xeni Kechagioglou, Maryloni Mayor as well as Tom, Grace, Jennifer, and friends from MSU Denver for the wonderful memories.

Ad Italia per i grandi insegnamenti e lezione di vita che mi ha permesso di vivere. A Piergiorgio Manciola per diventare una figura paterna ed di avermi ricevuto con le braccia aperte a casa sua durante il mio soggiorno a Perugia. Ringrazio a Marina Decuseara per il tempo meraviglioso che abbiamo condiviso insieme, così come il amore, esperienze, attenzioni, e le cure ricevute in tempi di difficoltà. Ad Antonio Annis, Ilaria Marini, Andrea Spasiano e Arturo Scalori che mi hanno permesso di vivere una esperienza italiana più significativa e arricchente con le sue famiglie, siete in un posto speciale nel mio cuore. A tutta la comunità che ho conosciuto grazie a ERASMUS Perugia, per i belli ricordi e approfondita della la cultura italiana e straniera. A Radiophonica Perugia e Rossella Biagi per la accoglienza e interessante esperienza nel settore della comunicazione scientifica. A

i ragazzi del calcetto per le partite mitiche. A i miei amici dottorandi di Firenze ed istituzioni accademique italiane che appartengono al settore, sopratutto Gabriele Freni, Camilo Bosco, Marco Lompi, Matteo Pampaloni, Claudia D'Angelo, Vincenzo Scotti e Vincenzo Totaro per le sue amicizie e suggerimenti nelle dubbi tecniche.

À mes chères amis Alexandre Alekhine, Mia Naakka, Christian Carreras, Juonas Juodas, Soufiane Ottmani et Jac Lanza qu'ils étaient toujours intéressé de ma vie, voyages et bien-être. Surtout je voudrais remercier à Maxime Stuber et Bastian Kamm pour son soutien pendant mon séjour en Suisse et fidélité inconditionnel.

To Noemi Gonzalez for the detailed explanations on coupling FLO-2D with MODFLOW-2005 and Marcia Steelman for always providing relevant output and background information of the Arch Creek Basin. To Robert Jane and Felix Santiago-Collazo for sharing their research findings and punctual advice at the latter stages of my journey. To my Miami roommates Michael, Tiago, Kelvin, and Greg for the barbecues and social gatherings in Miami. To my FIU friends Silvina, Oscar, Matthew, Angelica, Luke, Martina, Blake, Ryan, Marcel, Candice, Brad, Pau, Sage, Drew, Levente, Daniel, John, Cody, Miguel, Daniela, Nadia, Meenakshi, Jessica and many more for the good times.

A mi amada novia Mar por su amor, entrega y ser una gran inspiración para tomar un estilo de vida más natural, libre, equilibrado, trascendente y espiritual.

To my favorite motivational speakers Eric Thomas, Les Brown, and Jordan Peterson, for the daily doses of wisdom and motivation that strengthen my character and conviction at all times.

A mi primer mentor Daniel Salas Limón por impulsar mi carrera desde un inicio, y puntuales conversaciones en la UANL que me hizo reflexionar y replantear mi futuro. ¡Se logró el objetivo!

A mis amigos Juevesotes por los lazos de amistad, sana competitividad, debates interesantes, risas y retroalimentación de mis avances.

And last but not least, to my dear Mardela family that marked the beginning of my international journey. The acts of kindness, solidarity and love showed during my exchange year were instrumental to feel welcome in the community which lead to an amazing time. I feel that I would have settled down in Mexico long time ago if my experience was not that great. I am blessed to have you (yes you!) in my life. Thank you.

Declaration statement

I, **Francisco Peña Guerra**, declare that the **dissertation** entitled **"Integrating compound flood conditions through 2D hydraulic modeling for simulating flood risk processes in coastal cities"** is the result of my original research work and it has been written by myself under the supervision of my advisor, **Assefa Melesse**. Reference to the literature, and acknowledgement of collaborative research and discussions are made and appropriate credit has been given within this **dissertation**. I confirm that this work has not been submitted for any other degree qualification.

ABSTRACT

Low elevation coastal karst environments are highly vulnerable to flooding conditions due to climate change. Trends in rising global temperatures have increased the frequency and intensity of extreme precipitation, hydrometeorological phenomena and sea level rise, exacerbating the impact of pluvial, fluvial, coastal and groundwater flood hazards. Compound flooding events amplify flood hazards and pose a higher threat to residents and infrastructure in unison compared to independent phenomena.

Recent advancements in coupling hydrologic and hydraulic modeling frameworks have improved our ability to account for the combined effects of extreme pluvial, fluvial, and coastal flood hazards. This innovation in the hydroinformatics field facilitates more robust estimation of inundation, in turn improving floodplain mapping and mitigation strategies.

Although groundwater flooding is frequently overlooked in flood modeling due to its sporadic frequency worldwide and typically less severity compared to other flood hazards, the depth of the water table plays a crucial role in flood inundation dynamics, as high water table levels can diminish the soil infiltration rate and undermine the performance of storm drain systems, leading to chronic flooding scenarios.

In this study, we apply a two-way coupling technique to develop an integrated surface-subsurface water model capable of simulating the compound flooding potential of rainfall, tides, and groundwater mechanisms for the Arch Creek Basin located in North Miami, Florida (US), a region particularly prone to intense precipitation, hurricanes, king tides, high water tables, sunny day flooding and SLR.

The experiment suggests that groundwater-induced flooding is localized and influences the inundation area. In addition, copula-based statistical analyses were incorporated to simulate different combinations of flood drivers with predefined groundwater levels and sea level rise projections to characterize their relevance and impact in terms of inundation depth, extent, and building damage for current and future scenarios.

The contributions of this research are substantial and go beyond the numerical simulation scope, as it supports numerous fields and real applications including flood management, urban planning and design, flood mapping and zoning, flood insurance policies and policy making.

TABLE OF CONTENTS

LIST OF TABLES

TABLE PAGE

LIST OF FIGURES

FIGURE PAGE

ABBREVIATION AND ACRONYMS

1D	One Dimensional
2D	Two Dimensional
3D	Three Dimensional
AHED	Arch Hydro Enhanced Database
AIC	Akaike Information Criterion
ARF	Area Reduction Factors
CF	Compound Flooding
CCA	Climate Change Adaptation
CDF	Cumulative Density Function
CHD	Time-Variant Specified-Head
DEM	Digital Elevation Model
DRR	Disaster Risk Reduction
EPA	Environmental Protection Agency
GPD	General Pareto Distribution
GWF	Groundwater Flow Process
GHB	General-Head Boundary
GUI	Graphic User Interface
IPCC	Intergovernmental Panel on Climate Change
LECZ	Low Elevation Coastal Zones
LiDAR	Light Detection and Ranging
MDC	Miami Dade County

NEXRAD	Next-Generation Radar
NOAA	National Oceanic and Atmospheric Administration
OsWL	Ocean side Water Level
PDF	Probability Density Function
SFWMD	South Florida Water Management District
SLR	Sea Level Rise
USACE	United States Corps of Engineers
USGS	United States Geological Survey
VGI	Volunteered Geographic Information
WSE	Water Surface Elevation

CHAPTER I

Introduction

1 CHAPTER 1: INTRODUCTION

1.1 Introduction

The unsustainable rate of the world's human population exerts increasing pressure on the Earth's natural resources to unprecedented scales. Today, cities and urban agglomerations accommodate 56% of the world's 7.8 billion inhabitants (United Nations, 2019). As ongoing rural-urban migration patterns are expected to continue into the foreseeable future, urban land expansion, density trends, and environmental degradation are increasing cities' vulnerability of cities to climate hazards (de Sherbinin et al., 2007).

Extreme weather events dominate the top global risk outlook in terms of likelihood over the next ten years (World Economic Forum, 2019). Floods and tropical storms represent a national security threat worldwide as they account for 70% of all disaster events from 2000 to 2019, affecting 2.4 billion people and resulting in approximately 300,000 deaths (CRED & UNISDR, 2020). The significance of anthropogenic stresses in the hydrologic cycle has amplified the frequency and intensity of hydrometeorological disasters over the past decades, resulting in record-breaking floods with immediate societal impacts and billions in annual economic losses (Hallegatte et al., 2013).

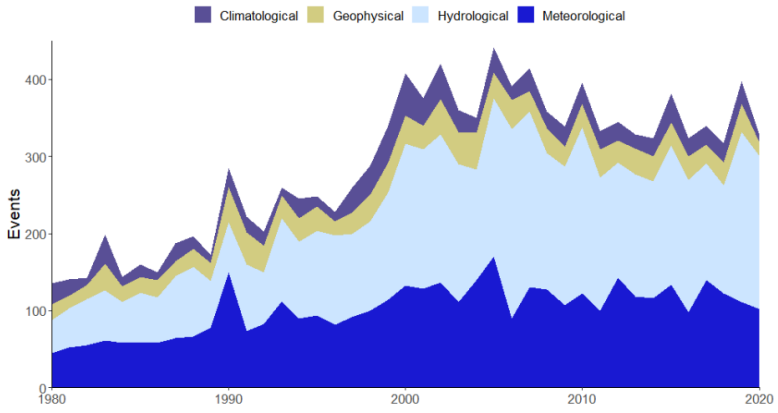

Figure 1.1. Number of disasters by type since 1980 (EM-DAT, 2020)

Despite the gradual integration of DRR and CCA practices build resilience through structural, non-structural, and nature-based solutions, urbanized LECZ remain susceptible to recurrent flooding conditions due to climate change. Trends on rising global temperatures, changes in weather patterns, increase of intensity and frequency of extreme events, and accelerated sea level rise exacerbate the impact of flood hazards, as well as the likelihood of compound flooding (CF) conditions, when the co-occurrence of two or more flood drivers over similar temporal and spatial scales lead to significant impacts (Bevacqua et al., 2017; Wahl et al., 2015; Zscheischler et al., 2018).

Although scientific and technological advancements have improved our knowledge of the characteristics, drivers, and effects of flooding at local, national, and continental levels, CF is an emerging field of study that analyze from a more accurate perspective the combination of pluvial, fluvial, coastal and groundwater flood drivers compared to traditional methods that only consider one variable at a time.

Several studies have applied probabilistic and deterministic approaches to analyze CF events. While stochastic models in copula-based probability analysis and extreme value theory examine the interrelationship between flood drivers from a mathematical perspective, hydrodynamic numerical simulations provide a tangible depiction of the flood dynamics for current and future climate projections.

The integration of stochastic output to feed physically-based models constitutes the idealistic realization of flood hazard mapping by rendering a more reliable product with lower sources of uncertainty and better estimation on the effects of catastrophic flood scenarios. This powerful synergy could represent a valuable tool for governments to shift from short term measures and underestimation of flooding into a long-term mentality to

drive and stimulate meaningful resilience policies that result in more balanced social, economic, and environmental tradeoffs.

1.2 Research questions

The main purpose of this research is to investigate

- Is it possible to simulate surface-subsurface water interactions by coupling FLO-2D with MODFLOW-2005?
- What is the role of univariate and multivariate forcing boundary conditions in assessing compound flooding scenarios in the Arch Creek Basin?
- What are the potential impacts of sea-level rise in compound flooding events in the Arch Creek Basin?

1.3 Research objectives

The main objective of this dissertation is to develop a tool capable of simulating complex compound flood hazard interactions (rainfall, coastal surge, and groundwater) within one hydrodynamic model to evaluate the magnitude of current and futures extreme conditions. In addressing this goal, we formulate three research objectives:

This dissertation is organized into five chapters and are described in more detail below: This dissertation is organized into five chapters and are described in more detail below: This dissertation is organized into five chapters and are described in more detail below:

- **Research objective 1 –** Calibrate and validate a loosely-coupled 2D hydrodynamic model able to simulate the compound flooding interactions between surface and

subsurface processes using crowdsourced data to effectively reproduce the flood dynamics caused by intense rainfall and unusually high-water table levels

- **Research objective 2 –** Simulate synthetic compound flooding scenarios based on "most-likely" combinations of different flood drivers derived from multivariate probabilistic analyses (bivariate and trivariate approaches)
- **Research objective 3 –** Assess the severity of compound flooding potential by accounting the effects of regional sea-level rise projections

1.4 Introduction

This dissertation is organized into five chapters and are described in more detail below:

Chapter 1 introduces a global perspective of the topic, poses research questions, and define research objectives.

Chapter 2 provides a detailed background of relevant flood driver mechanisms that trigger compound flooding events, followed by a complete description of modeling approaches and previous efforts that analyze groundwater and CF events regionally and overseas from a deterministic perspective. The Arch Creek Basin located in North Miami (Southern Florida) is selected as a case study site due to its acute vulnerability to flooding, low-lying terrain and complex hydrogeomorphology. In addition, the software used to develop the CF simulation is presented, with specific detail on the mathematical compatibility between a quasi-2D hydrodynamic model (FLO-2D) and a 3D finite-difference groundwater model (MODFLOW-2005). Details and the flood modeling set up and the storm events selected for calibration and validation are presented.

Chapter 3 focuses on the importance of linking probabilistic with deterministic modeling. The scientific methodology to perform the bivariate and multivariate statistical analyses of different flood drivers is presented. A detailed description of selected gauge stations located near the Arch Creek Basin used for the quantitative data collection are also included. Output from the most extreme isoline produced for a 100-year design events is used as input for the boundary conditions to run selected joint combinations of rainfall – surge samples under predefined water table thresholds to simulate compound flooding scenarios on the validated loosely-coupled physically-based model.

Chapter 4 extends the previous study as shown in **Chapter 3** to assess the compound flooding potential of future scenarios by accounting the influence of predefined water table thresholds and sea-level rise projections in terms of inundation depth, extent, and damage to buildings.

Finally, **Chapter 5** enlists the conclusions, recommendations, further research opportunities and major findings of the dissertation on the basis of the results reported in the previous chapters.

1.5 References

Bevacqua, E., Maraun, D., Hobæk Haff, I., Widmann, M., & Vrac, M. (2017). Multivariate statistical modelling of compound events via pair-copula constructions: Analysis of floods in Ravenna (Italy). *Hydrology and Earth System Sciences*, *21*(6), 2701–2723. https://doi.org/10.5194/hess-21-2701-2017

CRED, & UNISDR. (2020). *An overview of the last 20 years*. 1–28. https://reliefweb.int/sites/reliefweb.int/files/resources/Human Cost of Disasters 2000-2019 Report - UN Office for Disaster Risk Reduction.pdf

de Sherbinin, A., Schiller, A., & Pulsipher, A. (2007). The vulnerability of global cities to climate hazards. *Environment and Urbanization*, *19*(1), 39–64. https://doi.org/10.1177/0956247807076725

EM-DAT. (2020). *EM-DAT, the International Disaster Database*.

https://public.emdat.be/

Hallegatte, S., Green, C., Nicholls, R. J., & Corfee-Morlot, J. (2013). Future flood losses in major coastal cities. *Nature Climate Change*, *3*(9), 802–806. https://doi.org/10.1038/nclimate1979

United Nations. (2019). *World Urbanization Prospects: The 2018 Revision (ST/ESA/SER.A/420)*. https://population.un.org/wup/Publications/Files/WUP2018-Report.pdf

Wahl, T., Jain, S., Bender, J., Meyers, S. D., & Luther, M. E. (2015). Increasing risk of compound flooding from storm surge and rainfall for major US cities. *Nature Climate Change*, *5*(12), 1093–1097. https://doi.org/10.1038/nclimate2736

World Economic Forum. (2019). *The Global Risks Report*. *15*, 1–114. http://wef.ch/risks2019

Zscheischler, J., Westra, S., Van Den Hurk, B. J. J. M., Seneviratne, S. I., Ward, P. J., Pitman, A., Aghakouchak, A., Bresch, D. N., Leonard, M., Wahl, T., & Zhang, X. (2018). Future climate risk from compound events. *Nature Climate Change*, *8*(6), 469–477. https://doi.org/10.1038/s41558-018-0156-3

CHAPTER II

Compound flood modelling framework for rainfall-groundwater interactions

This chapter was reproduced and adapted from Peña, F., Nardi, F., Melesse, A., Obeysekera, J., Castelli, F., Price, R. M., Crowl, T., and Gonzalez-Ramirez, N. *Natural Hazards and Earth System Sciences Discussions,* **2021**, 1-3805520, *https://doi.org/10.5194/nhess-2021-259* with permission from Copernicus Publications.

2 CHAPTER 2: COMPOUND FLOOD MODELLING FRAMEWORK FOR RAINFALL-GROUNDWATER INTERACTIONS

2.1 Abstract

Compound floods are an active area of research where the complex interaction between pluvial, fluvial, coastal or groundwater flooding are analyzed. A number of studies have simulated the compound flooding impacts of precipitation, river discharge and storm surge variables with different numerical models and linking techniques. However, groundwater flooding is often neglected in flood risk assessments due to its sporadic frequency - as most regions have water tables sufficiently low that do not exacerbate flooding conditions -, isolated impacts and considerably less severity in respect to other types of flooding. This paper presents a physically-based, loosely-coupled modelling framework using FLO-2D and MODFLOW-2005 that is capable to simulate surface-subsurface water interactions to represent compound flooding events in North Miami. FLO-2D, responsible of the surface hydrology and infiltration processes, transfers the infiltration volume as recharge to MODFLOW-2005 until the soil absorption capacity is exceeded, while MODFLOW-2005 return exchange flow to the surface when groundwater heads are higher than the surface depth. The model calibration is based on three short-lived storm events that as individual processes represent minimum flooding conditions but in combination with pre-existing high-water table levels results in widespread flooding across the study area. Understanding groundwater flood risk is of particular interest to low-elevation coastal karst environments as the sudden emergence of the water table at ground surface can result in social disruption, adverse effects to essential services and damage infrastructure. Results are validated using FEMA's severe repetitive loss (SRL) property

records and crowdsourced data. Further research should assess the exacerbated impacts of high tides and sea level rise on water tables under current and future climate projections.

2.2 Introduction

Flood inundation modelling is of critical importance for better planning, forecasting and decision-making practices (Teng et al., 2017). Scientific and technological innovations in numerical algorithms have continuously improved the performance of physically-based hydrologic, ocean circulation and hydraulic modelling packages to simulate faster and more accurate flood physical processes over the computational domain at various scales and resolutions (Devia et al., 2015). However, most flood inundation models are designed to simulate specific flood hazards (i.e., pluvial, fluvial, coastal, groundwater) independently and are unable to assess complex flood dynamics per se due to code limitations and burdensome compatibility. To address these numerical constraints, some models have the ability to operate as linked units or groups by using coupling schemes (i.e. one-way, loosely, tightly, fully) to build compound models capable of simulating multiple flood drivers (Santiago-Collazo et al., 2019).

Compound floods (CF) are high-impact low-probability events characterized by a non-linearity behavior resulted from the complex interactions of interrelated flood drivers triggered at the same spatial and temporal scales (Field et al., 2012; Seneviratne et al., 2012; van Westen & Greiving, 2017; Zscheischler et al., 2018). Research on CF field has received increasing attention in recent years due to their adverse impacts at the global scale.

Deterministic and probabilistic approaches are preferred frameworks to analyze CF events. Stochastic models through copula-based probability analysis and extreme value theory examine the interrelationship between flood drivers, while physically-based

numerical simulations provide a tangible depiction of the flood dynamics for current and future climate projections. Several compound flooding studies have used physically-based hydrodynamic models as the reference model to simulate the combined effects of rainfall-runoff and storm surge (Christian et al., 2015; Ikeuchi et al., 2017; Karamouz et al., 2015; Kumbier et al., 2018; Olbert et al., 2017). Failure to consider the compound interactions of flood drivers can result in significant uncertainties in the magnitude, timing, and estimation of flood risk (Wahl et al., 2015). Therefore, the transition from traditional univariate approaches to a multivariate perspective is necessary to improve flood hazard understanding and predictions (Bates et al., 2021).

The significance of groundwater flooding is rarely disputed as it is only relevant to geographical regions sitting on top of permeable rock that are prone to groundwater emergence (i.e., Miami, Yucatán Peninsula, United Kingdom). Groundwater floods are events limited to prolonged rainfall in low-elevation karst watersheds characterized by unconfined aquifers that experience sudden increases of already high-water table levels above normal conditions (Finch et al. 2004). Although there has been a substantial increase in groundwater flooding literature since the 2000s as well as advances in understanding surface water/groundwater interactions (Brunner et al., 2017; Sophocleous, 2002), relevant knowledge gaps and lack of understanding of this phenomenon persist from the complex relationship between topography and hydrogeology (Bradford, 2002; Hughes et al., 2011; Ó Dochartaigh et al., 2019). The water table response time to hydrological events is controlled by the soil, vegetation and aquifer properties, which influence the infiltration capacity, recharge rate and response time (Nalesso, 2009). Similarly, the groundwater dynamics are influenced by spatial-temporal variations of single or compound flood drivers

(i.e. precipitation events, high river levels, above-average tides and sea level rise conditions) over long or repetitive periods of time (Ascott et al., 2017). Thus, the water table response to hydrological mechanisms (García-Gil et al., 2015), system fluctuations and residence time (MacDonald et al., 2014) determine the severity of groundwater flooding.

While probabilistic and empirical approaches have contributed to the development of regional groundwater flood maps (Cobby et al., 2009; Jacobs, 2007), physically-based models are scarce. Abboud et al. (2018) found that the June 2013 compound flood disaster in the Elbow River (Canada) was induced by steady precipitation and increased river flow discharges from upstream basins resulting in basement flooding due to the rise of the water table. The combined effects of fluvial and groundwater flooding were not considered on that study since the MODFLOW river package focused exclusively on groundwater flow. Similarly, Yu et al. (2019) applied the coupled surface-subsurface model PIHM to produce a comprehensive groundwater flood risk and damage assessment over the Koiliaris River (Greece). Yang & Tsai (2020) investigated the impacts of water table dynamics on groundwater flooding and levee under seepage in New Orleans, Louisiana using MODFLOW-USG for hazard mapping, flood delineation and levee breach analysis. Su et al. (2020) developed a coupled model to assess the improved response of the repaired storm drain system infrastructure with the shallow aquifer groundwater dynamics by coupling EPA SWMM with MODFLOW-2005 at the city of Hoboken in New Jersey (USA).

Previous efforts to model groundwater levels in South Florida have been developed in the form of hydrogeologic maps (Fish & Stewart, 1991), estimation of aquifer parameters to calculate groundwater flow (Cunningham et al., 2004), and statistical analysis of

hydrological measurements (Chebud & Melesse, 2011, 2012; Prinos & Dixon, 2016). Similarly, Hughes and White (2016) investigated the effect of pump practices and sea level rise on surface water routing and groundwater interactions in MDC using MODFLOW. Currently this is the main reference model for MDC regional research and planning purposes in hydrologic, ecologic, and environmental fields. Regarding the study area, Sukop et al. (2018) developed a MODFLOW model that analyzed the current and future response of the water table to rainfall events in a portion of the Arch Creek Basin. The study highlighted precipitation as the main trigger for groundwater-induced flooding, with tidal fluctuations and sea level rise increasing the shallow water table. Researching the flood risk potential from surface-subsurface water interactions in MDC where the water table is near to the ground surface is critical as it could reveal hidden risks from the compound impact of major storms and coastal forcing variables for present and future scenarios.

The main purpose of this study is to develop a loosely-coupled modeling framework capable of addressing complex compound flood phenomena. To better understand the combined effects of pluvial and groundwater flooding in a low elevation coastal zone, a methodology is developed to couple the 2D hydrodynamic software FLO-2D and the groundwater model MODFLOW-2005. The Arch Creek Basin in North Miami was selected as an ideal test site due to its unique hydrogeomorphology, low-lying topography, influence of tides on drainage outlets, and high vulnerability to flooding events. Three events characterized by short-lived heavy precipitation events and unusually high-water tables were selected to simulate the surface groundwater interaction. Finally, the coupled model results were validated based on official reports and volunteered geographic

information (VGI) flood observations from the study area. This study aims to highlight the importance of groundwater flooding as a potential flood driver in urbanized karst coasts. The paper is organized as follows: a complete description of the study area is introduced (Section 2), followed by data collection and the methodology presented in Sections 3 and 4. Results illustrate the main findings (Section 5); the discussion compares the results with similar work in the region (Section 6); and the conclusion section including the advantages, limitations, and future research (Section 7).

2.3 Study Area

2.3.1 Site description

The Arch Creek Basin is located in the northeastern part of Miami-Dade County (MDC), along the coast of Biscayne Bay in the city of North Miami, Florida. Prior to anthropogenic interventions, the Arch Creek River served as an important flow corridor that connected the Everglades to Biscayne Bay, controlling the flood pulse dynamics in the tropical wetland system (Figure 2.1)

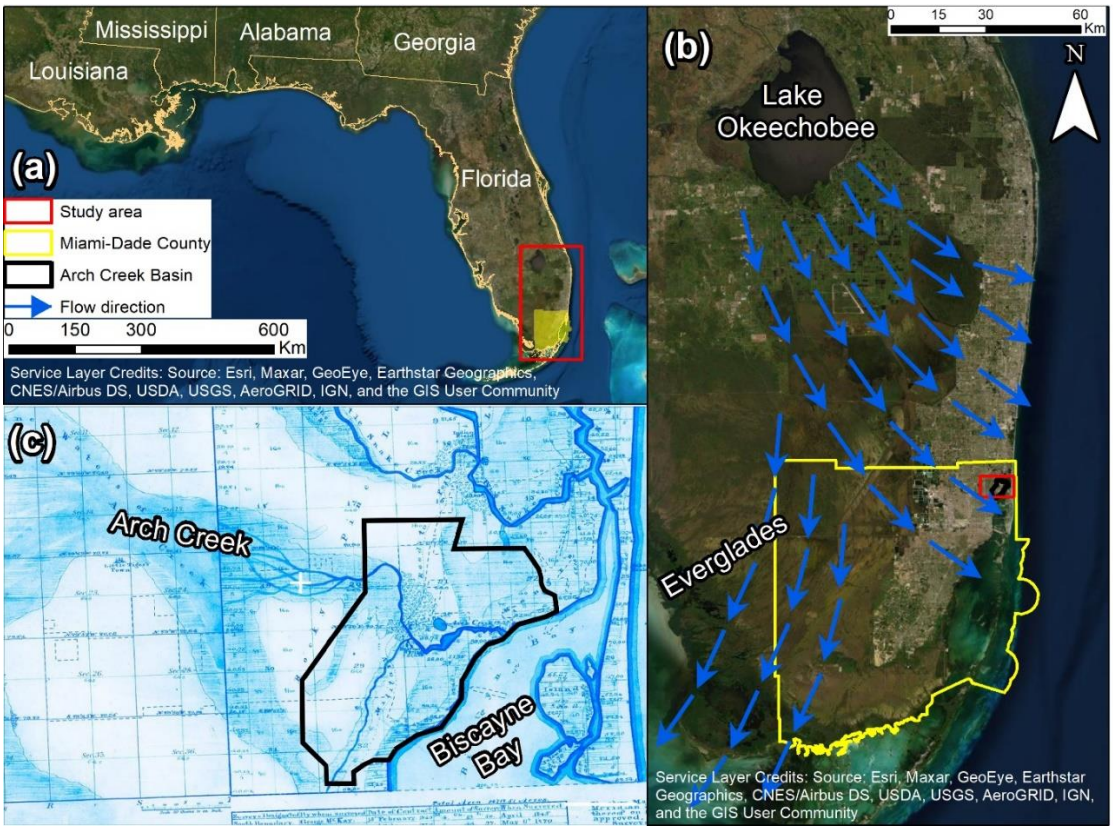

Figure 2.1. Location map of the study area. (a) MDC located in Southeast Florida, USA (b) current Everglades water flow from Lake Okeechobee towards the Atlantic Coast and Gulf of Mexico, and (c) land survey from 1870 that illustrates the natural flow direction of the Arch Creek to discharge into the Biscayne Bay prior urbanization (Miami Herald, 2019).

The gradual modifications in land use and the construction of the Biscayne Canal in the 1920s marked the transition of the natural environment to agricultural lands. Variations in the soil moisture conditions and infiltration levels due to changes in the streamflow and drainage patterns in the area caused unsustainable farming practices that lead to a shift to residential development (Figure 2.2). The urbanization process along Biscayne Bay required considerable cut and fill earthworks to create ideal urban development conditions (Miami-Dade, 2016).

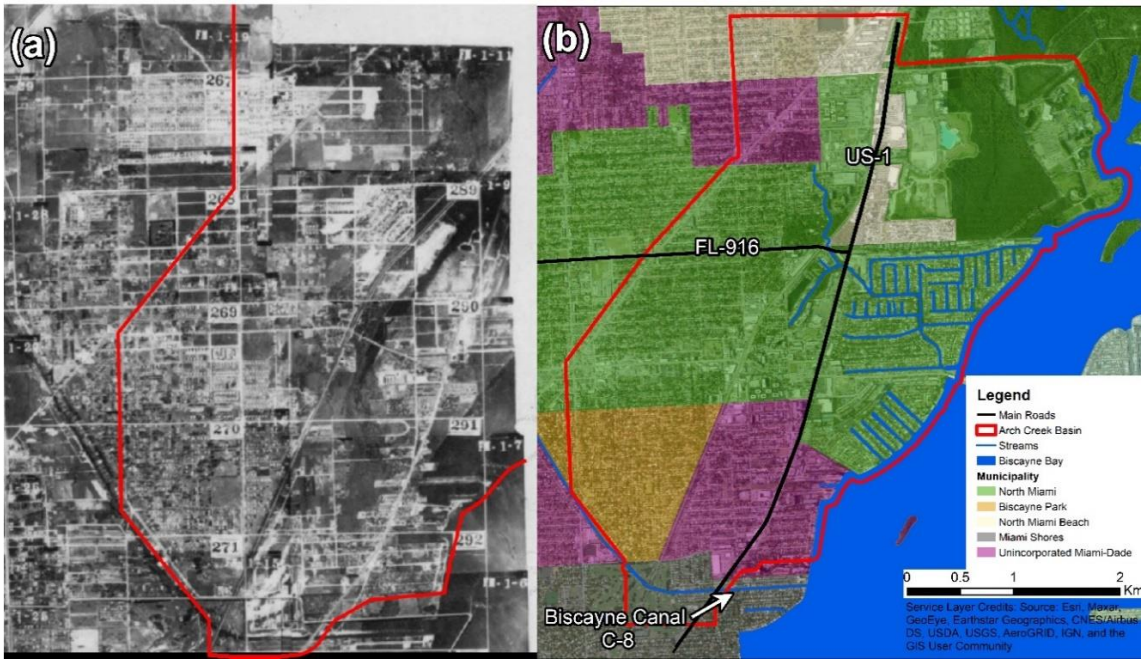

Figure 2.2. Aerial photography of historical (1948) and current urbanized environment in the study area. (a) Major civil and drainage works contributed to the rapid urbanization of the Arch Creek Basin; (b) Municipality map, including North Miami, Biscayne Park, North Miami Beach, Miami Shores and Unincorporated Miami-Dade (U.S. Department of Agriculture, 1948).

The Arch Creek Basin (16.95 km^2) is a low-lying coastal zone predominantly urbanized (90.1%) and economically diverse. The population is distributed within five jurisdictions, primarily concentrated in North Miami and North Miami Beach (Table 2.1). Although the topography is predominantly low and flat, some areas within the basin are considered the highest elevations in MDC ranging from 5 to 15 meters.

Frameworks to integrate flood risk mitigation and climate change adaptation strategies are a main component in Miami Dade County's policy agenda (GM&B, 2019). As a result, the Arch Creek Basin received the designated status of "Adaptation Action Area", the first pilot project in Florida to build social, environmental and economic resilience (Miami-Dade, 2016).

Table 2.1. Population and land elevations of Arch Creek Basin jurisdictions. Population totals account for the whole jurisdiction area (U.S. Census Bureau, 2020)

Jurisdiction	Population*	Area (km^2)	Area ACB (km^2)	Percentage of land elevation (meters)				
				< 0	0 - 1	1 - 2	2 - 5	> 5
North Miami	62489	26.09	11.00	7.88	18.64	39.67	31.27	2.54
Biscayne Park	3124	1.64	1.44	0.00	1.48	77.20	21.32	0.00
North Miami Beach	42971	13.79	1.43	0.01	11.53	20.05	68.41	0.00
Miami Shores	10459	9.80	0.54	4.82	19.68	38.91	36.56	0.03
Unincorporated MDC	N/A	25467	2.54	3.65	14.60	47.08	34.67	0.00

2.3.2 Climate

The climate of southeast Florida is characterized by wet (May to October) and dry seasons (November through April) with 75% of the annual rainfall occurring in the wet season (Abiy et al., 2019). The average annual rainfall in Miami is above 1500 mm and the average monthly precipitation during the wet season is above 150 mm (Abiy et al., 2019). Rainfall can vary from year to year (1000 – 2000 mm/yr), due to tropical storms and extreme hydrometeorological events which highly influence rainfall amounts. A reported increasing trend in rainfall of 2.1 mm/yr from 1906 to 2016, mainly attributable to an increase in wet season rainfall (Abiy et al., 2019), underscores that south Florida is under a continued threat from flooding.

2.3.3 Hydrology and groundwater

The Arch Creek Basin sits atop one of the most permeable aquifers in the world, known as the Biscayne Aquifer. The Biscayne Aquifer stores 34 billion m^3 of water and spans an area of 10,000 km^2 (Price et al., 2020) tapering from near the center of peninsula Florida towards the eastern coastline where its maximum thickness is about 38 meters (Parker & Cooke, 1944) and hydraulic conductivities exceeding 3,000 m/day (Fish & Stewart, 1991).

The stratigraphy of Biscayne aquifer consists entirely of unconfined permeable limestones of the Fort Thompson and Miami Limestone Formations and contains numerous solution conduits, resulting in rapid infiltration and recharge to the aquifer (Cunningham & Florea, 2009; Hoffmeister et al., 1967; Parker & Cooke, 1944). Recharge via precipitation occurs primarily in the Everglades and groundwater flows eastward towards the shore where it discharges to Biscayne Bay (Cunningham & Florea, 2009).

2.4 Data description

This section presents the data sets required to build the 2D surface-subsurface flood modelling study, including the topographic input, and hydrologic monitoring stations that provide rainfall, tide and well gauge records, as well as verified flood observations.

2.4.1 Topography

The Light Detection and Ranging (LiDAR) digital elevation model (DEM) is a 2-meter spatial resolution produced by Miami-Dade County, Florida. The LiDAR scanner corresponds to the actual bare-earth surface, removing tops of vegetation, buildings, and vehicles, and the project coordinate system is UTM zone 17N Horizontal Datum WGS84. In terms of elevation, the North American Vertical Datum of 1988 (NAVD 88) was assigned as the reference geodetic vertical datum for this study, substituting the original measurements based on the National Geodetic Vertical Datum of 1929 (NGVD 29).

2.4.2 Hydrologic input

Hydrologic modeling included hydrologic conditions of the time periods 1-4 October 2000, 6-8 June 2013, and 23-26 May 2020. Boundary and initial hydrologic inputs such as precipitation, tide and ocean-side water levels, and groundwater heads over the specified time periods were obtained from the following sources.

2.4.2.1 Rainfall

The NEXRAD Radar Rainfall Application is a scientific web map interface developed by the South Florida Water Management District (SFWMD) on which rainfall data is reported based on spatial coverage configurations in the form of the entire district, counties, Arch Hydro Enhanced Database (AHED) watersheds, or Rain Grid. The NEXRAD Rain Grid Layer is a 2 km grid resolution that provides an accurate

representation of precipitation every 15 minutes. Rainfall Grid cell 10044042 was selected to characterize the Arch Creek Basin's rainfall conditions.

2.4.2.2 Tides and ocean-side water levels

DBHYDRO is the official SFWMD repository for climate, hydrologic, and environmental databases (https://www.sfwmd.gov/science-data/dbhydro). Ocean-side water levels were obtained from stations S28_H and S28_T, located in the Biscayne Canal Number C-8 on the Arch Creek southern boundary edge.

The NOAA Tides & Currents website (https://tidesandcurrents.noaa.gov/) provides local water levels, tides, current predictions, and other oceanographic and meteorological conditions. The closest coastal sensor to the Arch Creek Basin is located at the Virginia Key, Biscayne Bay Station (ID #8723214).

2.4.2.3 Groundwater heads

The Unites States Geological Survey (USGS) National Water Information System (https://waterdata.usgs.gov/nwis/gw), in cooperation with the SFWMD, records daily summary data of maximum groundwater levels in the south Florida region. The groundwater level data was obtained from well G-852 adjacent to the outer western boundary of the study area (Figure 2.3). Daily field water level measurements have been recorded since 1973, and 15-minute intervals since October 2007.

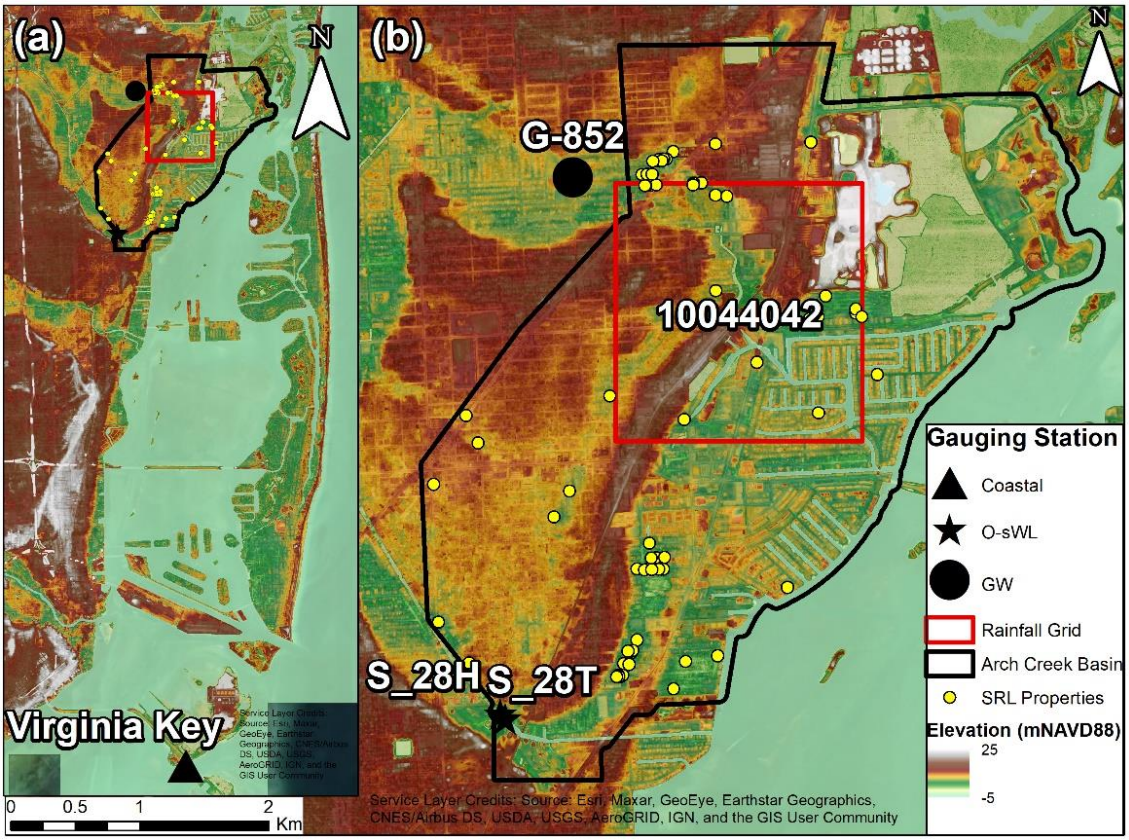

Figure 2.3. Geographical location of selected data in the study site. (a-b) Topographic map showing the location of the Arch Creek Basin (black polygon), and the distribution of closest gauging stations to the study site (black), rainfall grid (red square), and FEMA's SRL claims (yellow).

2.4.3 Repetitive flood claims

FEMA's severe repetitive loss (SRL) properties program is designed to provide grants and financial assistance to residential properties that have experienced frequent flood losses over the years (FEMA, 2021). Currently, seventy-five properties have requested financial assistance for property acquisition or to recoup with some of their investments due to flood damages in the Arch Creek Basin (Miami-Dade, 2017). The database stores detailed information on the date of loss, building type, flood zone designation, type of insurance and claim payments between 1995 to 2015, providing a clear footprint of flooding risk hotspots and flood prone communities.

2.5 Methodology

2.5.1 Hydraulic Model: FLO-2D

FLO-2D is a physically-based volume conservation model capable of simulating the propagation of water dynamics over confined and unconfined environments using the dynamic wave approximation to the momentum equation (O'Brien et al., 1993). The flood routing model combines hydrology and hydraulics in a computational square grid system environment that moves the flood volume across the tile's boundary one step at a time.

Rainfall-runoff processes can come in the form of rainfall data over the domain or distributed input flood hydrographs in the channel or floodplain. 1D equations are applied for channel flow routing movement in a downstream direction as long as the flow remains in the channel cross-section. Conversely, 2D equations are activated when the maximum capacity of the channel is exceeded, and during overland runoff in the floodplain.

The model can represent high-resolution environments and urban features, including buildings, streets, levees, obstructions, and drainage systems. These can influence the flow distribution dynamics, which are governed by the topography and Manning roughness coefficient. Similarly, the flow propagation and velocity can be influenced by abrupt changes in slope, depressions, unsteady flow conditions, and hydraulic structures.

The FLO-2D model input data are the floodplain topographic digital terrain model (DTM), channel geometry, inflow and outflow boundary conditions, as well as grid cell parameters representing the presence of artificial features on the bare earth (i.e., levees, building, bridges) (O'Brien, 2011).

The equations implemented in the model consist of the Continuity Equation (Eq. 2.1):

$$i = \frac{\partial h}{\partial t} + \frac{\partial hV}{\partial x} \quad \text{Eq. 2.1}$$

and the Momentum Equation (Eq. 2.2):

$$S_f = S_o - \frac{\partial h}{\partial x} - \frac{V}{g} \cdot \frac{\partial V}{\partial x} - \frac{1}{g} \cdot \frac{\partial V}{\partial t} \quad \text{Eq. 2.2}$$

where h is the flow depth, t is the time variable, V is the depth-averaged velocity in one of the potential eight flow directions x, i is the excess rainfall intensity (if the rainfall component is considered), So is the bed slope, g is the gravity acceleration, and Sf is the friction slope based on the Manning Equation. For the Momentum Equation, the bed slope is subtracted by the pressure gradient, local, and convective acceleration variables respectively, to represent the one-dimensional depth-averaged channel flow.

FLO-2D uses the abovementioned equations of motion to calculate the average flow velocity across a grid element boundary one direction at a time in eight potential flow directions over the floodplain, four cardinal directions (North, East, South, and West), and four diagonal directions (NE, NW, SE, and SW). The calculation of each velocity is one dimensional and solved independently from the other boundary cells; thus, velocity vectors are not calculated when the flow is shared with adjacent grid cells. The stability of this explicit numerical scheme is based on strict criteria to control the magnitude of the variable computational time-step.

2.5.2 MODFLOW-2005

MODFLOW is the world's leading open-source groundwater flow model used by hydrologists. MODFLOW is a computer code developed by the USGS since 1984 that uses Fortran language to simulate groundwater flow aquifer layers (confined or unconfined) using a block-centered finite-difference approach (Harbaugh, 2005). Technological developments have contributed to overall updates in the code, resulting in the much-improved version of MODFLOW-2005. MODFLOW-2005 processes are structured as flow packages, which are divided into multiple subroutines that are responsible for simulating optional processes that deal with a single aspect of the simulation, including block-centered flow (BCF6), layer property flow (LPF), unsaturated zone flow (UZF), and seawater intrusion (SWI2) to mention a few. Similarly, the model offers several solvers to solve matrix equations, as well as subsidence, observations, surface-water routing, and transport packages.

The geometric discretization of the aquifer(s) is fundamental to transform the aquifer components into discrete elements. The aquifer is broken down in grid elements to obtain the number of rows, the number of columns, and the width of each row and column for the horizontal direction. The vertical water pressure direction is delineated in the model by specifying the number of layers to be used, and the top/bottom elevations of every cell and layer. The number of layers corresponds to the number of aquifers. The spatial grid resolution must be appropriate to the domain and scale to set the model boundary conditions, as well as the aquifer characterization and parameters in specific cells, to represent with the highest standard of accuracy the modeling components for surface-subsurface flow interactions. At the end of the simulation, all cell centroids (also known as

nodes) will record the flow stresses of the hydrogeological system, such as water heads, recharge, and zetas.

The following expression (Eq. 2.3) illustrates the three-dimensional groundwater movement at constant density through porous earth material using MODFLOW:

$$\frac{\partial}{\partial x}\left(K_{xx}\frac{\partial h}{\partial x}\right)+\frac{\partial}{\partial y}\left(K_{yy}\frac{\partial h}{\partial y}\right)+\frac{\partial}{\partial z}\left(K_{zz}\frac{\partial h}{\partial z}\right)+W=S_S\frac{\partial h}{\partial t} \qquad \text{Eq. 2.3}$$

where K_{xx}, K_{yy}, and K_{zz} are values of hydraulic conductivity along the x, y, and z coordinate axes, which are assumed to be parallel to the principal axes of hydraulic conductivity, h is the potentiometric head, W is a volumetric flux per unit volume representing sources or sinks of water, with $W < 0.0$ for flow out of the groundwater system, $W > 0.0$ for flow into the system, S_S is the specific storage of the porous material, and t is time.

The presented groundwater flow equation follows the application of the continuity equation, preserving the balance of flow between inputs-outputs with changes in the storage capacity. Under the premise that water density remains constant, the continuity equation (Eq. 2.4) expressing the balance of flow for a cell is calculated as:

$$\sum Q_i = S_S\frac{\Delta h}{\Delta t}\Delta V \qquad \text{Eq. 2.4}$$

where Q_i is the flow rate into the cell, S_S is the specific storage or the volume of water that can be injected per unit volume of aquifer material per unit change in head, ΔV is the volume of the cell, and Δh is the change in head over a time interval of length Δt.

2.5.3 Coupling surface-groundwater models

FLO-2D is capable of simulating coupled hydrodynamic interactions of surface and subsurface flow components with MODFLOW-2005. A loosely-coupled technique interaction approach was applied to combine FLO-2D, and MODFLOW-2005 Groundwater Flow Process (GWF) package input to solve the flood routine and groundwater flow numerical equations separately by exchanging information in an iterative matter (Santiago-Collazo et al., 2019) (Figure 2.4).

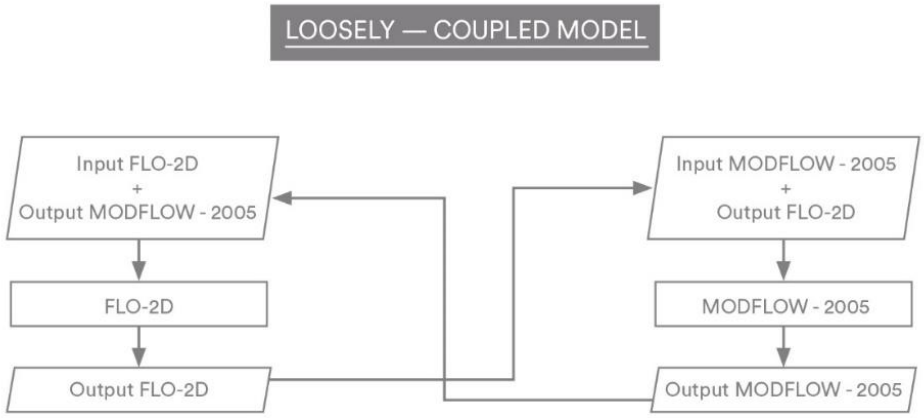

Figure 2.4. Flowchart representing the loosely-coupled joining technique between FLO-2D and MODFLOW-2005.

The resulted surface-subsurface water exchanges under unsteady flow can occur at any given time of the simulation in the discretized domain, as groundwater recharge from water infiltration in floodplains and rivers or as groundwater return exchange flow when the water table reaches the surface.

The main factors determining the coupling compatibility process between FLO-2D and MODFLOW-2005 include the algorithms' mathematical solver compatibility to calculate and transfer the exchanged volumes in opposite directions and share consistent

spatial and temporal scales. A significant advantage in the coupling process is that both numerical codes are written in FORTRAN programming language and shared the same explicit finite difference method. Thus, the spatial and temporal intervals of FLO-2D and MODFLOW-2005 are separated into a selected number of time steps, and the solution is calculated by solving the two- and three-dimensional equations, respectively. From a numerical perspective, this independence is beneficial to satisfy the numerical stability criteria and accuracy.

In terms of the spatial scale, a perfect match between FLO-2D and MODFLOW-2005 surface elevation layers is necessary for the surface and subsurface water interactions to happen. This agreement is subject to identical geographical position, reference system, size resolution, and topographic cell elevations (Figure 2.5).

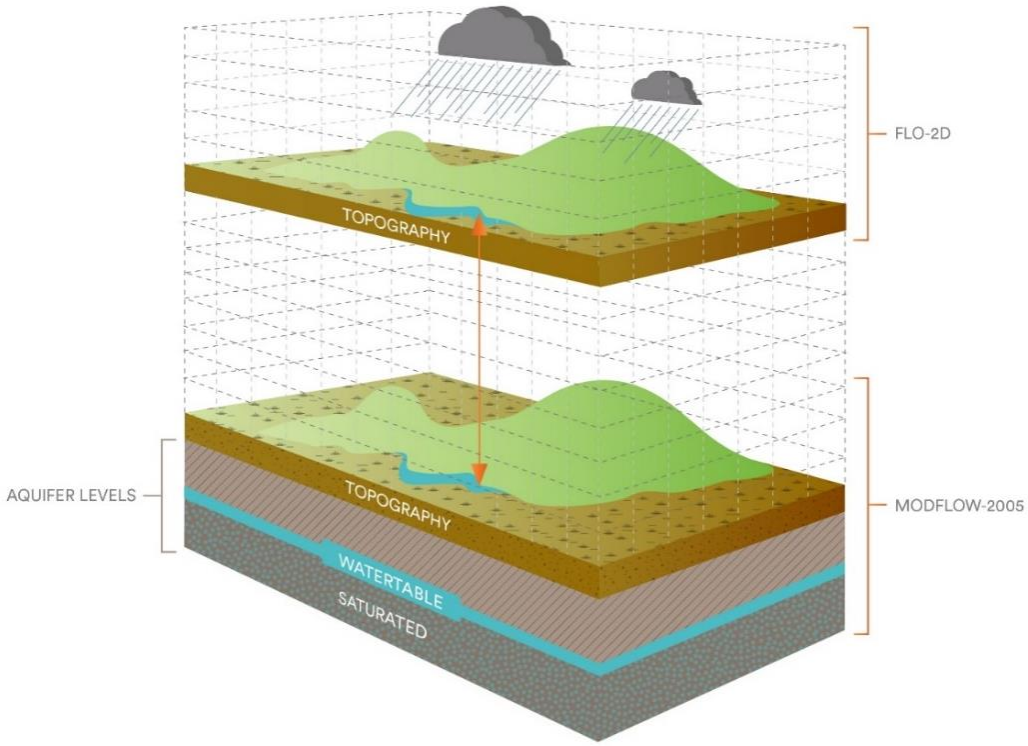

Figure 2.5. Spatial compatibility between FLO-2D and MODFLOW-2005

Although the coupled models can have variations in the number of cells and domains, FLO-2D cells must overlap the MODFLOW-2005 grid domain system to compute results and transfer the output data from one model to another and vice versa until the end of the simulation.

It is important to note that FLO-2D and MODFLOW-2005 design structures present significant operability differences to perform calculations. In MODFLOW-2005, the simulation is divided into a series of stress periods within which specified data are constant. Each stress period, in turn, is divided into a series of time steps. The solution of the finite difference equations can be written in matrix form as given by Eq. 2.5:

$$[A]\{h\} = \{q\} \qquad \text{Eq. 2.5}$$

where $[A]$ is a matrix of the coefficients of the head for all active nodes in the grid, $\{h\}$ is a vector of head values at the end of time step n for all grid nodes, and $\{q\}$ is a vector of the constant heads for each timestep.

MODFLOW-2005 has three internal nested loops, the stress period loop (outer), time step loop (intermediate), and iteration loop (inner). A predetermined procedure is implemented at the beginning as a routine setup function to read the domain set-up (i.e., grid resolution, number of layers, and simulation time), model data in the form of boundary conditions, aquifer hydraulic characteristics (i.e., hydraulic conductivity, specific storage, transmissivity), initial head conditions, and selected solution method.

The outer loop is responsible for calculating the resulted heads for each timestep from defined boundary conditions, including specified heads (i.e., time-variant or head boundary packages), specified flux (i.e., recharge or wells), and head-dependent flux (i.e.,

drain, evapotranspiration or river recharge). The intermediate loop accounts for the total simulation time, as well as additional output processing, and the inner loop for calculation purposes to approximate the head solution until the maximum number of iterations is achieved. At the end of the iteration loop, specified output control files are created in the form of heads, budget terms, or flow in the domain. The intermediate and outer loops repeat until all timesteps are completed for all stress periods (Harbaugh, 2005).

FLO-2D model works with variable time steps that are automatically adjusted internally based on stability criteria requirements. Because FLO-2D uses an explicit finite difference method to solve the surface water equations, its time step is usually much smaller than that defined for the MODFLOW-2005 model, resulting in an increasing number of 2D computational sweeps to match the MODFLOW-2005 simulation time (FLO-2D, 2018). A time-synchronization scheme was developed to achieve the coupling, as the MODFLOW-2005 intermediate loop is in charge of transferring the information between models. For example, the FLO-2D iterative calculations start until reaching MODFLOW-2005 time step one. Then, the MODFLOW-2005 intermediate loop performs its respective calculations from time step one and is shared in both directions to continue with the following time step (Nalesso, 2009). The process repeats itself until the simulation time of FLO-2D is completed. Similarly, MODFLOW-2005 can experience numerous stress periods during the simulation. Figure 2.6 depicts the time step synchronization procedure between both models.

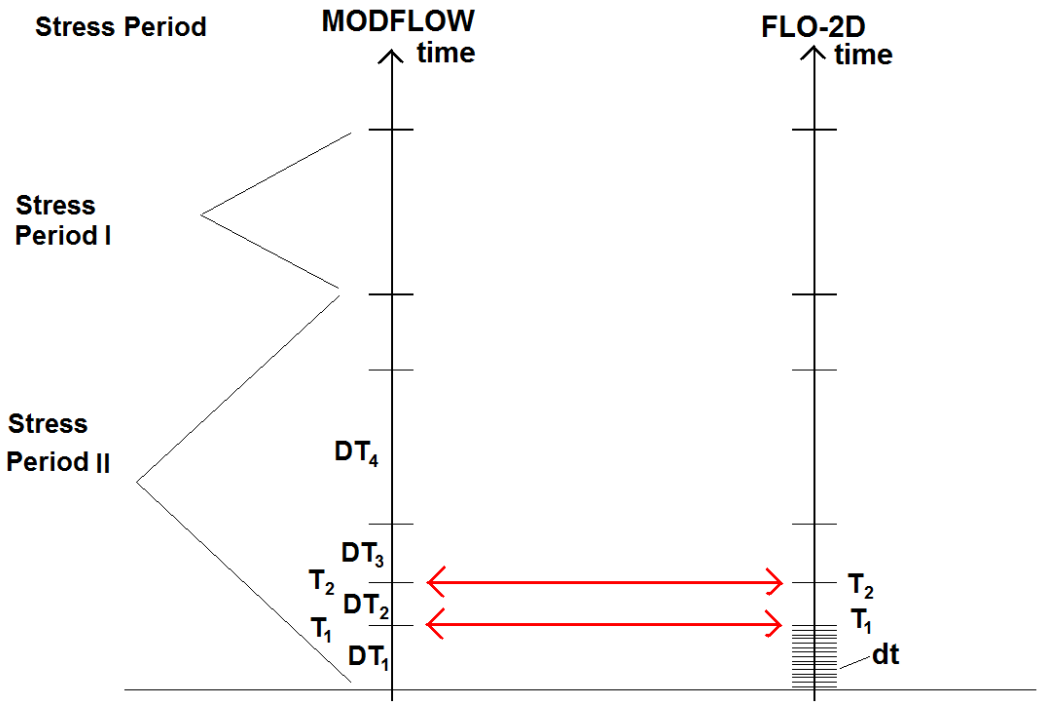

Figure 2.6. Time-step synchronization of FLO-2D and MODFLOW-2005

The FLO-2D algorithm calculates the accumulated volume of water that infiltrates from the floodplain before each MODFLOW-2005 stress time. In this study, the Green-Ampt method (1911) was selected for being the most complete function to estimate infiltration. With this method, the rainfall intensity predominantly influences the infiltration process as runoff and is generated when the maximum infiltration capacity is exceeded. Several variables are accounted for in the Green and Ampt infiltration function, including initial abstraction, hydraulic conductivity, soil porosity, volumetric moisture deficiency (initial and final soil saturation conditions), soil suction and soil storage depth. The development of the G&A method in FLO-2D is based on the application of Darcy's Law principle that the infiltration process begins as soon as the surface water moves in a vertical direction through the permeable medium and can be written as given by Eq. 2.6:

$$\frac{\Delta F}{\gamma} - ln\left(1 + \frac{\Delta F}{\gamma + F(t)}\right) = \frac{K_w}{\gamma}\,\Delta t \qquad \text{Eq. 2.6}$$

Where:

ΔF = change in infiltration over the computational time step

K_w = hydraulic conductivity at natural saturation (mm/hr)

$\gamma = (PSIF + Head) * DTHETA$

$PSIF$ = capillary suction (mm)

$Head$ = incremental rainfall for the time step plus flow depth on the grid element (mm)

$DTHETA$ = volumetric soil moisture deficit (dimensionless)

$F(t)$ = total infiltration at time t

Δt = computational time step

Fullerton (1983) developed an explicit equation ΔF by using a power series expansion for infiltration with respect of time to approximate the logarithmic term in the latter equation (Eq. 2.7):

$$\Delta F = \frac{-[2F(t) - K_w\Delta t] + [(2F(t) - K_w\Delta t)^2 + 8K_w\Delta t(\gamma + F(t))]^2}{2} \qquad \text{Eq. 2.7}$$

Conversely, the water exchange can also occur in the opposite direction due to flash flood events, fast recharge, or high-water surface levels in channels due to a sudden rise in the water table. If the groundwater heads calculated in MODFLOW-2005 are higher than the surface depth in FLO-2D, the depth of water from groundwater will be added to the surface depth. The infiltration calculation is switched off at each node as long as the saturation condition persists, meaning that infiltration will not be calculated until the soil absorption capacity is reestablished.

2.5.4 Model configuration and set-up

The FLO-2D hydraulic model requires a grid of square cells to represent the topography of the floodplain domain. The structured grid size of the computational domain defines the hydraulic model resolution. The LIDAR DTM was used as source floodplain topographic information, and an interpolation algorithm was implemented to produce a resampled DTM floodplain model to be used as input elevation of the hydraulic model. The nearest neighbor interpolation method was selected to resample data from the high-resolution 2 m LiDAR to a 20m resolution (≈ 43,000 cells).

In addition to the topographic features, a detailed representation of the built environment is relevant for urban flood modeling to simulate the flow wave propagation dynamics realistically. All buildings in the domain (7827 features) were imported to the FLO-2D computational domain. The polygon vectors are represented as Area Reduction Factors (ARF = 1) where the grid element surface area is considered impervious and is removed from potential water interactions.

Bathymetric measures were available for the Little Arch Creek River. A 1D hydraulic model with natural cross-sections was imported into FLO-2D extending from NE 143rd Street to structure G-58 located downstream of the Enchanted Forest Elaine Gordon Park. Official bathymetry from the Biscayne shore, Keystone Island, and Sans Souci canals was not available for this study due to jurisdiction restrictions. To compensate for the missing geometry, aerial imagery Google Earth was used to measure the canal's width, while a 10-meter bottom elevation was used as constant depth based on the Miami Florida Intracoastal Topography database from the Oleta River.

The infiltration method selected for the case study was the Green-Ampt, and the global soil parameters correspond to the pavement and the porous limestone environment to account for the surface water and groundwater interactions. For simplicity, the Manning roughness coefficient was assumed as 0.40 for green land cover areas and 0.04 for the impervious urbanized environment, canals bed, and Biscayne coast. Rainfall and tides were considered for the hydrologic forcing, setting the precipitation over the whole domain and tide levels in the Biscayne Bay's easternmost cells.

Concerning MODFLOW-2005, a simple model was developed based on two groundwater models, the regional MDC by USGS (Hughes & White, 2016) and the Arch Creek Basin (Sukop et al., 2018). The aquifer is composed of one-layer of about 36 meters, hydraulic conductivity parameters (Kx, Kz, Ss, Sy, and initial head), and four boundary conditions. The CHD package feature in the easternmost boundary represents the tide conditions of the Biscayne Bay, and the ocean-side water levels from Canal C-8 in the southern boundary edge. In respect to the groundwater heads, the GHB package was used to set the water table levels from gauge station G-852 in the westernmost boundary of the domain.

After the models are set-up, the compatibility process validates the perfect agreement between grid structure, position, and vertical elevations. A perfect match between the surface layers is required for the loosely-coupled model to link the floodplain-aquifer hydrodynamics. If so, FLO-2D will act as the base hydraulic model capable of simulating rainfall and discharge, ocean levels, and groundwater elevations, with the support of MODFLOW-2005, to create a compound inundation model (Figure 2.7).

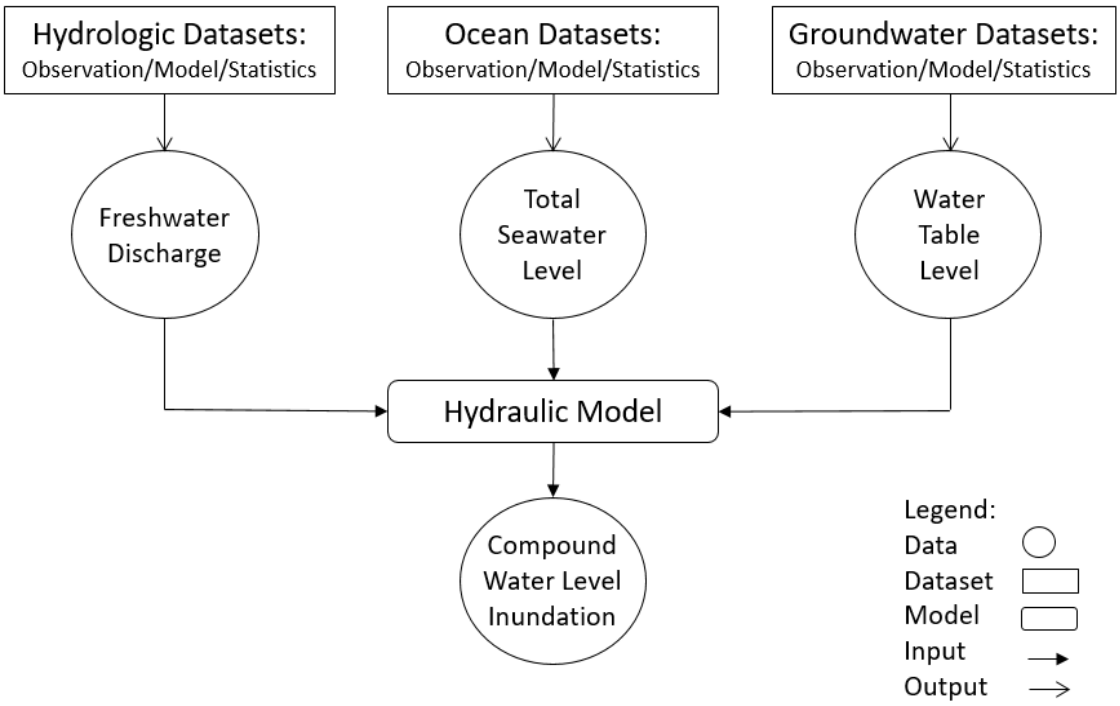

Figure 2.7. Flowchart representing the CF simulation using FLO-2D as the based hydraulic model to connect hydrologic, ocean and groundwater datasets, the latter with the support of MODFLOW-2005. Adapted from Santiago-Collazo et al. (2019)

2.5.5 Flood events

Three flood events (2-4 October 2000, 6-8 June 2013, and 25 May 2020) characterized by similar high intensity rainfall, low storm surge levels, and unusually high-water table levels with different response times were selected to compare the surface-subsurface model results (Figure 2.8).

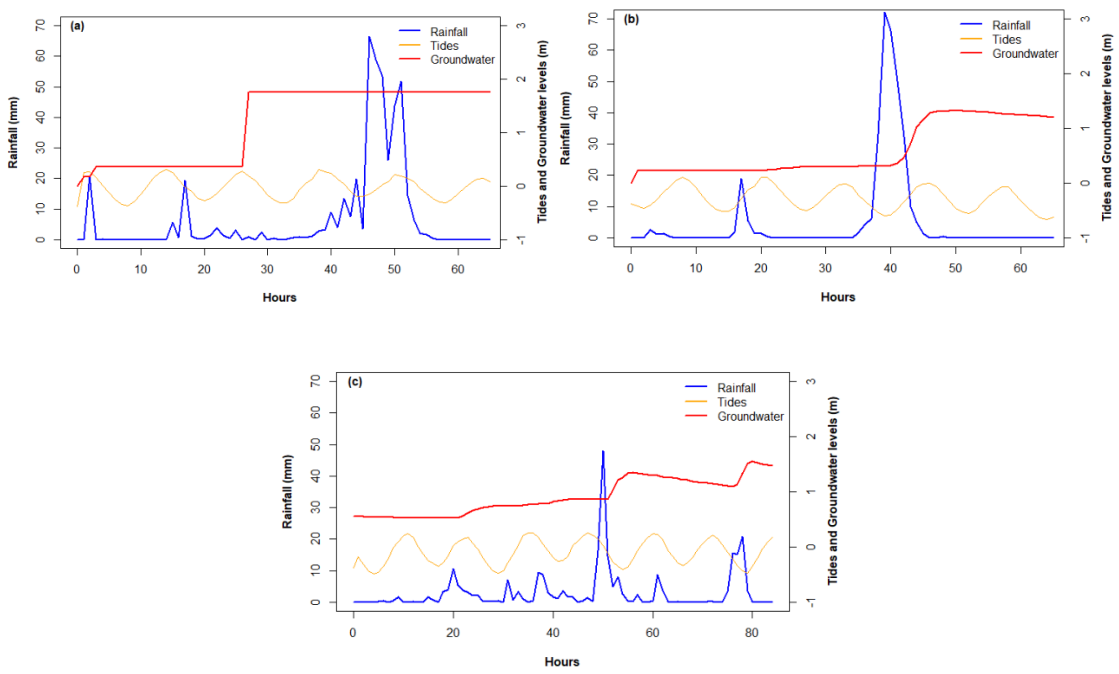

Figure 2.8. Time series of rainfall, tides, and groundwater levels for: (a) Tropical Storm Leslie; (b) Tropical Storm Andrea; (c) 25 May 2020 storm. The simulation time was determined based on the rainfall duration and groundwater fluctuations to properly characterized each event, being 64-hours for both Tropical Storms and 84-hours for the May 2020 event.

On 2-4 October 2000, Tropical Storm Leslie was responsible of one of the most severe events of North Miami in recent history in terms of flooding and property damages, with an accumulated rainfall of 454 mm over 65 hours and an estimated return period of 50 years. The highly permeable limestone and hydraulic conductivity of the Biscayne Aquifer is sensitive and strongly influenced by the direct and rapid response of ground-water levels to local scale rainfall events. As a result, a large area covered by heavy showers in Broward and MDC contributed to the sharp increase in the water table levels prior to the localized precipitation (≈ 20 hours) in the Arch Creek Basin (Franklin et al., 2001).

Similarly on 6-8 June 2013, Tropical Storm Andrea was a short-lived storm that formed in the Gulf of Mexico which produced very heavy precipitation across Broward and MDC (Beven II, 2013), recording a storm total rainfall of 317 mm in the Arch Creek Basin. The intense precipitation over 11 hours promoted the groundwater recharge rates significantly which led to a sudden increase of 1 meter in the water table.

The 25 May 2020 event is categorized as a 25-year storm with a total daily rainfall depth of 263 mm, producing localized rainfall in the North Biscayne Bay watershed, specifically in the Arch Creek Basin. Although the rainfall intensity and peak flow per-se did not represent a major threat to the study site and the storm hydrograph is less severe compared to Tropical Storm Leslie and Andrea, antecedent rainfall and soil moisture conditions exacerbated the magnitude of this event. Low-intensity storms contributed to the consistent recharge of the aquifer since mid-April 2020. It should be noted that May 2020 is also considered the second wettest May on record. As a result, the 25 May 2020 storm resulted in the fast gradual increase of groundwater table levels from 0.7 to 1.55 meters (NAVD 88) in ≈ 60 hours, leading to a CF event from pluvial and groundwater sources.

2.6 Results

2.6.1 Compound simulation

The interaction of groundwater and surface water physical processes are relevant and meaningful to better assess the severity of CF risks in low elevation coastal karsts environments. Figure 2.9 illustrates substantial flood magnitude differences when the subsurface hydrology and the infiltration depth are omitted from the 2D flood modelling framework. While the joint impact of rainfall and tide levels per se do not pose significant

threats to infrastructure as the surface runoff rapidly infiltrates into the porous permeable soil (Figure 2.9ace), the shallow water table of the Biscayne Aquifer quickly responds to high-intensity short-duration storms which results in the sudden increase of groundwater levels, leading to extensive urban flooding in parts of the Arch Creek Basin (Figure 2.9bdf). The simulation proves reasonable in terms of maximum flood depth and extent due to the similarities in the hydrologic conditions, being Tropical Storm Leslie the most severe of all three storms.

Figure 2.10 shows the flood mapping results and the water table timeseries for Tropical Storm Leslie. Although rainfall-runoff is the primary source of flooding in the urbanized Arch Creek Basin, abnormally high groundwater levels triggered groundwater-induced flooding resulting in the amplification of chronic flooding near historic waterways or zones below the County's land elevation flood criteria within North Miami and Unincorporated MDC, with flood depths $\approx$ 1 meter (Figure 2.10a, Figure 2.10b). The groundwater plots illustrate the effect of tidal and groundwater boundary conditions on the behavior of the simulated water table, in turn demonstrating the importance of both variables in the modeling set-up and influence in subsurface dynamics, as a cyclic high-low pattern characterize the tide fluctuations of the Biscayne Bay (Figure 2.10b, Figure 2.10e) compared to the defined water heads behavior from well G-852 in the western boundary of the domain (Figure 2.10a, Figure 2.10f).

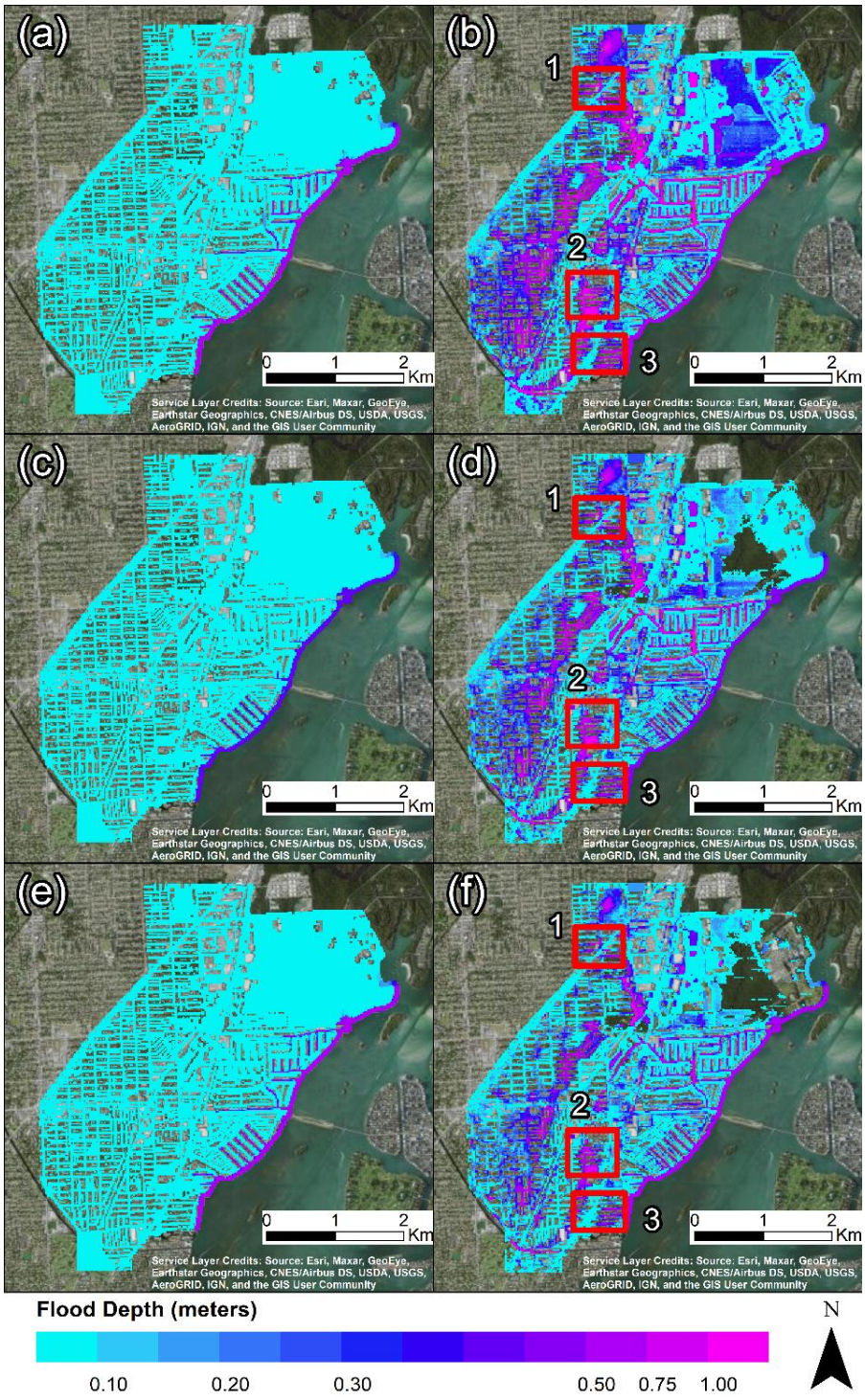

Figure 2.9. Spatial distribution of maximum inundation depths for rainfall and tides (left) and the compound flooding interaction of rainfall, tides, and water table (right) for Tropical Storm Leslie (a-b), Tropical Storm Andrea (c-d), and 25 May 2020 event (e-f).

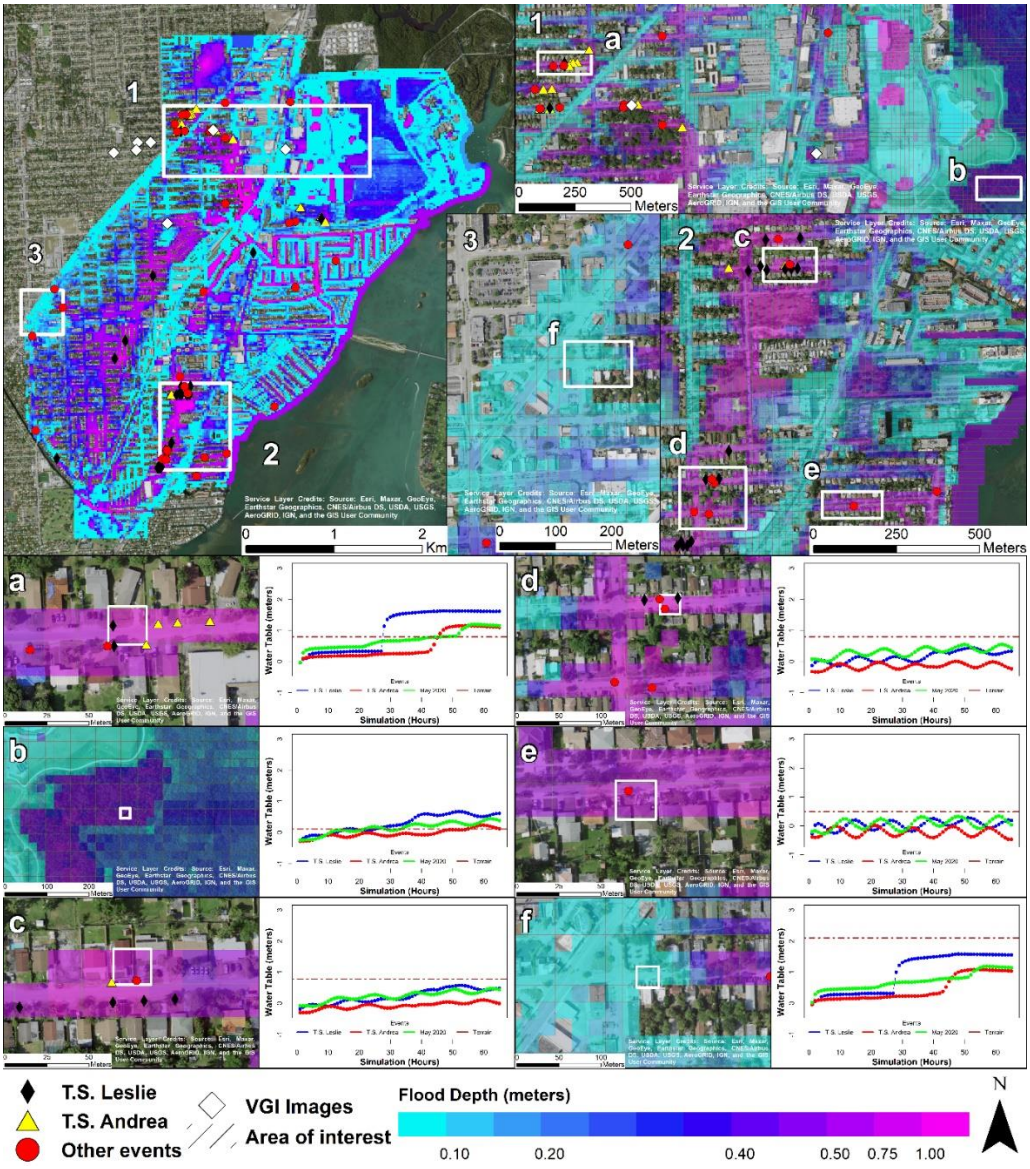

Figure 2.10. Distribution of maximum water surface elevations and groundwater table profiles in six sample locations across the Arch Creek Basin for Tropical Storm Leslie.

2.6.2 Identification of flooding hotspots

Despite the absence of post-disaster mapping products, measurements, and limited crowdsourced data in the study area, FEMA's SRL records were used to compare the model results with flood observations. Although the available records do not specify the observed inundation depths, an agreement between the property locations and maximum water levels

may offer sufficient validation to identify properties and neighborhoods at risk where shallow water tables can exacerbate the flooding conditions. The simulated storm events illustrate that most of the properties experienced moderate to high flood depths in predefined locations. For example, the housing infrastructure of Unincorporated MDC are particularly vulnerable to the impacts of surface flooding, even when the water table remains below the surface (Figure 2.10b, Figure 2.10e). Figure 2.11 presents a consistent agreement between the reported claims and localized flooding, indicating that the housing infrastructure in these neighborhoods have experienced SLR and are likely to experience additional flood losses at some point in the future.

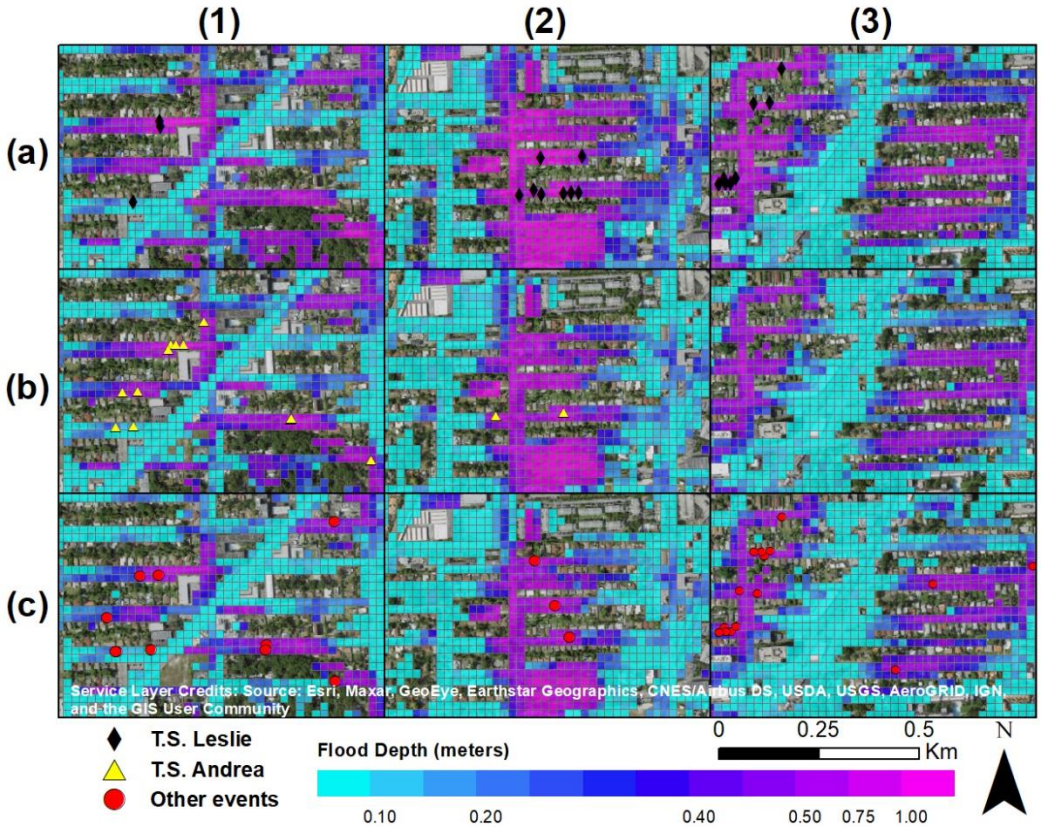

Figure 2.11. Distribution of maximum water surface elevations in three sample locations (Figure 2.9) for Tropical Storm Leslie (a), Tropical Storm Andrea (b), and 25 May 2020 event (c) against FEMA's SRL database (yellow). A high rate of agreement between FEMA's claims and high flood depths is achieved by the compound flood simulations.

In terms of residential damage, Tropical Storm Leslie and Tropical Storm Andrea may be considered the costliest events in the Arch Creek Basin as both account for the 60% of the reported claims (25 and 17 respectively) (Table 2.2).

Table 2.2. Quantitative analysis of simulated flood depths in respect to FEMA's SRL database by events.

Flood depth (mts)	T.S. Leslie	T.S.	Other Events
0 - 0.1	2	0	3
0.1 - 0.2	1	1	5
0.2 - 0.3	0	1	3
0.3 - 0.4	1	1	5
0.4 - 0.5	0	2	5
0.5 - 0.75	4	5	10
0.75 - 1.0	13	7	2
1.0 - 2.0	4	0	0
Total	25	17	33

Sources of uncertainty in the coupled numerical model could be reduced by increasing the model's resolution and incorporating storm-water infrastructure features. For example, the increase of the water table levels could challenge the ability of the storm drain system to convey water towards the Bay, resulting in prolonged flooding conditions, or anti-flood pump stations may alleviate the impacts of flooding by draining water from the streets and swales back to the ocean. Nevertheless, these records only reflect a small percentage of the damaged infrastructure and cannot be generalized at the Basin scale as the property owners may not meet the criteria to file the claim.

2.6.3 Validation using crowdsourced data from Tropical Storm Andrea

A limited number of real-time and post-flood crowdsourced flooding observations in the Arch Creek Basin were available during Tropical Storm Andrea (Figure 2.12). The visual comparison indicates a consistent spatial agreement between the maximum flood

depth of the coupled simulation and the interpreted depth of the crowdsourced data (Table 2.3).

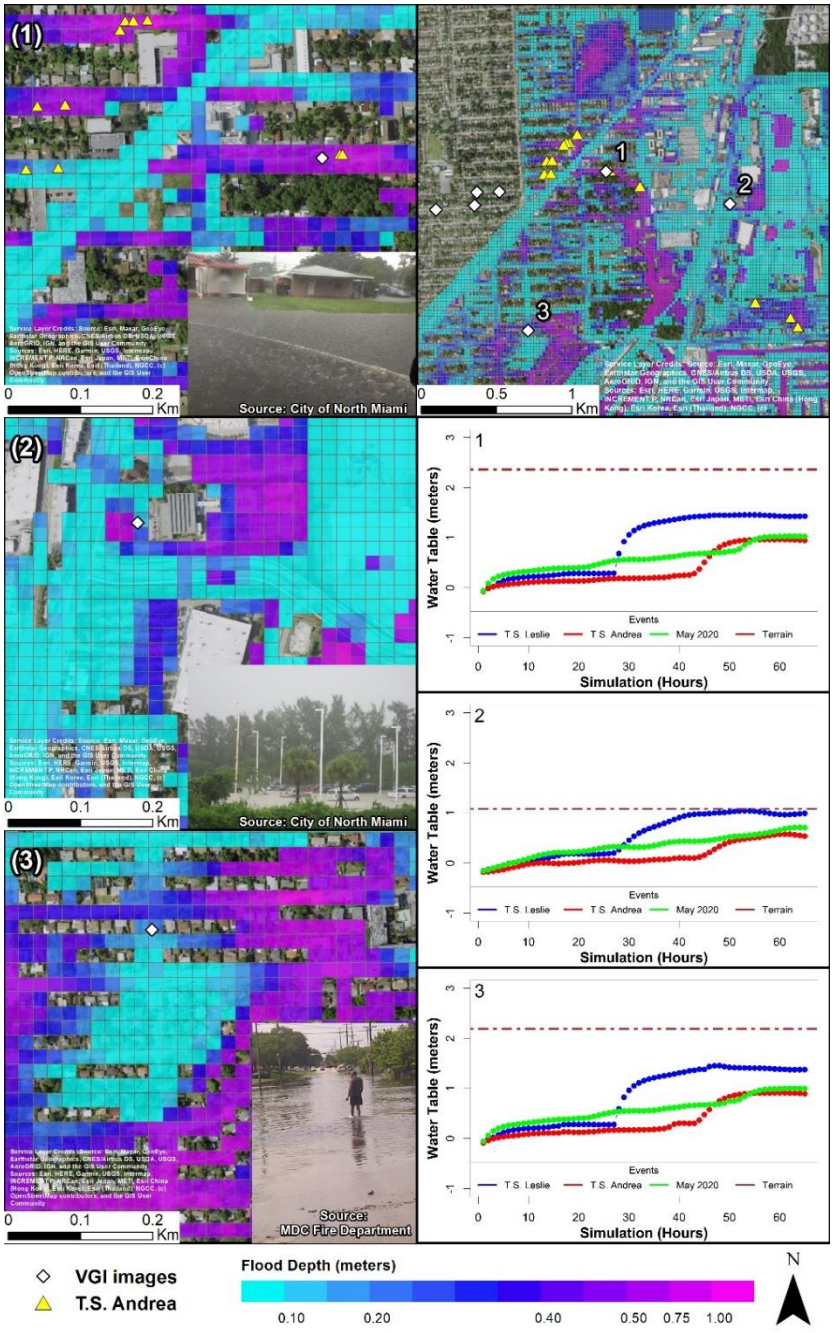

Figure 2.12. Maximum surface water depths of Tropical Storm Andrea in the Northwestern portion of the Arch Creek Basin (top right). Three selected subdomains (left) with available crowdsourced observations (white) are compared against FEMA's claims (yellow) and the simulated groundwater levels, resulting in rainfall-induced flooding as the water table remained below the terrain elevation (brown).

Table 2.3. Comparison between simulated maximum water flood depths and VGI imagery obtained during and after Tropical Storm Andrea

No.	Latitude	Longitude	Image category	Interpreted depth (m)	Max simulated depth (m)	Difference (m)
1	-80.165579	25.910225	During storm	0.20	0.67	-0.47
2	-80.157365	25.908227	During storm	0.55	0.54	0.01
3	-80.170807	25.900715	After storm	0.25	0.23	0.02

Figure 2.12a associates high flow depths (> 0.5 meters) with several properties that have experienced regular chronic flooding conditions, while the crowdsourced photograph displays an estimated inundation depth of 0.20 meters. Despite the model's overestimation, this comparison can be seen as an effective form of validation considering the changes in land use associated with the Arch Creek flow (Figure 2.1c) and low topographic elevation (Figure 2.3b).

Regarding Figure 2.12b, the US Post Office exhibits chronic flooding in the parking lot. We observe a reasonable level of accuracy in terms of flood depth validation results derived from the coupled model. Figure 2.12c displays stagnant flood water accumulated after the event in a portion of the NE 14 Ave. The results suggest that the rise in the water table influence the inundation extents, water levels and flood timeline.

Although the limitations on the amount of collected crowdsourced data in the study area, a larger georeferenced dataset including the date and time could improve the reliability of VGI data to validate hydrodynamic models. Similarly, a higher spatial resolution could reduce the level of uncertainty and biases from the modelling results.

2.7 Discussion

2.7.1 Flood risk and vulnerability

Floods resulting from extreme weather and climate events represent a major threat to low-lying neighborhoods and housing infrastructure in the Arch Creek Basin. Historically, frontal systems and summer cloudbursts are responsible for most of the significant pluvial flooding events in the study area compared to strong tropical systems, with Hurricane Irene (1999), Katrina (2005), Irma (2017), and No-Name storms as the only exceptions (Miami-Dade, 2015).

Most of the population of MDC lives in high-risk areas, only 1.2 meters (4 feet) above sea-level. In regard to the Arch Creek Basin, three-quarters of the urban landscape (67%) are located in a 100-year flood-prone area, and over 80% of the housing stock was built prior the development of the 1973 Flood Insurance Rate Map (Miami-Dade, 2016). For instance, properties in the Arch Creek Estates and localized areas East of US-1 such as the Key Stone Islands and Sans Souci Estates experienced repetitive flood losses since these settlements were built in the former riverbed of the Arch Creek Rivers or in land reclamation areas. The capacity of these communities to respond to hydrometeorological phenomena is limited or non-existent, resulting in repetitive negative impacts on livelihoods and residential property, expanding the socio-economic gap and inequality of MDC communities (Keenan et al., 2018).

2.7.2 Groundwater level fluctuations

The results of this investigation determined that groundwater tables rise rapidly with rainfall events leading to surface flooding in the Arch Creek Basin. Similar results were obtained by Sukop et al. (2018) who found that precipitation as the main trigger for

groundwater-induced flooding, with tidal fluctuations and sea level rise increasing the shallow water table, contributing to the reduction of the storm drain capacity. The present study also determined that antecedent rainfall events were important in the height of the water table at the start of the rainfall events investigated.

Seasonal water table fluctuations are expected throughout the year, presenting a higher level frequency during the winter and spring seasons due to climate variability and hydrological forcing (Gurdak et al., 2009; Taylor & Alley, 2001). Nevertheless, as we observed with Tropical Storm Leslie and Tropical Storm Andrea, the potential rise of groundwater levels to the surface during dry season cannot be ruled out since the hydraulically non-restrictive nature of the carbonate strata in MDC allows for rapid infiltration and high recharge rates during heavy precipitation events. The hydrologic forcing input and modeling results suggest that the joint occurrence of a high-intensity short-duration precipitation (> 50 mm peak, 250 mm total) with already high groundwater levels (> 1 meter) result in a CF event. Further research on linking multivariate statistical analysis with coupled hydrodynamic modeling frameworks may prove beneficial to identify thresholds that trigger CF conditions (Couasnon et al., 2018; Jane et al., 2020; Moftakhari et al., 2019; Saksena et al., 2019; Sebastian et al., 2017).

2.7.3 Tides and sea level rise

MDC is already experiencing the cascading effects of climate change with a record of 39 high-tide flooding events in 2019 (Wdowinski, 2019), costliest and most active hurricane seasons in records (2017 and 2020) (NOAA, 2021), steady increase in higher water table anomalies since 2010 (SFWMD, 2021), continuous saltwater intrusion (Guha & Panday, 2012; Obeysekera et al., 2011), and more frequent groundwater flooding events

(Compact, 2020; Sukop et al., 2018). Current SLR projections are expected to amplify future flood hazards in MDC including the variability in hydrological processes and extreme events, as well as the frequency and duration of nuisance flooding and shallow water tables (Obeysekera & Salas, 2016; Sweet et al., 2016).

Although this investigation determined that rainfall and sea levels alone did not produce significant flooding, the modeling efforts did not include storm surge flooding that can often accompany large hurricanes (Zhang et al., 2013). Nonetheless SLR projections and induced storm surge flooding conditions are beyond the scope of this study, future work on assessing the impact of high tide and storm surge induced flooding are fundamental to assess CF events and future flood risk scenarios (Obeysekera et al., 2019).

2.7.4 Wastewater and pollutants

Understanding the potential for groundwater tables to rise above the ground surface is important as Smith et al. (2021) determined that rising groundwater tables can carry contaminants from below ground septic systems to surface waters. Wastewater in septic systems often contain fecal coliforms, nitrate, phosphate as well as a number of pharmaceutical compounds such as antibiotics, analgesics and synthetic hormones (Yang et al., 2016). Rising groundwater tables not only present a concern to property damage as documented in this investigation, but also raise concerns for human exposure to wastewater pollutants. Furthermore, as floodwaters run-off, they can transport pollutants to adjacent surface water bodies such as Biscayne Bay. Wastewater contaminants have been found to persist in south Florida coastal waters (Singh et al., 2010). Future flood management efforts should consider flood water treatment to alleviate polluting adjacent surface waters.

2.8 Conclusions

Compound flooding hazards are increasing in coastal cities due to multiple factors related to climate change. The Arch Creek Basin in North Miami, which served as a vital flow corridor that connected the Everglades to the Biscayne Bay, is an appropriate location to study CF conditions. Results corroborate that groundwater-induced flooding is localized; thus, becoming an underlying condition that must be considered in low elevation coastal karst environments where the water table dynamics are subject to swift fluctuations caused by rainfall events.

A knowledge gap regarding a consolidated groundwater modelling framework was identified and addressed by proposing a loosely-coupled flood model that integrates surface hydrology and groundwater. The ability to produce more comprehensive flood hazard mapping from couple surface and subsurface water interactions is scientifically relevant to professionals in hydroinformatics since it improves the replicability of flood dynamics, setting the path to improve the understanding, prediction, and response time of groundwater levels as a potential trigger to compound flooding phenomena that can exacerbate floodwater depth and areal extent. This work opens new horizons on the development of CF models from a holistic perspective.

The quality and accuracy of flood hazard mapping in urban areas are strictly related to the model spatial resolution considering that the vertical datum and built-up environment influence flow propagation dynamics. A 20-meters grid resolution was selected to balance the computational demands with a certain level of precision without compromising the quality of the simulation. However, the investigation of higher and coarser resolutions in

CF studies might yield insights into the estimation of inundated areas and time performance at different scales.

Considering Miami's hydrogeomorphology is one of the most complex globally, the compounding effects of flood drivers may respond differently in diverse geographic settings. Therefore, further research should consider the proposed modeling framework to assess the CF risk in different geographical regions prone to multiple flood drivers, specifically in areas that have access to post-event flooding maps in the form of remote sensing products or VGI data for calibration and validation purposes.

The ability to simulate rising groundwater levels and sea level rise will be of great interest to Miami-Dade authorities on the impact of flooded septic systems from an ecological and public health perspective, providing a clearer view on the spread of septic tank effluent and contamination hotspots.

The contributions of this research are substantial and go beyond the numerical simulation scope, as it supports numerous fields and real applications including flood management, urban planning and design, flood mapping and zoning, disaster risk reduction, flood insurance policies and policy making. Ultimately, this research is a small piece of multidisciplinary work that analyzes the ripple effects of flooding in a wide range of fields (such as socio-economic costs, urban and ecological degradation, and health) and can set the basis for prevention, protection, accommodation, and even retreat/relocation policies.

2.9 References

Abboud, J. M., Ryan, M. C., & Osborn, G. D. (2018). Groundwater flooding in a river-connected alluvial aquifer. *Journal of Flood Risk Management*, *11*(4), 1–11. https://doi.org/10.1111/jfr3.12334

Abiy, A. Z., Melesse, A. M., Abtew, W., & Whitman, D. (2019). Rainfall trend and variability in Southeast Florida: Implications for freshwater availability in the Everglades. *PLoS ONE*, *14*(2), 1–20. https://doi.org/10.1371/journal.pone.0212008

Ascott, M. J., Marchant, B. P., Macdonald, D., McKenzie, A. A., & Bloomfield, J. P. (2017). Improved understanding of spatio-temporal controls on regional scale groundwater flooding using hydrograph analysis and impulse response functions. *Hydrological Processes*, *31*(25), 4586–4599. https://doi.org/10.1002/hyp.11380

Bates, P. D., Quinn, N., Sampson, C., Smith, A., Wing, O., Sosa, J., Savage, J., Olcese, G., Neal, J., Schumann, G., Giustarini, L., Coxon, G., Porter, J. R., Amodeo, M. F., Chu, Z., Lewis-Gruss, S., Freeman, N. B., Houser, T., Delgado, M., … Krajewski, W. F. (2021). Combined Modeling of US Fluvial, Pluvial, and Coastal Flood Hazard Under Current and Future Climates. *Water Resources Research*, *57*(2), 1–29. https://doi.org/10.1029/2020wr028673

Beven II, J. L. (2013). *Tropical Storm Andrea (AL012013)* (Issue August). https://www.nhc.noaa.gov/data/tcr/AL012013_Andrea.pdf

Bradford, R. B. (2002). Volume-duration growth curves for flood estimation in permeable catchments. *Hydrology and Earth System Sciences*, *6*(5), 939–947. https://doi.org/10.5194/hess-6-939-2002

Brunner, P., Therrien, R., Renard, P., Simmons, C. T., & Franssen, H. J. H. (2017). Advances in understanding river-groundwater interactions. *Reviews of Geophysics*, *55*(3), 818–854. https://doi.org/10.1002/2017RG000556

Chebud, Y., & Melesse, A. (2011). Operational Prediction of Groundwater Fluctuation in South Florida using Sequence Based Markovian Stochastic Model. *Water Resources Management*, *25*(9), 2279–2294. https://doi.org/10.1007/s11269-011-9808-z

Chebud, Y., & Melesse, A. (2012). Spatiotemporal Surface-Groundwater Interaction Simulation in South Florida. *Water Resources Management*, *26*(15), 4449–4466. https://doi.org/10.1007/s11269-012-0156-4

Christian, J., Fang, Z., Torres, J., Deitz, R., & Bedient, P. (2015). Modeling the Hydraulic Effectiveness of a Proposed Storm Surge Barrier System for the Houston Ship Channel during Hurricane Events. *Natural Hazards Review*, *16*(1), 04014015. https://doi.org/10.1061/(asce)nh.1527-6996.0000150

Cobby, D., Morris, S., Parkes, A., & Robinson, V. (2009). Groundwater flood risk management: Advances towards meeting the requirements of the EU floods directive. *Journal of Flood Risk Management*, *2*(2), 111–119. https://doi.org/10.1111/j.1753-318X.2009.01025.x

Couasnon, A., Sebastian, A., & Morales-Nápoles, O. (2018). A Copula-based bayesian network for modeling compound flood hazard from riverine and coastal interactions at the catchment scale: An application to the houston ship channel, Texas. *Water*

(Switzerland), *10*(9). https://doi.org/10.3390/w10091190

Cunningham, K. J., Carlson, J. L., Wingard, G. L., Robinson, E., & Wacker, M. A. (2004). Characterization of aquifer heterogeneity using cyclostratigraphy and geophysical methods in the upper part of the Karstic Biscayne Aquifer, Southeastern Florida. In *Water-Resources Investigations Report*. https://doi.org/10.3133/wri034208

Cunningham, K. J., & Florea, L. J. (2009). *The Biscayne Aquifer of Southeastern Florida The Biscayne Aquifer of Southeastern Florida*. 196–199.

Devia, G. K., Ganasri, B. P., & Dwarakish, G. S. (2015). A Review on Hydrological Models. *Aquatic Procedia*, *4*(Icwrcoe), 1001–1007. https://doi.org/10.1016/j.aqpro.2015.02.126

FEMA. (2021). *https://www.fema.gov/case-study/repetitive-flood-claims-program-benefits-city-and-homeowners*.

Field, C., Barros, V., & Stocker, T. (2012). *Managing the risks of extreme events and disasters to advance climate change adaptation. Special report of the Intergovernmental Panel on Climate Change (IPCC)*.

Finch, J. W., Bradford, R. B., & Hudson, J. A. (2004). The spatial distribution of groundwater flooding in a chalk catchment in southern England. *Hydrological Processes*, *18*(5), 959–971. https://doi.org/10.1002/hyp.1340

Fish, J. E., & Stewart, M. T. (1991). Hydrogeology of the surficial aquifer system, Dade County, Florida. In *Water-Resources Investigations Report*. https://doi.org/10.3133/wri904108

FLO-2D. (2018). *FLO-2D Reference Manual*.

Franklin, J. L., Avila, L. A., Beven, J. L., Lawrence, M. B., Pasch, R. J., & Stewart, S. R. (2001). Atlantic hurricane season of 2000. *Monthly Weather Review*, *129*(12), 3037–3056. https://doi.org/10.1175/1520-0493(2001)129<3037:AHSO>2.0.CO;2

Fullerton, W. T. (1983). *Water and Sediment Routing from Complex Watersheds and Example Application to Surface Mining*. Colorado State University.

García-Gil, A., Vázquez-Suñé, E., Sánchez-Navarro, J. Á., Mateo Lázaro, J., & Alcaraz, M. (2015). The propagation of complex flood-induced head wavefronts through a heterogeneous alluvial aquifer and its applicability in groundwater flood risk management. *Journal of Hydrology*, *527*, 402–419. https://doi.org/10.1016/j.jhydrol.2015.05.005

Greater Miami & the Beaches. (2019). *Resilient 305*.

Guha, H., & Panday, S. (2012). Impact of Sea Level Rise on Groundwater Salinity in a Coastal Community of South Florida. *Journal of the American Water Resources*

Association, *48*(3), 510–529. https://doi.org/10.1111/j.1752-1688.2011.00630.x

Gurdak, J. S., Hanson, R. T., & Green, T. R. (2009). Effects of Climate Variability and Change on Groundwater Resources of the United States. In *Fact Sheet*. https://doi.org/10.3133/fs20093074

Harbaugh, A. W. (2005). MODFLOW-2005 : the U.S. Geological Survey modular ground-water model--the ground-water flow process. In *Techniques and Methods*. https://doi.org/10.3133/tm6A16

Hoffmeister, J. E., Stockman, K. W., & Multer, H. G. (1967). Miami Limestone of Florida and Its Recent Bahamian Counterpart. *GSA Bulletin*, *78*(2), 175–190. https://doi.org/10.1130/0016-7606(1967)78[175:MLOFAI]2.0.CO;2

Hughes, A. G., Vounaki, T., Peach, D. W., Ireson, A. M., Jackson, C. R., Butler, A. P., Bloomfield, J. P., Finch, J., & Wheater, H. S. (2011). Flood risk from groundwater: Examples from a Chalk catchment in southern England. *Journal of Flood Risk Management*, *4*(3), 143–155. https://doi.org/10.1111/j.1753-318X.2011.01095.x

Hughes, J. D., & White, J. T. (2016). Hydrologic conditions in urban Miami-Dade County, Florida, and the effect of groundwater pumpage and increased sea level on canal leakage and regional groundwater flow. *U.S. Geological Survey*, *Scientific Investigations Report 2014-5162*, 175.

Ikeuchi, H., Hirabayashi, Y., Yamazaki, D., Muis, S., Ward, P. J., Winsemius, H. C., Verlaan, M., & Kanae, S. (2017). Compound simulation of fluvial floods and storm surges in a global coupled river-coast flood model: Model development and its application to 2007 Cyclone Sidr in Bangladesh. *Journal of Advances in Modeling Earth Systems*, *9*(4), 1847–1862. https://doi.org/10.1002/2017MS000943

Jacobs. (2007). *Groundwater flooding records collation, monitoring and risk assessment (reference HA5): consolidated report*.

Jane, R., Cadavid, L., Obeysekera, J., & Wahl, T. (2020). Multivariate statistical modelling of the drivers of compound flood events in south Florida. *Natural Hazards and Earth System Sciences*, *20*(10), 2681–2699. https://doi.org/10.5194/nhess-20-2681-2020

Karamouz, M., Zahmatkesh, Z., Goharian, E., & Nazif, S. (2015). Combined Impact of Inland and Coastal Floods: Mapping Knowledge Base for Development of Planning Strategies. *Journal of Water Resources Planning and Management*, *141*(8), 04014098. https://doi.org/10.1061/(asce)wr.1943-5452.0000497

Keenan, J. M., Hill, T., & Gumber, A. (2018). Climate gentrification: From theory to empiricism in Miami-Dade County, Florida. *Environmental Research Letters*, *13*(5). https://doi.org/10.1088/1748-9326/aabb32

Kumbier, K., Carvalho, R. C., Vafeidis, A. T., & Woodroffe, C. D. (2018). Investigating

compound flooding in an estuary using hydrodynamic modelling: A case study from the Shoalhaven River, Australia. *Natural Hazards and Earth System Sciences*, *18*(2), 463–477. https://doi.org/10.5194/nhess-18-463-2018

MacDonald, A. M., Lapworth, D. J., Hughes, A. G., Auton, C. A., Maurice, L., Finlayson, A., & Gooddy, D. C. (2014). Groundwater, flooding and hydrological functioning in the Findhorn floodplain, Scotland. *Hydrology Research*, *45*(6), 755–773. https://doi.org/10.2166/nh.2014.185

Miami-Dade. (2015). *Little Arch Creek Salinity Control Structure; Arch Creek Basin Drainage Evaluation Report*.

Miami-Dade. (2016). *Arch Creek Study Area, Miami-Dade County, Florida; Briefing Book for ULI Advisory Services Panel, May 22-27 2016*.

Miami-Dade. (2017). *Repetitive losses*. http://www.miamidade.gov/environment/repetitive-%0Alosses.asp

Miami Herald. (2019). *North Miami bought her flooded home. Now it's going to become a park to fight sea rise*. https://www.miamiherald.com/news/local/environment/article235403232.html

Moftakhari, H., Schubert, J. E., AghaKouchak, A., Matthew, R. A., & Sanders, B. F. (2019). Linking statistical and hydrodynamic modeling for compound flood hazard assessment in tidal channels and estuaries. *Advances in Water Resources*, *128*(April), 28–38. https://doi.org/10.1016/j.advwatres.2019.04.009

Nalesso, M. (2009). Integrated surface-ground water modeling in wetlands with improved methods to simulate vegetative resistance to flow. *ProQuest ETD Collection for FIU*.

NOAA. (2021). *Storm events database*. https://www.ncdc.noaa.gov/stormevents/

O'Brien, J. S. (2011). *FLO-2D Users Manual*.

O'Brien, J. S., Julien, P. Y., & Fullerton, W. T. (1993). Two-dimensional water flood and mudflow simulation. *Hydrol. Eng.*, *119*, 244–261.

Ó Dochartaigh, B., Archer, N. A. L., Peskett, L., MacDonald, A. M., Black, A. R., Auton, C. A., Merritt, J. E., Gooddy, D. C., & Bonell, M. (2019). Geological structure as a control on floodplain groundwater dynamics. *Hydrogeology Journal*, *27*(2), 703–716. https://doi.org/10.1007/s10040-018-1885-0

Obeysekera, J., Irizarry, M., Park, J., Barnes, J., & Dessalegne, T. (2011). Climate change and its implications for water resources management in south Florida. *Stochastic Environmental Research and Risk Assessment*, *25*(4), 495–516. https://doi.org/10.1007/s00477-010-0418-8

Obeysekera, J., & Salas, J. D. (2016). Frequency of Recurrent Extremes under

Nonstationarity. *Journal of Hydrologic Engineering*, *21*(5), 04016005. https://doi.org/10.1061/(asce)he.1943-5584.0001339

Obeysekera, J., Sukop, M., Troxler, T., Irizarry, M., & Rogers, M. (2019). *Potential Implications of Sea-Level Rise and Changing Rainfall for Communities in Florida using Miami-Dade County as a Case Study*. https://slsc.fiu.edu/_assets/pdfs/fbc_fiu_finalreport_22aug2019.pdf

Olbert, A. I., Comer, J., Nash, S., & Hartnett, M. (2017). High-resolution multi-scale modelling of coastal flooding due to tides, storm surges and rivers inflows. A Cork City example. *Coastal Engineering*, *121*(January), 278–296. https://doi.org/10.1016/j.coastaleng.2016.12.006

Parker, G. G., & Cooke, C. W. (1944). Late Cenozoic Geology of Southern Florida with a Discussion of the Ground Water. *U.S. Geological Survey*, *27*.

Pellenbarg, N. P. (1989). Groundwater management in the Netherlands: Background and legislation groundwater in the Netherlands. *Groundwater Management: Sharing Responsibility for an Open Access Resource, March 1984*, pp137-149.

Price, R., Schwartz, K., Anderson, B., Boucek, R., Briceño, H., Cook, M., Fitz, C., Onsted, J., Rehage, J., Rivera-Monroy, V., Roy Chowdhury, R., & Saha, A. (2020). *Chapter 3: Water, Sustainability, and Survival, in Childers, D.L., E.E. Gaiser and L.A. Ogden (eds.) The Coastal Everglades: The Dynamics of Social-Ecological Transformation in the South Florida Landscape. Oxford University Press : New York, New York.*

Prinos, S. T., & Dixon, J. F. (2016). Statistical analysis and mapping of water levels in the Biscayne aquifer, water conservation areas, and Everglades National Park, Miami-Dade County, Florida, 2000–2009. In *Scientific Investigations Report*. https://doi.org/10.3133/sir20165005

Rotzoll, K., & Fletcher, C. H. (2013). Assessment of groundwater inundation as a consequence of sea-level rise. *Nature Climate Change*, *3*(5), 477–481. https://doi.org/10.1038/nclimate1725

Saksena, S., Merwade, V., & Singhofen, P. J. (2019). Flood inundation modeling and mapping by integrating surface and subsurface hydrology with river hydrodynamics. *Journal of Hydrology*, *575*(December 2018), 1155–1177. https://doi.org/10.1016/j.jhydrol.2019.06.024

Santiago-Collazo, F. L., Bilskie, M. V., & Hagen, S. C. (2019). A comprehensive review of compound inundation models in low-gradient coastal watersheds. *Environmental Modelling and Software*, *119*(June), 166–181. https://doi.org/10.1016/j.envsoft.2019.06.002

Sebastian, A., Dupuits, E. J. C., & Morales-Nápoles, O. (2017). Applying a Bayesian network based on Gaussian copulas to model the hydraulic boundary conditions for

hurricane flood risk analysis in a coastal watershed. *Coastal Engineering*, *125*(August 2016), 42–50. https://doi.org/10.1016/j.coastaleng.2017.03.008

Seneviratne, S., Nicholls, N., Easterling, D., Goodess, C., Kanae, S., Kossin, J., Luo, Y., Marengo, J., Mcinnes, K., Rahimi, M., Reichstein, M., Sorteberg, A., Vera, C., & Zhang, X. (2012). *Changes in climate extremes and their impacts on the natural physical environment*.

SFWMD. (2021). *DBHYDRO*. http://my.sfwmd.gov/dbhydroplsql/show_dbkey_info.main_menu

Singh, S. P., Azua, A., Chaudhary, A., Khan, S., Willett, K. L., & Gardinali, P. R. (2010). Occurrence and distribution of steroids, hormones and selected pharmaceuticals in South Florida coastal environments. *Ecotoxicology*, *19*(2), 338–350. https://doi.org/10.1007/s10646-009-0416-0

Smith, M. A., Kominoski, J. S., Gaiser, E. E., Price, R. M., & Troxler, T. G. (2021). Stormwater runoff and tidal flooding transform dissolved organic matter composition and increase bioavailability in urban coastal ecosystems. *Journal of Geophysical Research: Biogeosciences*, 1–19. https://doi.org/10.1029/2020jg006146

Sophocleous, M. (2002). Interactions between groundwater and surface water: The state of the science. *Hydrogeology Journal*, *10*(1), 52–67. https://doi.org/10.1007/s10040-001-0170-8

Southeast Florida Regional Climate Change Compact Sea Level Rise Work Group (Compact). (2020). *A document prepared for the Southeast Florida Regional Climate Change Compact Climate Leadership Committee*. http://www.southeastfloridaclimatecompact.org/wp-content/uploads/2015/10/2015-Compact-Unified-Sea-Level-Rise-Projection.pdf

Su, X., Liu, T., Beheshti, M., & Prigiobbe, V. (2020). Relationship between infiltration, sewer rehabilitation, and groundwater flooding in coastal urban areas. *Environmental Science and Pollution Research*, *27*(13), 14288–14298. https://doi.org/10.1007/s11356-019-06513-z

Sukop, M. C., Rogers, M., Guannel, G., Infanti, J. M., & Hagemann, K. (2018). High temporal resolution modeling of the impact of rain, tides, and sea level rise on water table flooding in the Arch Creek basin, Miami-Dade County Florida USA. *Science of the Total Environment*, *616–617*, 1668–1688. https://doi.org/10.1016/j.scitotenv.2017.10.170

Sweet, W. V., Menendez, M., Genz, A., Obeysekera, J., Park, J., & Marra, J. J. (2016). In tide's way: Southeast Florida's September 2015 sunny-day flood. *Bulletin of the American Meteorological Society*, *97*(12), S25–S30. https://doi.org/10.1175/BAMS-D-16-0117.1

Taylor, C. J., & Alley, W. M. (2001). Ground-water-level monitoring and the importance

of long-term water-level data. *US Geological Survey Circular*, *1217*, 1–68. https://pubs.usgs.gov/circ/circ1217/pdf/circ1217_final.pdf

Teng, J., Jakeman, A. J., Vaze, J., Croke, B. F. W., Dutta, D., & Kim, S. (2017). Flood inundation modelling: A review of methods, recent advances and uncertainty analysis. *Environmental Modelling and Software*, *90*, 201–216. https://doi.org/10.1016/j.envsoft.2017.01.006

U.S. Census Bureau. (2020). *American Community Survey 5-Year Data (2009-2019)*. https://www.census.gov/data/developers/data-sets/acs-5year.html

U.S. Department of Agriculture. (1948). *Aerial photographs of Dade County*. https://ufdc.ufl.edu/UF00071738/00034/1x?search=dade

van Westen, C. J., & Greiving, S. (2017). Multi-hazard risk assessment and decision making. *Environmental Hazards Methodologies for Risk Assessment and Management*, 31–94. https://doi.org/10.2166/9781780407135_0031

Wahl, T., Jain, S., Bender, J., Meyers, S. D., & Luther, M. E. (2015). Increasing risk of compound flooding from storm surge and rainfall for major US cities. *Nature Climate Change*, *5*(12), 1093–1097. https://doi.org/10.1038/nclimate2736

Wdowinski, S. (2019). Coherent saptio-temporal variations in the rate of sea level rise along the US Atlantic and Gulf coasts. *AGU Fall Meeting Abstracts*, *2019*, OS21A-07.

Winston, R. B. (2009). *ModelMuse: A Graphical User Interface for MODFLOW-2005 and PHAST: U.S. Geological Survey Techniques and Methods 6–A29*. http://pubs.usgs.gov/tm/tm6A29/tm6A29.pdf

Yang, S., & Tsai, F. T. C. (2020). Understanding impacts of groundwater dynamics on flooding and levees in Greater New Orleans. *Journal of Hydrology: Regional Studies*, *32*(July), 100740. https://doi.org/10.1016/j.ejrh.2020.100740

Yang, Y., Toor, G., Wilson, P. C., & Williams, C. F. (2016). Septic systems as hot-spots of pollutants in the environment: Fate and mass balance of micropollutants in septic drainfields. *The Science of the Total Environment*, *566–567*, 1535–1544.

Yu, X., Moraetis, D., Nikolaidis, N. P., Li, B., Duffy, C., & Liu, B. (2019). A coupled surface-subsurface hydrologic model to assess groundwater flood risk spatially and temporally. *Environmental Modelling and Software*, *114*(September 2018), 129–139. https://doi.org/10.1016/j.envsoft.2019.01.008

Zhang, K., Li, Y., Liu, H., Xu, H., & Shen, J. (2013). Comparison of three methods for estimating the sea level rise effect on storm surge flooding. *Climatic Change*, *118*(2), 487–500. https://doi.org/10.1007/s10584-012-0645-8

Zscheischler, J., Westra, S., Van Den Hurk, B. J. J. M., Seneviratne, S. I., Ward, P. J.,

Pitman, A., Aghakouchak, A., Bresch, D. N., Leonard, M., Wahl, T., & Zhang, X. (2018). Future climate risk from compound events. *Nature Climate Change*, *8*(6), 469–477. https://doi.org/10.1038/s41558-018-0156-3

CHAPTER III

Investigating compound flooding in a low elevation coastal karst environment using multivariate statistical and 2D hydrodynamic modeling: A case study in the Arch Creek Basin, Miami-Dade County Florida USA

3 CHAPTER 3: INVESTIGATING COMPOUND FLOODING IN A LOW ELEVATION COASTAL KARST ENVIRONMENT USING MULTIVARIATE STATISTICAL AND 2D HYDRODYNAMIC MODELING: A CASE STUDY IN THE ARCH CREEK BASIN, MIAMI-DADE COUNTY FLORIDA USA

3.1 Abstract

Miami-Dade County is vulnerable to flash, pluvial, fluvial, coastal and groundwater flooding due to its low-elevation and karst morphology. Despite considerable advances in understanding the impact of compound flooding events by considering major flood drivers (precipitation, river discharge, and coastal surge), little is known regarding the severity of groundwater hazards in this region. This study links a multivariate statistical analysis with a coupled physically-based 2D hydraulic model to estimate the flood hazard in the Arch Creek Basin located in North Miami. A bivariate copula analysis was used to capture the joint probability of key flood drivers with predefined water table thresholds to set-up the flood modeling conditions. Results demonstrate the high vulnerability to extreme precipitation events compared to coastal surge in the study area. Similarly, groundwater flooding is relevant in shallow water table environments, as it influences the severity of flood hazards in terms of flood inundation depth, extent, and damage to building infrastructure. This research demonstrates that groundwater flooding is a latent risk that should be incorporated in flood hazard mapping in regions susceptible to high water tables and sea level rise.

3.2 Introduction

Miami-Dade County (MDC) is the world's most exposed metropolitan area in terms of coastal flooding, due to its low elevation, high population density and economic importance (OECD, 2007). The value of assets at risk of coastal flooding is projected to

increase from $416 billion in 2011 to $3,513 trillion by 2070 (Hanson et al., 2011). Florida has been hit by 120 hurricanes since 1851, representing 40% of the total number in the U.S. (NOAA, 2021). Of the 56 hurricanes to make landfall in southeast Florida, 20 are classified as major hurricanes (Category 3 or higher) with Irma (2017), Wilma (2005), and Andrew (1992) the most destructive of recent times. In the same context, anthropogenic changes of the natural landscape have resulted in significant modifications of the hydrological cycle, watershed hydrology, and flow regimes leading to an increase in urban runoff and pluvial flooding (Leopold et al., 2005). MDC highly relies on flood control systems, designed to minimize the impacts of pluvial flooding among other functions, to remain functional during prolonged heavy rainfall events. In general, the drainage systems can convey low return periods of rainfall events (≈10-year storms).

Groundwater flooding has received significantly less attention by the scientific community compared to the impacts of pluvial, fluvial, and coastal flooding events (Cobby et al., 2009). Low elevation coastal floodplains underlaid by unconfined aquifers are susceptible to groundwater flooding as long-duration precipitation events can trigger shallow water tables to rise through the permeable strata and emerge at surface level (Macdonald et al., 2008; Sophocleous, 2002). Higher water tables are becoming more common in coastal karst environments, due to reduced rates of groundwater abstraction in urban areas (groundwater rebound) and to a lesser extent in mining areas (Hardt & Hutchinson, 1978; Hughes & White, 2016; Pellenbarg, 1989). Rising groundwater levels put additional pressure on the drainage system, increase the chances of flooding as may cause structural damage to urban settlements and infrastructure. Permeable alluvial river

systems and paleo valleys with limited storage capacity are also potential environments for groundwater flooding (Cantafio and Ryan, 2014; Larkin and Sharp Jr., 1992). The high hydraulic conductivity and transmissivity rates of alluvial streams favor the exchange of high river stage flows from the riparian zone into the aquifer (Abboud et al., 2018; Guinn Garrett et al., 2012; Woessner, 2000), which can be detrimental to productive farming systems (Kozlowski and Pallardy, 1984).

Karst landscapes are distinctive environments characterized by the direct hydrologic connection between any surface water and the underlying highly transmissive aquifer, and are particularly vulnerable to groundwater flooding and a multiple of geohydrological hazards due to their swift hydrodynamic response to precipitation and limited storage capacity (Gutiérrez et al., 2014; Martinotti et al., 2017; Naughton et al., 2018). The surficial limestone of the Biscayne Aquifer - among the most permeable in the world – allows for rapid infiltration and recharge, initiating in the Everglades the laterally-dominated flow system moving throughout MDC to discharge in the Biscayne Bay (Cunningham and Florea, 2009; Price et al., 2020). South Florida's low-lying geomorphology and karst terrain face complex environmental and engineering challenges posed by rising water tables and sea level rise (Czajkowski et al., 2018; Sukop et al., 2018; Sweet et al., 2016; Wdowinski et al., 2016).

Compound events are defined as the co-occurrence of two or more flooding drivers e.g. rainfall and storm tide, that are not necessarily individually extreme but combined produce an extreme impact (Bevacqua et al., 2017; Leonard et al., 2014; Zscheischler et al., 2018). Many of the variables are causally linked as they are driven by the same large

scale synoptic conditions, consequently there is often statistically significant dependence between the drivers (e.g., Nasr et al., 2021; Wahl et al., 2015). Copulas and Fréchet transformations allow the modeling of the dependence structure to be decoupled marginal distributions (Genest and Favre, 2007) and are increasingly used to analyze the joint probabilities of river discharge and storm surge at locations around the U.S. In general, the more localized the study, the more complex the approach adopted. Global scale analyses by Ward et al. (2018) and Wahl et al. (2015) applied bivariate copulas to in situ observational records, the latter adopting precipitation as a proxy for discharge. To improve spatial coverage in the aforementioned studies, Couasnon et al. (2020) applied bivariate copulas to the output of climate models. Moftakhari et al. (2017), again utilizing bivariate copulas, demonstrated that sea level rise significantly increases the probability of observing a predefined hazardous river discharge and coastal water level events at least once in a given design lifetime at eight major U.S. cities. Moftakhari et al. (2019) and Muñoz et al. (2020) employed a similar approach to capture the dependence between annual maximum coastal surge and river discharge in Southern California, and near Savannah Georgia, respectively. Couasnon et al. (2018) meanwhile adopted a gaussian copula-based Bayesian network to model the pairwise dependencies between discharge records in a Texas catchment, as well as between these records and the non-tidal residual recorded at Galveston. Jane et al. (2020) applied a vine copula and a conditional extreme value model to precipitation, ocean side water level seaward of flood control structures and groundwater level at three sites in MDC. Serafin et al. (2019) modelled the dependence between the wave height component of the total water level and maximum daily discharge along the Quillayute River in Washington by a logistic model.

The simulation of individual mechanisms or superposition of results ignoring the dynamic often nonlinear interaction of the different flood processes significantly miscalculate flood risk (e.g. Kumbier et al., 2018). Compound inundation models attempt to account for the complex interaction of multiple flood drivers, to simulate the compound effects of either pluvial, fluvial and coastal flooding phenomena (Eilander et al., 2020; Wahl et al., 2015), or even predictions of the three flood drivers at large-scales (Bates et al., 2021). Integrated models able to calculate the inundation due to the combination of storm surge and river discharge are sparse, consequently, storm surge models are typically coupled with a hydrological/hydraulic model through boundary conditions either by running one model after another (i.e. one-way coupled) or by the exchange of information at each synchronized time-step (dynamic coupling) (Santiago-Collazo et al., 2019). Several studies have focused on quantifying the compound effects of inundation at local levels. For example, Saleh et al. (2017) found out important differences on the types of inundation processes caused by hurricanes Irene and Sandy in New Jersey, as a number of characteristics influence the severity of the storm surge and precipitation caused by hurricanes. Similarly Olbert et al. (2017) identified fluvial flooding as the dominant mechanism behind a 2009 coastal flood event in Cork, Ireland.

In recently developed hybrid approaches, the output of multivariate statistical analyses, typically long synthetic records, act as the boundary conditions for hydraulic models. The approaches identify transition zones, where the dominant driver changes, and flooding can be induced from hydrologic and coastal sources as well as their collective interaction (Bilskie and Hagen, 2018). Unless the synthetic record is relatively short (e.g.,

Couasnon et al., 2018), the computational expensive of running a hydraulic model for every synthetic event can be prohibitive. To alleviate the computational burden, Moftakhari et al. (2019) and Muñoz et al. (2020) employed a hazard scenario approach that only required four runs of the physics-based model for a given return period. The T-year discharge paired with a moderate ocean water level and vice versa as well as the T-year events associated with the "AND" and "OR" hazard scenarios that the observation records imply are "most likely". Serafin et al. (2019) ran a HEC-RAS model for a carefully selected subset of 50, 700-year records, and estimated the along river levels of the remainder from surrogate models trained at discrete points along the river based on the limited model runs. By analyzing long synthetic records rather pre-determined return period events Serafin et al. (2019) were able to show the disparity in the along-river levels derived by pairing the upstream and downstream forcing's with the same marginal return periods with (response) water levels, those derived empirically at each location using the model output.

Although linking probabilistic frameworks with hydrodynamic modeling for coastal structural design to simulate extreme scenarios are a common practice (Couasnon et al., 2018; Moftakhari et al., 2019; Sebastian et al., 2017), studies on surface-groundwater interactions are limited. Saksena et al. (2019) highlighted groundwater processes as indispensable for realistic estimates of flood inundation for the Upper Wabash River basin in Indiana. The river hydrodynamics calculations were obtained based on the ICPR model (Streamline Technologies, 2016), a fully coupled 2D surface-subsurface modeling framework that incorporates the vadose zone as the linking medium between the surface hydraulics and the water table. Yang & Tsai (2020) investigated the impacts of water table

dynamics on groundwater flooding and levee under seepage to identify potential levee breach locations in New Orleans. Similarly, Mancini et al. (2020) simulated through a 1D-2D hydraulic model (HEC-RAS 2D) the groundwater flooding conditions over an area of reclaimed land in Rome, Italy. Several studies acknowledge the importance of groundwater flooding in South Florida. For example, Nalesso (2009) coupled FLO-2D with MODFLOW-2005 to simulate the bidirectional exchange of flow in wetlands considering the resistant effect of vegetation as an additional soil parameter to better estimate the hydrogeological process. Hughes & White (2016) investigated the effect of pump practices and sea level rise on surface water routing and groundwater interactions in MDC using MODFLOW. Sukop et al. (2018) developed a MODFLOW model that analyzed the current and future response of the water table to precipitation in a portion of the Arch Creek Basin. The study highlighted precipitation as the main trigger for groundwater-induced flooding, with tidal fluctuations and sea level rise increasing the shallow water table.

The aim of this paper is to leverage an established multivariate statistical approach with a loosely coupled hydrodynamic model able to simulate surface-groundwater interaction to potentially yield a more robust estimation of flood hazard, facilitating better urban planning, resilience investments and adaptation strategies. Meeting this aim will require the achievement of three objectives. The first objective is to apply a multivariate statistical analysis to model the joint distribution of precipitation with storm tide and groundwater level in the joint tail regions. A bivariate conditional exceedance sampling - copula-based approach is adopted to calculate the “most-likely” combinations of flood drivers and an ensemble realizations of design events for a 100-year return period. The

second objective is to use a physically-based compound inundation model to investigate the combined effects of pluvial and coastal flooding in the Arch Creek Basin in North Miami based on the most extreme realization from the statistical analysis. The third objective is to incorporate predefined groundwater levels into different combinations of precipitation and surge levels scenarios to compare the contribution and relevance of flooding mechanisms in respect to flood depth, extent, and damage potential. To conclude, a flood damage assessment is presented to estimate the economic impact to the building infrastructure from the above mentioned scenarios through adopting a globally available depth-damage curve dataset.

3.3 Site Description and Data

3.3.1 Study Area

The Arch Creek Basin is an urbanized catchment located in the northeastern boundary of MDC Southeast Florida (Figure 3.1). Surface water flows in a predominantly southerly direction from Lake Okeechobee across the Everglades agricultural and water conservation areas towards Florida's coastlines (Figure 3.1). Upstream flow from the C-8 watershed enters the North Biscayne Bay watershed through the northwest boundary and follows the same direction as the natural flow towards the Arch Creek Basin before discharging into Biscayne Bay (Figure 3.1).

The study site is underlaid by the surficial rock of the Biscayne Aquifer, a highly permeable aquifer composed by the Fort Thompson and Miami Limestone Formations with a maximum thickness of about 38 meters at the Atlantic coastline (Fish and Stewart, 1991; Halley et al., 1977; Hoffmeister et al., 1967; Parker, 1951). The porous limestone landscape

is susceptible to dynamic water influxes in horizontal and vertical directions due to numerous solution conduits, resulting in rapid infiltration and recharge processes (Parker, 1951; Parker and Cooke, 1944). The hydrologic connectivity of the Everglades Water Conservation Areas with the Biscayne Bay watershed is of critical importance to the wetland and aquatic ecosystems, fisheries, and water purification, where the freshwater surface flow moves through canals and structures towards the shore or through underground aquifers (Cunningham and Florea, 2009). Nearly 50% of rainfall that recharges the Biscayne Aquifer discharges to the sea (Klein and Hull, 1978).

3.3.2 Data

Rainfall, tides, and water table level records were collected from official sources near the Arch Creek Basin (Figure 3.2). Localized convection events can cause substantial variation in rainfall totals and groundwater levels at stations located within close proximity of each other. To explore the sensitivity of flood hazard estimates to the choice of rainfall and groundwater levels records from multiple stations are analyzed in this work. A list of gauging stations is presented in Table 4.1.

Daily rainfall totals were collected from the NEXRAD Radar Rainfall Application which provides gridded rainfall data at a 2km x 2km resolution, and from rainfall gauges operated by National Oceanic and Atmospheric Administration (NOAA) National Climatic Data Center (NCDC). NEXRAD Rain Grid cell 10044042 was selected as it is centered on the Arch Creek Basin (Figure 3.2). Rain gauges S27_R and S29_R are selected as they are the closest of the NOAA NCNC's gauges to the Arch Creek Basin.

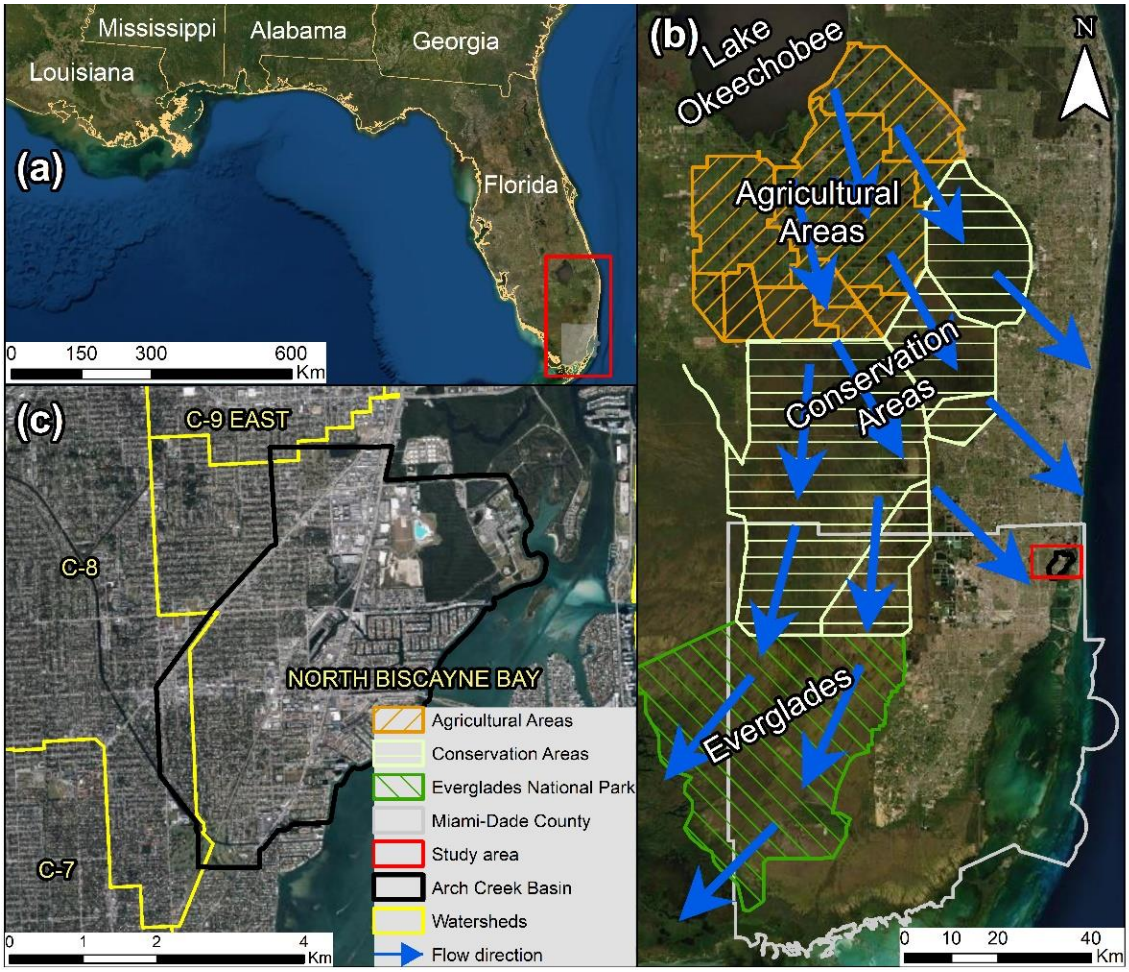

Figure 3.1. Study site location. (a) MDC (grey) located in Southeast Florida, USA (b) current water flow from Lake Okeechobee towards Florida's coastline, and (c) watersheds (yellow) near the study area, being the North Biscayne Bay watershed the most influential to the Arch Creek Basin.

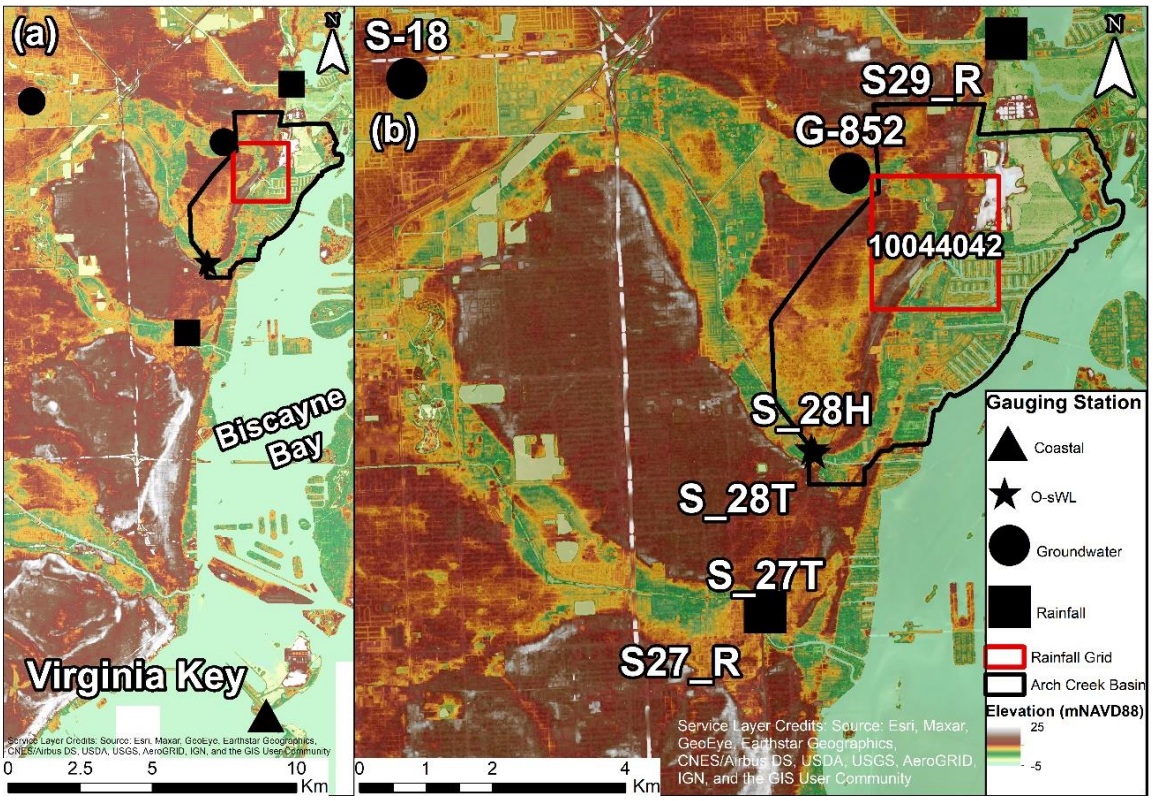

Figure 3.2. Topographic map and distribution of gauge stations closest to the Arch Creek Basin (a-b). The topographic elevations correspond to a LiDAR DEM 2-meter spatial resolution.

Table 3.1. List of gauge stations considered for the statistical analysis

No.	Type	Station Name	Start Date	Source
1	Rainfall	NEXRAD Grid 10044042	1-1-1996	NEXRAD SFWMD
2	Ocean	Virginia Key	1-26-1994	NOAA Tides & Currents
3	Ocean-side Water Level	S28_T	5-31-1985	DBHYDRO
4	Groundwater	G-852	10-1-1973	DBHYDRO
5	Groundwater	S-18	1-1-1955	DBHYDRO
6	Ocean-side Water Level	S27_T	5-31-1985	DBHYDRO
7	Rainfall	S27_R	3-18-1997	DBHYDRO
8	Rainfall	S29_R	3-18-1997	DBHYDRO

Daily maxima of tide levels from the NOAA Tides & Currents website were extracted from the Virginia Key (VK), Biscayne Bay Station (ID #8723214), located 25 km south the study area to characterize the coastal conditions. The VK record starts on 26 January 1994. Similarly, ocean-side water levels from stations S28_T and S27T were extracted from DBHYDRO. S28_T station is the tidal stream structure that forms part of the North Biscayne Bay Basin and is located in the Biscayne Canal Number C-8 on the Arch Creek southern boundary edge, the record starts on 31 May 1985. Station S28_H which located upstream of S28_T will not be considered for the statistical analysis but exclusively for the boundary conditions of the hydrodynamic model. Similarly, station S27_T is located further south in the Little River, providing records of ocean-side water levels from the same period.

The United States Geological Survey (USGS) National Water Information System, in cooperation with the SFWMD is responsible for recording daily summary data of maximum groundwater levels in the South Florida region. The groundwater level time-series data from well G-852 adjacent to the outer western boundary of the study area has recorded daily maximum field observations since 1 October 1973, and 15-minute intervals since October 2007. Similarly, Well S-18, located 3 km west from the study area, is also included in the statistical analysis as it provides 65 years of records.

Considering the proximity of all gauge stations and seldom gaps of missing records, a linear interpolation procedure was applied to infill missing values.

3.4 Methodology

Section 3.4.1 provides a detailed description of the procedure to implement the full statistical analysis of rainfall, tide levels, and groundwater observation records to derive 100-year design events, in which the most extreme combination will be selected for the flood modeling framework. Section 3.4.2 describes the mathematical background of the coupled 2D hydraulic-hydrologic flow models, followed by the modeling set-up to define the digitized domain and boundary conditions. Section 3.4.3 introduces the employment of depth-damage function approaches in different regions to develop damage assessments, ultimately describing a global database that is adjusted to national scale values to forecast expected damage.

3.4.1 Bivariate statistical analysis

A copula C is a multivariate cumulative distribution function CDF with uniform [0,1] marginal probability distributions. Copulas offer more flexibility in the modeling of multivariate distributions than traditional multivariate statistical models. More specifically, copulas allow the dependence structure among two or more variables to be modeled independently of their marginal distributions (Maity, 2018).

For illustrative purposes, let us assume a pair of continuous random variables X and Y with CDFs $F_x(x) = P(X \leq x)$ and $G_y(y) = P(Y \leq y)$, and a joint CDF $H_{x,y}(x,y) = P[X \leq x, Y \leq y]$. Their association in the distribution functions $F_x(x)$, $G_y(y)$, and $H_{x,y}(x,y)$ are contained within the defined unit square interval margins based on the number of variables. For example, in a 2D case, $\boldsymbol{I}^2 = [0,1]^2$ resulting in $F(x_1 x_2) = C(F_1(x_1), F_2(x_2))$. Thus, any pair (X, Y) corresponds to a point $(F_x(x), G_y(y))$ in the unit

dimensional space $\boldsymbol{I} = [0,1] \times [0,1]$, in which the latter ordered pair set a designated number $H_{x,y}(x, y)$ in the $\boldsymbol{I}$ matrix (Grimaldi et al., 2011; Nelsen, 2006).

The fundamental theorem for copulas was first introduced by Sklar (1959), it describes how the copula function constructs a joint CDF by coupling marginal CDFs, and in the bivariate case is given by Eq. 3.1:

$$F(x_1, \dots, x_d) = C(F_1(x_1), \dots, F_d(x_d)) \quad \text{Eq. 3.1}$$

This work adopts the methodology developed by Jane et al. (2020) as a benchmark procedure due to similarities in the scope of the two studies. The copula will only be fit to bivariate extremes, as often relationships between the variables in the joint tails of a distribution can be different from the bulk of the distribution. We adopt the two-sided conditional sampling approach (e.g., Wahl et al. 2015) where an observation is considered as a 'bivariate extreme' if at least one of the variables is in an extreme state i.e., above a high threshold.

Design events are only uniquely defined in the univariate setting. Finding design events in the bivariate and higher dimensional domains requires the specification of a hazard scenario (Salvadori et al., 2016). In the bivariate setting, a fixed probability (or return period) combined with a hazard scenario yields a contour, also referred to as an isoline, containing an infinite set of events with the probability under the specified hazard scenario (Salvadori et al., 2011). There are several hazard scenario definitions, each representing a different underlying probability i.e., set of events associated with a fixed probability (e.g., Salvadori et al., 2016). The hazard scenario should be carefully chosen to

reflect the failure mechanism under investigation, however, their adoption in practice was described by Serinaldi (2015) as "somewhat arbitrary and subjective". This work focuses on flooding caused by simultaneous occurrences of heavy rainfall and either storm tide or elevated groundwater levels, therefore we adopt the "AND" hazard scenario in common with similar recent studies on compound flooding (e.g., Ghanbari et al., 2021; Jane et al., 2020; Moftakhari et al., 2019).

The steps required for the identification of bivariate extreme events of rainfall and either storm tide or groundwater level, using copulas to model the conditional samples and simulate an event with a user-specified return period under the “AND” hazard scenario are explained below:

1) Water level records are detrended. The mean sea level trend is removed using a linear fit. A three-month moving average window is then applied to the linearly detrended series to remove any seasonality. The residuals are then transformed to present-day levels by adding the mean of the most recent five years of observations.
2) The two times series are declustered using a user specified (quantile) threshold and 3-day separation criterion to identify independent cluster maxima.
3) Two-sided conditional sampling is implemented where the declustered excesses of one variable are paired with the co-occurring value of the other variable yielding two conditional samples.
4) The VineCopula R package (Schepsmeier et al., 2018) is used to find the best fitting according to the Akima Information Criterion (AIC) of 40 copula families, plus the ‘independence copula’ to each conditional sample.

5) The conditioned variables are fitted to the Generalized Pareto Distribution (GPD) where the goodness of fit is assessed via probability-probability (pp), quantile-quantile (qq), density and return level plots.
6) Repeat steps 2-5 choosing a quantile threshold that ensures the correlations in the conditional sample and best fitting copula remains stable and a sufficient goodness-of-fit is achieved in the GPD distribution.
7) A range of relevant (i.e., bounded or unbounded) parametric marginal distributions are fit to each non-conditioned variable and the best fitting as determined by the AIC is adopted.
8) The full isoline associated with a user-specified return period is given by the envelope created by overlapping the quantile isolines (with the same return period) obtained from each conditional sample as per Bender et al. (2016).

The single "most-likely" designed event is the event on the isoline associated with the highest probability density given the observed data. An ensemble of design events can be obtained by sampling along the isoline using the (relative) probability density assigned to events on the isoline by the observed data.

3.4.2 Coupled model

3.4.2.1 Description

A loosely-coupled technique interaction approach was applied to combine FLO-2D, and MODFLOW-2005 Groundwater Flow Process (GWF) package input to solve the flood routine and groundwater flow numerical equations separately by exchanging information in an iterative matter (Santiago-Collazo et al., 2019). FLO-2D (O'Brien et al.,

1993) is a quasi-2D hydraulic model based on flood volume conservation and hydraulic routing scheme simulating channel–floodplain exchange, flood wave attenuation, and the alteration of inundation dynamics due to artificial obstructions (levees, buildings, streets, etc.) on a gridded topographic surface. MODFLOW simulates groundwater flow in aquifer layers (confined or unconfined) using a block-centered finite-difference approach (Harbaugh, 2005) based on Darcy's Law. The loosely-coupled surface-subsurface water model can simulate the exchange of flow in opposite directions, as groundwater recharge or groundwater return flow depending on the infiltration capacity and water table levels.

The main factors determining the coupling compatibility process between FLO-2D and MODFLOW-2005 include the algorithms' mathematical solver compatibility to calculate and transfer the exchanged volumes in opposite directions and share consistent spatial and temporal scales. A perfect overlap between FLO-2D and MODFLOW-2005 spatial (domain, coordinate system, grid resolution, and topography) and temporal scales (time units) is necessary for the coupled model to transfer the output data in a synchronized systematic manner (Figure 4.3). A more detailed description of the coupling process is provided in Peña et al., 2021.

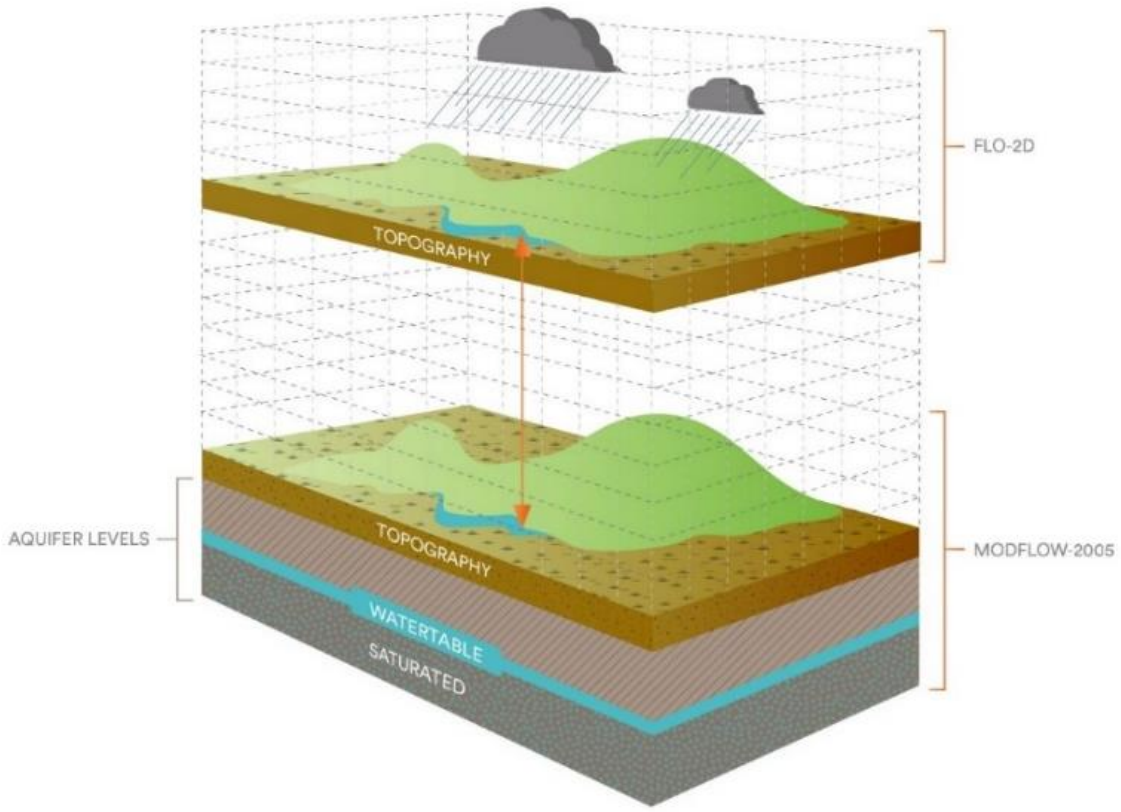

Figure 3.3. Spatial compatibility between FLO-2D and MODFLOW-2005

3.4.2.2 Configuration

The Arch Creek Basin is represented by a grid square mesh of 20-meter resolution with a total of 42,621 cells in the discretized domain from a LiDAR DEM 2-meter spatial resolution. The boundary conditions represent the hydrologic forcing input in FLO-2D and MODFLOW-2005. The rainfall distribution, which is uniform on every FLO-2D grid element, denotes a short-duration high intensity behavior. The Biscayne Bay's coastal boundary conditions are represented on the easternmost side of the FLO-2D and MODFLOW-2005 domains, while the groundwater boundary conditions are represented at the westernmost side of the domain in MODFLOW-2005. Two regional groundwater

models that characterize the complex hydrogeomorphology and subsurface hydraulics of MDC and a portion of the Arch Creek Basin respectively (Hughes and White, 2016; Sukop et al., 2018) were used as reference to build a simplified MODFLOW-2005 model.

The Green-Ampt infiltration method was selected to account for the infiltration process in FLO-2D and transfer the infiltrated volume as recharge to MODFLOW-2005. The FLO-2D soil infiltration properties exemplify the very high hydraulic conductivity of the porous permeable soil. The infiltration depth parameter determines the storage limit between the ground surface and the water table (≈ 2 meters). To simplify the model set-up some assumptions were made. A 0.40 Manning roughness coefficient was used for green areas and 0.04 for the urbanized impervious surface, canal bed, and Biscayne coast. A total of 7827 building features were imported into the FLO-2D domain as completely blocked grid elements preventing potential water interactions.

With respect to the canals and ocean floor bathymetry, most of this information is not available due to lack of data and jurisdiction restrictions. As a result, a uniform 10-meter bottom elevation was considered for the Biscayne coast and canals to replicate the constant depth of the Intracoastal Topography database located at the northern boundary of the study site. Canals features, streets and hydraulic structures were not considered in this study.

3.4.2.3 Flood damage assessment

The quantification of flood damage is a crucial element for flood risk management practices, urban planning, decision-making, insurance policies and the world economy (Dobrovičová et al., 2015; Smith, 1994). The financial impact of urban flood risk is

commonly assessed by flood depth-damage functions to estimate the tangible direct damage to exposed infrastructure and assets based on maximum flooding water levels. Approaches on estimating flood risk damage potential vary in terms of scale and level of uncertainty, ranging from calibrated depth-damage curves using historical data (Freni et al., 2010) to potential flood damage based on land-use at the national level (De Moel et al., 2011) and global scale (Jongman et al., 2012).

Regarding MDC, different methodologies have been applied to estimate potential economic losses from flooding using quantitative local data. McAlpine and Porter (2018) calculated the economic cost of current and future inundation scenarios on property values through the combination of hydrological, topographic, and local sea level rise projections. Similarly, Ghanbari et al. (2020) applied the HAZUS-MH coastal model and loss estimation tool (Scawthorn et al., 2006) to quantify the average annual losses from the combination of extreme and nonextreme flood events with flooding thresholds and sea level rise scenarios. Keenan et al. (2018) evaluated the influence of topographic elevation on long-term market price appreciation for residential properties by jurisdiction, as rates are highly influenced by the threat of potential flooding.

In the present study, we apply the global flood depth-damage functions developed by the Joint Research Centre (Huizinga et al., 2017) to calculate the flood damage assessment for the Arch Creek Basin. The database provides maximum damage values with respect to damage class (residential buildings, commercial buildings, industrial buildings, and agriculture) and flood depth at the country and continent level. Note that all data pertaining to the US are based on the HAZUS-MH model, and economic values were

transformed to the current exchange rate (1€ = $0.84). An object-based approach was used to calculate direct flood damage statistics from the building features in the study area.

3.5 Results and Discussion

In this section, results from the multivariate statistical – hydrodynamic modeling frameworks are presented. 3.5.1 is dedicated to the multivariate statistical analysis of selected rainfall, tides, and groundwater sites nearby the Arch Creek Basin. 3.5.2 is focused on the simulation results, providing a graphical representation of the compound flooding conditions based on selected events determined by the copula statistical analysis to simulate the most extreme joint probability isoline. In addition, a flood damage assessment presents the economic losses of selected events under predefined groundwater levels.

3.5.1 Multivariate statistical analysis

The 100-year design events is presented in **Figure 3.4**. Results show that design events are present in most rainfall gauge – storm tide or groundwater combinations with different degrees of magnitude. For instance, for VK, the 100-year most likely design event given by S29_R is more severe in terms of storm tide than NEXRAD and S27_R. Despite marginal rainfall most severe at S29, for the VK combination the most likely design event in terms of rainfall is when the S27 record is adopted. Isoline S27_R for instance the curve contains the most events with storm tide greater than 0.5m and rainfall greater than 200mm.

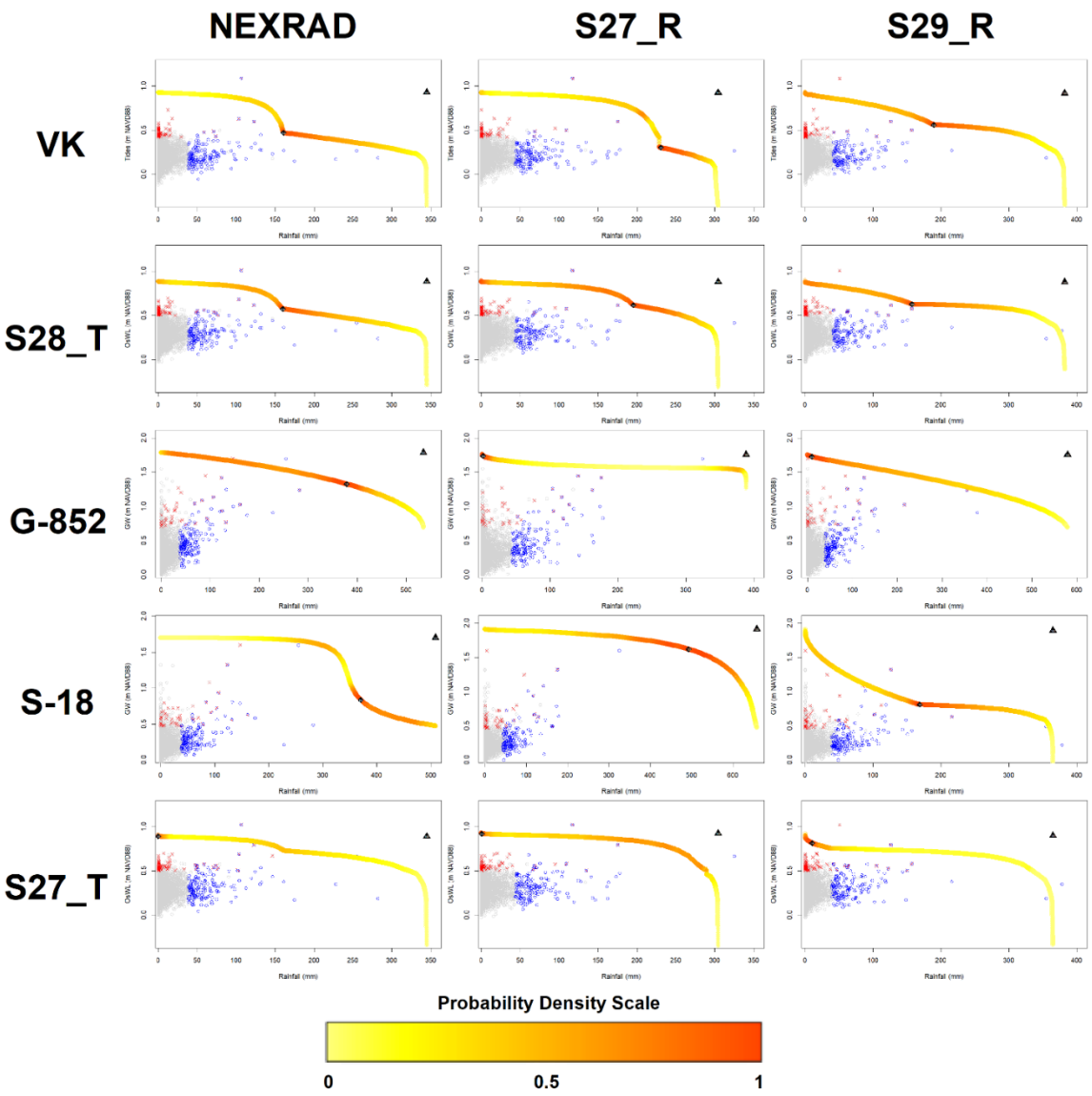

Figure 3.4. Comparison of 100-year isolines obtained using the two-sided sampling approach for different combinations of rainfall, tides, and groundwater gauge stations. The colored contour signifies the likelihood of events on the isoline implied by the observations. The plot displays observations (grey) including those that exceed specific thresholds for rainfall (blue), tides and groundwater levels (red) along with the "most likely" (diamond) and full dependence (triangle) design events.

The design events given by G-852 (c) and S-18 (d) show contrasting dependency and change in behavior between variables in all three scenarios. Based on NEXRAD, the design events are more dependent on rainfall amounts than groundwater levels. Regarding S27_R and S29R, there is a lack of statistical dependence with G-852, as the design events remain close to the maximum water table levels, while the disparity between the isoline and full dependence design event is greatest for the S27_R - S-18 and S29_R – S-18, reflecting that these rainfall gauges are located far and downstream of the groundwater well.

From all possible combinations between rainfall and tides, the most extreme behavior was captured by stations S29_R and S28_T (**Figure 3.5**). The design and four ensemble events from the generated quantile isoline were extracted to be used as input for the model boundary conditions. The hydrologic conditions were adjusted based on the Tropical Storm Andrea timeseries (6-8 June 2013), characterized by a short-duration extreme precipitation, constant tide levels and unusually high antecedent groundwater levels that experienced a sudden increase right after the peak rainfall intensity, resulting in a groundwater induced flooding event in the study area (Peña et al., 2021).

In respect to the rainfall and groundwater joint probabilities, all copulas present a spatial homogeneity on water table levels (0.5 – 2.0 meters), being S-18 and S27_R the combination that exhibits the most extreme behavior. Based on a pragmatic approach, six water table thresholds (0.0, 1.0, 1.5, 2.0, 2.5, and 3.0 meters) are proposed as predefined groundwater conditions to simulate the compound effects of the selected ensemble

realizations for the S29_R and S28_T isoline. The idea is to select water table levels closer to the surface to validate the assumption that higher water table influence flood risk.

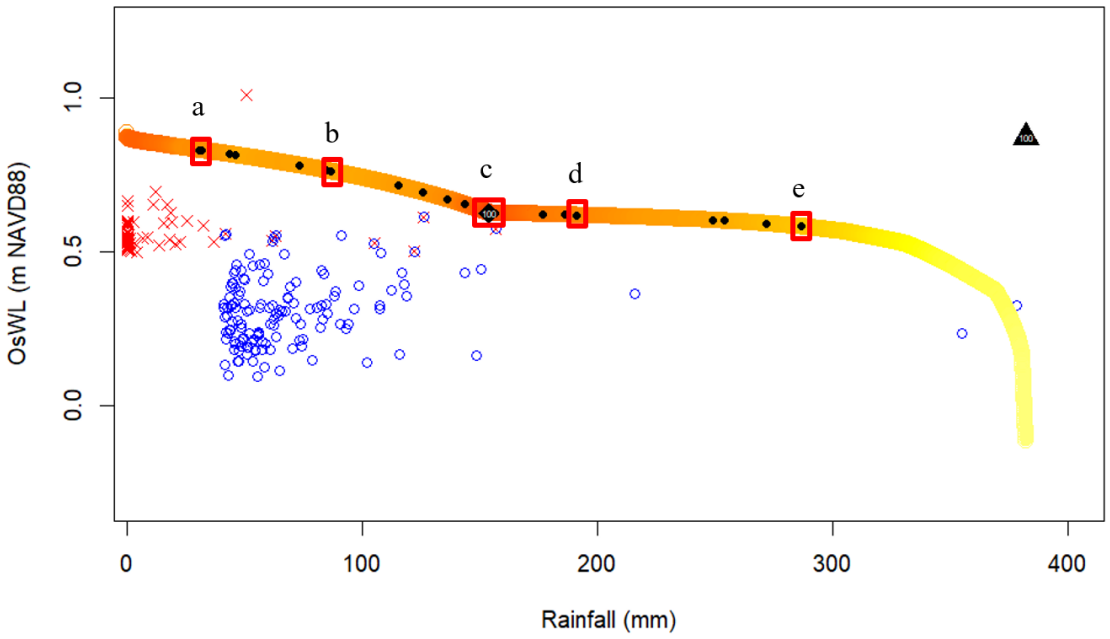

Figure 3.5. Quantile isoline for a 100-year return period between rainfall and Ocean-side Water Level at sites S29_R and S28_T, containing the design (black diamond), ensemble (black dots) and selected events (red squares) to set-up the modeling boundary conditions.

3.5.2 Physically-based coupled model

Sensitivity to composite pluvial, coastal and groundwater flooding events was explored by applying different combinations of hydrological forcing variables to assess the compound inundation impacts of extreme scenarios. Five selected events from the copula isoline were tested using six groundwater threshold levels. The inundation maps (**Figure 3.6**) suggest that the Arch Creek Basin is more vulnerable to short-duration heavy precipitation resulting in flash floods events compared to tidal flooding conditions.

Although the effect of tidal flooding is relatively low, high tide stages have a direct impact on the canals flow, representing a localized hazard to coastal and waterfront properties.

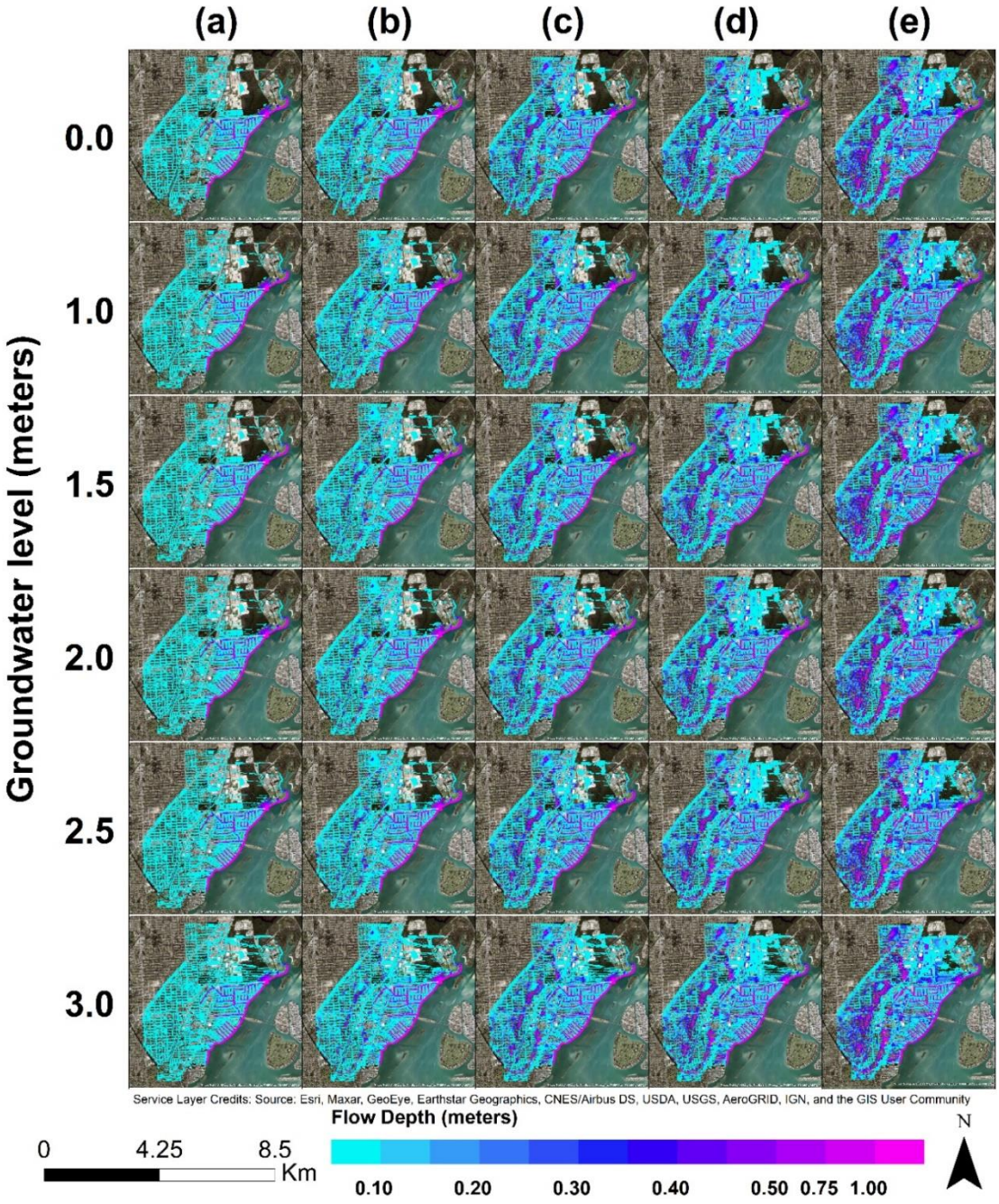

Figure 3.6. Simulated compound flooding scenarios from the interaction of precipitation, coastal surge, and predefined water table levels.

Flooding stages are directly correlated with the progressive increase in precipitation, as the surface runoff is either absorbed into the green permeable spaces or is accumulated above impervious surfaces. The shallow infiltration depth plays an important role in the system flood dynamics as the flooded area increased once the maximum infiltration capacity is exceeded (**Table 2.2**).

Table 3.2. Percentage of flood-influenced areas based on different compound scenarios

Water table (meters)	% Flooded area				
	a	b	c	d	e
0	44.0	53.3	55.4	59.9	63.6
1	47.7	55.6	57.3	61.4	65.0
1.5	48.0	55.8	57.7	61.7	65.2
2	48.5	56.1	58.0	62.0	65.4
2.5	49.6	56.8	58.7	62.5	66.0
3	53.9	60.2	62.0	64.7	67.9

The contrast in behavior between combinations of low precipitation – high tides and high precipitation – low tides reflect the susceptibility of the urban environment to pluvial flooding, as it is not directly affected by storm surge events since it is protected by the Surfside, North Beach, and Bay Harbor Islands. In addition, the Keystone Island and Sans Souci canals act as ‘buffer’ zones, mitigating the impact of waves to extend inland with a fraction of the Arch Creek Basin building infrastructure facing the coast.

As expected, when the groundwater component is considered the surface-groundwater exchange also increases the flood inundation extent. Although higher water table levels may not necessarily reach the surface, the increase in threshold resulted in the

expansion of inundation depth and extent across the study area affecting the overall surface flooding conditions.

The economic damage assessment of the presented flood combinations is showed in **Table 2.3**. The total damage is slight underestimated when the groundwater component is not considered in the modeling framework. Based on a conservative approach, it should be noted that most of the 75% of the 7827 buildings in the Arch Creek Basin experience minor (< 0.5 meters) to moderate (0.5 – 1.0 meters) flooding with isolated cases of major flood damage above 1 meter. Although higher water table thresholds do not represent an increase in the number of damaged properties, it does exacerbate the overall impact. Residential properties in the Arch Creek Basin are mostly affected by the increase in the water table where most of the urbanized environment has a land elevation below 2.0 meters (Miami-Dade, 2016; Peña et al., 2021).

Although the presented simulations balance spatial resolution (20 m resolution) with computational performance (≈ 30 minutes per simulation), city-scale flood models benefit from higher mesh resolutions which improve the accuracy of localized flood inundation depth and extent, in particular the flood propagation dynamics on streets and green areas. Further studies should consider the storm drain infrastructure (drainage wells and French drains) and pump stations in the simulation, as both features improve flood control and alleviate the impacts of flooding in flat low-elevation areas.

Table 3.3. Estimated compound flooding damage potential from the interaction of precipitation, coastal surge, and predefined water table levels for residential, commercial, and industrial buildings

Water table (meters)	Category	a		b		c		d		e	
		# Buildings	Total Damage (Million)	# Buildings	Total Damage (Million)	# Buildings	Total Damage (Million)	# Buildings	Total Damage (Million)	# Buildings	Total Damage (Million)
0	Residential	5003	$29.598	5003	$29.761	5003	$30.339	5004	$31.078	5005	$33.078
	Commercial	880	$0.480	887	$0.509	887	$0.548	888	$0.613	888	$0.755
	Industrial	2	$0.002	20	$0.015	36	$0.027	38	$0.029	47	$0.053
	Total	5885	$30.079	5910	$30.285	5926	$30.914	5930	$31.720	5940	$33.886
1	Residential	5003	$29.598	5003	$29.754	5003	$30.451	5004	$31.191	5005	$33.244
	Commercial	881	$0.480	888	$0.510	888	$0.555	889	$0.614	889	$0.762
	Industrial	2	$0.002	20	$0.015	36	$0.027	39	$0.029	47	$0.053
	Total	5886	$30.080	5911	$30.279	5927	$31.033	5932	$31.834	5941	$34.059
1.5	Residential	5003	$29.598	5003	$29.761	5003	$30.494	5004	$31.205	5005	$33.315
	Commercial	881	$0.480	888	$0.510	888	$0.561	889	$0.626	889	$0.762
	Industrial	2	$0.002	20	$0.015	36	$0.027	39	$0.029	47	$0.053
	Total	5886	$30.080	5911	$30.286	5927	$31.082	5932	$31.861	5941	$34.130
2	Residential	5003	$29.598	5003	$29.761	5003	$30.543	5004	$31.237	5005	$33.364
	Commercial	881	$0.480	888	$0.510	888	$0.561	889	$0.626	889	$0.762
	Industrial	2	$0.002	20	$0.015	36	$0.027	39	$0.029	47	$0.053
	Total	5886	$30.080	5911	$30.286	5927	$31.132	5932	$31.893	5941	$34.179
2.5	Residential	5005	$29.610	5005	$29.773	5004	$30.563	5004	$31.237	5005	$33.407
	Commercial	881	$0.480	888	$0.510	888	$0.568	889	$0.626	889	$0.792
	Industrial	2	$0.002	20	$0.015	36	$0.027	40	$0.030	47	$0.053
	Total	5888	$30.091	5913	$30.298	5928	$31.158	5933	$31.894	5941	$34.251
3	Residential	5005	$29.610	5005	$29.787	5005	$30.569	5005	$31.290	5005	$33.453
	Commercial	882	$0.481	888	$0.510	888	$0.568	889	$0.626	889	$0.792
	Industrial	2	$0.002	20	$0.015	36	$0.027	40	$0.030	47	$0.053
	Total	5889	$30.092	5913	$30.312	5929	$31.164	5934	$31.946	5941	$34.297

3.6 Conclusions

In this work, we proposed the linkage of multivariate statistical – hydrodynamic modeling frameworks to map potential compound flooding scenarios in the Arch Creek Basin in North Miami. Copulas served to assess the statistical correlation between precipitation, tide levels and water table records by producing overlapped quantile isolines of "most likely" design events under a full dependence assumption A loosely-coupled physically-based 2D hydraulic model (FLO-2D and MODFLOW-2005) was used to simulate different combinations of flood drivers with predefined groundwater levels to characterize their relevance and impact in terms of inundation depth and extent.

Predictions suggest that "most likely" design events do not produce most inundation of the events on an isoline, hence it is advantageous to use an ensemble of design events to evaluate the inundation potential. Groundwater levels must be accounted for to robustly estimate flood risk in the Arch Creek Basin. Lowland and bayfront locations are particularly vulnerable to compound flood risks and will require significant adaptation strategies to cope with the extreme nature of these events. For instance, the combination of structural measures (i.e., pump stations, flood gates, raising roads), nature-based solutions (i.e., flood parks, hybrid green-recreation spaces, ecological restoration) and regulations (i.e., home buyout programs, building codes) could help reduce the effects of flooding.

Nearby in situ hydrologic forcing records can substantially change the shape of the isolines in turn the design events. As a result, the analysis of different combinations may provide insights on the selection of statistical output to simulate conditions from a conservative perspective. The significance of estimating potential monetary losses due to

compound flooding scenarios is of paramount importance to urban planners, decision makers and local officials for designing smart strategies to build a more resilient community that can withstand and bounce back from future flood events.

The consolidation of both methodologies into an integrated approach represents a solid step to establish a holistic flood risk assessment framework. Climate change is expected to amplify the effects of rainfall events, storm surge, and tides as potential sources of flooding in MDC (Obeysekera et al., 2019, 2011) as well as compound flooding events (Wahl et al., 2015) increasing the gradual inundation process of anthropogenic and natural systems (Zhang, 2011). Further research should consider climate and sea level rise projections to evaluate future flood risks.

3.7 References

Abboud, J.M., Ryan, M.C., Osborn, G.D., 2018. Groundwater flooding in a river-connected alluvial aquifer. J. Flood Risk Manag. 11, 1–11. https://doi.org/10.1111/jfr3.12334

Bates, P.D., Quinn, N., Sampson, C., Smith, A., Wing, O., Sosa, J., Savage, J., Olcese, G., Neal, J., Schumann, G., Giustarini, L., Coxon, G., Porter, J.R., Amodeo, M.F., Chu, Z., Lewis-Gruss, S., Freeman, N.B., Houser, T., Delgado, M., Hamidi, A., Bolliger, I., McCusker, K., Emanuel, K., Ferreira, C.M., Khalid, A., Haigh, I.D., Couasnon, A., Kopp, R., Hsiang, S., Krajewski, W.F., 2021. Combined Modeling of US Fluvial, Pluvial, and Coastal Flood Hazard Under Current and Future Climates. Water Resour. Res. 57, 1–29. https://doi.org/10.1029/2020wr028673

Bender, J., Wahl, T., Müller, A., Jensen, J., 2016. A multivariate design framework for river confluences. Hydrol. Sci. J. 61, 471–482. https://doi.org/10.1080/02626667.2015.1052816

Bevacqua, E., Maraun, D., Hobæk Haff, I., Widmann, M., Vrac, M., 2017. Multivariate statistical modelling of compound events via pair-copula constructions: Analysis of floods in Ravenna (Italy). Hydrol. Earth Syst. Sci. 21, 2701–2723. https://doi.org/10.5194/hess-21-2701-2017

Bilskie, M. V., Hagen, S.C., 2018. Defining Flood Zone Transitions in Low-Gradient

Coastal Regions. Geophys. Res. Lett. 45, 2761–2770. https://doi.org/10.1002/2018GL077524

Cantafio, L.J., Ryan, M.C., 2014. Quantification du débit de base et des impacts sur la qualité de l'eau imputables à l'aquifère alluvial à prédominance graveleuse, dans la section urbaine d'une grande rivière canadienne. Hydrogeol. J. 22, 957–970. https://doi.org/10.1007/s10040-013-1088-7

Cobby, D., Morris, S., Parkes, A., Robinson, V., 2009. Groundwater flood risk management: Advances towards meeting the requirements of the EU floods directive. J. Flood Risk Manag. 2, 111–119. https://doi.org/10.1111/j.1753-318X.2009.01025.x

Couasnon, A., Eilander, D., Muis, S., Veldkamp, T.I.E., Haigh, I.D., Wahl, T., Winsemius, H.C., Ward, P.J., 2020. Measuring compound flood potential from river discharge and storm surge extremes at the global scale. Nat. Hazards Earth Syst. Sci. 20, 489–504. https://doi.org/10.5194/nhess-20-489-2020

Couasnon, A., Sebastian, A., Morales-Nápoles, O., 2018. A Copula-based bayesian network for modeling compound flood hazard from riverine and coastal interactions at the catchment scale: An application to the houston ship channel, Texas. Water (Switzerland) 10. https://doi.org/10.3390/w10091190

Cunningham, K.J., Florea, L.J., 2009. The Biscayne Aquifer of Southeastern Florida The Biscayne Aquifer of Southeastern Florida 196–199.

Czajkowski, J., Engel, V., Martinez, C., Mirchi, A., Watkins, D., Sukop, M.C., Hughes, J.D., 2018. Economic impacts of urban flooding in South Florida: Potential consequences of managing groundwater to prevent salt water intrusion. Sci. Total Environ. 621, 465–478. https://doi.org/10.1016/j.scitotenv.2017.10.251

De Moel, H., Aerts, J.C.J.H., Koomen, E., 2011. Development of flood exposure in the Netherlands during the 20th and 21st century. Glob. Environ. Chang. 21, 620–627. https://doi.org/10.1016/j.gloenvcha.2010.12.005

Dobrovičová, S., Dobrovič, R., Dobrovič, J., 2015. The Economic Impact of Floods and their Importance in Different Regions of the World with Emphasis on Europe. Procedia Econ. Financ. 34, 649–655. https://doi.org/10.1016/s2212-5671(15)01681-0

Eilander, D., Couasnon, A., Ikeuchi, H., Muis, S., Yamazaki, D., Winsemius, H.C., Ward, P.J., 2020. The effect of surge on riverine flood hazard and impact in deltas globally. Environ. Res. Lett. 15. https://doi.org/10.1088/1748-9326/ab8ca6

Fish, J.E., Stewart, M.T., 1991. Hydrogeology of the surficial aquifer system, Dade

County, Florida, Water-Resources Investigations Report. https://doi.org/10.3133/wri904108

Freni, G., La Loggia, G., Notaro, V., 2010. Uncertainty in urban flood damage assessment due to urban drainage modelling and depth-damage curve estimation. Water Sci. Technol. 61, 2979–2993. https://doi.org/10.2166/wst.2010.177

Genest, C., Favre, A.C., 2007. Everything You Always Wanted to Know about Copula Modeling but Were Afraid to Ask. J. Hydrol. Eng. 12, 347–368. https://doi.org/10.1061/(ASCE)1084-0699(2007)12:4(347)

Ghanbari, M., Arabi, M., Kao, S.C., Obeysekera, J., Sweet, W., 2021. Climate Change and Changes in Compound Coastal-Riverine Flooding Hazard Along the U.S. Coasts. Earth's Futur. 9, 1–17. https://doi.org/10.1029/2021EF002055

Ghanbari, M., Arabi, M., Obeysekera, J., 2020. Chronic and Acute Coastal Flood Risks to Assets and Communities in Southeast Florida. J. Water Resour. Plan. Manag. 146, 04020049. https://doi.org/10.1061/(asce)wr.1943-5452.0001245

Grimaldi, S., Kao, S.C., Castellarin, A., Papalexiou, S.M., Viglione, A., Laio, F., Aksoy, H., Gedikli, A., 2011. Statistical Hydrology, Treatise on Water Science. https://doi.org/10.1016/B978-0-444-53199-5.00046-4

Guinn Garrett, C., Vulava, V.M., Callahan, T.J., Jones, M.L., 2012. Groundwater-surface water interactions in a lowland watershed: Source contribution to stream flow. Hydrol. Process. 26, 3195–3206. https://doi.org/10.1002/hyp.8257

Gutiérrez, F., Parise, M., De Waele, J., Jourde, H., 2014. A review on natural and human-induced geohazards and impacts in karst. Earth-Science Rev. 138, 61–88. https://doi.org/10.1016/j.earscirev.2014.08.002

Halley, R.B., Shinn, E.A., Hudson, J.H., Lidz, B.H., 1977. Pleistocene barrier bar seaward of ooid shoal complex near Miami, Florida. Am. Assoc. Pet. Geol. Bull. 61, 519–526.

Hanson, S., Nicholls, R., Ranger, N., Hallegatte, S., Corfee-Morlot, J., Herweijer, C., Chateau, J., 2011. A global ranking of port cities with high exposure to climate extremes. Clim. Change 104, 89–111. https://doi.org/10.1007/s10584-010-9977-4

Harbaugh, A.W., 2005. MODFLOW-2005 : the U.S. Geological Survey modular ground-water model--the ground-water flow process, Techniques and Methods. https://doi.org/10.3133/tm6A16

Hardt, W.F., Hutchinson, C.B., 1978. Model aids planners in predicting rising ground-water levels in San Bernardino, California. Groundwater 16, 424–431.

https://doi.org/10.1111/j.1745-6584.1978.tb03257.x

Hoffmeister, J.E., Stockman, K.W., Multer, H.G., 1967. Miami Limestone of Florida and Its Recent Bahamian Counterpart. GSA Bull. 78, 175–190. https://doi.org/10.1130/0016-7606(1967)78[175:MLOFAI]2.0.CO;2

Hughes, J.D., White, J.T., 2016. Hydrologic conditions in urban Miami-Dade County, Florida, and the effect of groundwater pumpage and increased sea level on canal leakage and regional groundwater flow. U.S. Geol. Surv. 175.

Huizinga, J., Moel, H. De, Szewczyk, W., 2017. Global flood depth-damage functions: Methodology and the database with guidelines, EUR 28552. ed. Publications Office of the European Union, Luxembourg. https://doi.org/10.2760/16510

Jane, R., Cadavid, L., Obeysekera, J., Wahl, T., 2020. Multivariate statistical modelling of the drivers of compound flood events in south Florida. Nat. Hazards Earth Syst. Sci. 20, 2681–2699. https://doi.org/10.5194/nhess-20-2681-2020

Jongman, B., Ward, P.J., Aerts, J.C.J.H., 2012. Global exposure to river and coastal flooding : Long term trends and changes. Glob. Environ. Chang. 22, 823–835. https://doi.org/10.1016/j.gloenvcha.2012.07.004

Keenan, J.M., Hill, T., Gumber, A., 2018. Climate gentrification: From theory to empiricism in Miami-Dade County, Florida. Environ. Res. Lett. 13. https://doi.org/10.1088/1748-9326/aabb32

Klein, H., Hull, J.E., 1978. Biscayne aquifer, southeast Florida, Water-Resources Investigations Report. https://doi.org/10.3133/wri78107

Kozlowski, T.T., Pallardy, S.G., 1984. CHAPTER 5 - Effect of Flooding on Water, Carbohydrate, and Mineral Relations, in: KOZLOWSKI, T.T.B.T.-F. and P.G. (Ed.), Physiological Ecology. Academic Press, San Diego, pp. 165–193. https://doi.org/https://doi.org/10.1016/B978-0-12-424120-6.50010-9

Kumbier, K., Carvalho, R.C., Vafeidis, A.T., Woodroffe, C.D., 2018. Investigating compound flooding in an estuary using hydrodynamic modelling: A case study from the Shoalhaven River, Australia. Nat. Hazards Earth Syst. Sci. 18, 463–477. https://doi.org/10.5194/nhess-18-463-2018

Larkin, R.G., Sharp Jr., J.M., 1992. On the relationship between river-basin geomorphology, aquifer hydraulics, and ground-water flow direction in alluvial aquifers. GSA Bull. 104, 1608–1620. https://doi.org/10.1130/0016-7606(1992)104<1608:OTRBRB>2.3.CO;2

Leonard, M., Westra, S., Phatak, A., Lambert, M., van den Hurk, B., Mcinnes, K.,

Risbey, J., Schuster, S., Jakob, D., Stafford-Smith, M., 2014. A compound event framework for understanding extreme impacts. Wiley Interdiscip. Rev. Clim. Chang. 5, 113–128. https://doi.org/10.1002/wcc.252

Leopold, L.B., Huppman, R., Miller, A., 2005. Geomorphic effects of urbanization in forty-one years of observation. Proc. Am. Philos. Soc. 149, 349–371.

Macdonald, D., Bloomfield, J., Hughes, A., MacDonald, A., Adams, B., McKenzie, A., 2008. Improving the understanding of the risk from groundwater flooding in the UK. Flood Risk Manag. Res. Pract. 1071–1080. https://doi.org/10.1201/9780203883020.ch125

Maity, R., 2018. Statistical Methods in Hydrology and Hydroclimatology. https://doi.org/10.1007/978-981-10-8779-0

Mancini, C.P., Lollai, S., Volpi, E., Fiori, A., 2020. Flood modeling and groundwater flooding in urbanized reclamation areas: The case of Rome (Italy). Water (Switzerland) 12. https://doi.org/10.3390/w12072030

Martinotti, M.E., Pisano, L., Marchesini, I., Rossi, M., Peruccacci, S., Brunetti, M.T., Melillo, M., Amoruso, G., Loiacono, P., Vennari, C., Vessia, G., Trabace, M., Parise, M., Guzzetti, F., 2017. Landslides, floods and sinkholes in a karst environment: The 1-6 September 2014 Gargano event, southern Italy. Nat. Hazards Earth Syst. Sci. 17, 467–480. https://doi.org/10.5194/nhess-17-467-2017

McAlpine, S.A., Porter, J.R., 2018. Estimating Recent Local Impacts of Sea-Level Rise on Current Real-Estate Losses: A Housing Market Case Study in Miami-Dade, Florida. Popul. Res. Policy Rev. 37, 871–895. https://doi.org/10.1007/s11113-018-9473-5

Miami-Dade, 2016. Arch Creek Study Area, Miami-Dade County, Florida; Briefing Book for ULI Advisory Services Panel, May 22-27 2016.

Moftakhari, H., Salvadori, G., AghaKouchak, A., Sanders, B.F., Matthew, R.A., 2017. Compounding effects of sea level rise and fluvial flooding. Proc. Natl. Acad. Sci. U. S. A. 114, 9785–9790. https://doi.org/10.1073/pnas.1620325114

Moftakhari, H., Schubert, J.E., AghaKouchak, A., Matthew, R.A., Sanders, B.F., 2019. Linking statistical and hydrodynamic modeling for compound flood hazard assessment in tidal channels and estuaries. Adv. Water Resour. 128, 28–38. https://doi.org/10.1016/j.advwatres.2019.04.009

Muñoz, D.F., Moftakhari, H., Moradkhani, H., 2020. Compound Effects of Flood Drivers and Wetland Elevation Correction on Coastal Flood Hazard Assessment. Water Resour. Res. 56, 1–21. https://doi.org/10.1029/2020WR027544

Nalesso, M., 2009. Integrated surface-ground water modeling in wetlands with improved methods to simulate vegetative resistance to flow. ProQuest ETD Collect. FIU.

Nasr, A.A., Wahl, T., Rashid, M.M., Camus, P., Haigh, I.D., 2021. Assessing the dependence structure between oceanographic, fluvial, and pluvial flooding drivers along the United States coastline. Hydrol. Earth Syst. Sci. Discuss. 2021, 1–31. https://doi.org/10.5194/hess-2021-268

Naughton, O., Mccormack, T., Gill, L., Johnston, P., 2018. Groundwater flood hazards and mechanisms in lowland karst terrains. Geol. Soc. Spec. Publ. 466, 397–410. https://doi.org/10.1144/SP466.9

Nelsen, R., 2006. An Introduction to Copulas, Second. ed. Springer Science+Business Media, Inc., New York, USA. https://doi.org/10.2307/1271100

NOAA, 2021. Storm events database [WWW Document]. URL https://www.ncdc.noaa.gov/stormevents/ (accessed 3.29.21).

O'Brien, J.S., Julien, P.Y., Fullerton, W.T., 1993. Two-dimensional water flood and mudflow simulation. Hydrol. Eng. 244–261.

Obeysekera, J., Irizarry, M., Park, J., Barnes, J., Dessalegne, T., 2011. Climate change and its implications for water resources management in south Florida. Stoch. Environ. Res. Risk Assess. 25, 495–516. https://doi.org/10.1007/s00477-010-0418-8

Obeysekera, J., Sukop, M., Troxler, T., Irizarry, M., Rogers, M., 2019. Potential Implications of Sea-Level Rise and Changing Rainfall for Communities in Florida using Miami-Dade County as a Case Study. Miami FL.

OECD, 2007. Ranking port cities with high exposure and vulnerability to climate extremes: exposure estimates. Environment 1, 53–57. https://doi.org/10.1787/011766488208

Olbert, A.I., Comer, J., Nash, S., Hartnett, M., 2017. High-resolution multi-scale modelling of coastal flooding due to tides, storm surges and rivers inflows. A Cork City example. Coast. Eng. 121, 278–296. https://doi.org/10.1016/j.coastaleng.2016.12.006

Parker, G.G., 1951. Geologic and Hydrologic Factors in the Perennial Yield of the Biscayne Aquifer. J. AWWA 43, 817–834. https://doi.org/https://doi.org/10.1002/j.1551-8833.1951.tb19032.x

Parker, G.G., Cooke, C.W., 1944. Late Cenozoic Geology of Southern Florida with a Discussion of the Ground Water. U.S. Geol. Surv.

Pellenbarg, N.P., 1989. Groundwater management in the Netherlands: Background and legislation groundwater in the Netherlands. Groundw. Manag. Shar. Responsib. an open access Resour. pp137-149.

Peña, F., Nardi, F., Melesse, A., Obeysekera, J., Castelli, F., Price, R.M., Crowl, T., Gonzalez-Ramirez, N., 2021. Compound flood modelling framework for rainfall-groundwater interactions. Nat. Hazards Earth Syst. Sci. Discuss. 2021, 1–38. https://doi.org/10.5194/nhess-2021-259

Price, R., Schwartz, K., Anderson, B., Boucek, R., Briceño, H., Cook, M., Fitz, C., Onsted, J., Rehage, J., Rivera-Monroy, V., Roy Chowdhury, R., Saha, A., 2020. Chapter 3: Water, Sustainability, and Survival, in Childers, D.L., E.E. Gaiser and L.A. Ogden (eds.) The Coastal Everglades: The Dynamics of Social-Ecological Transformation in the South Florida Landscape. Oxford University Press : New York, New York.

Saksena, S., Merwade, V., Singhofen, P.J., 2019. Flood inundation modeling and mapping by integrating surface and subsurface hydrology with river hydrodynamics. J. Hydrol. 575, 1155–1177. https://doi.org/10.1016/j.jhydrol.2019.06.024

Saleh, F., Ramaswamy, V., Wang, Y., Georgas, N., Blumberg, A., Pullen, J., 2017. A multi-scale ensemble-based framework for forecasting compound coastal-riverine flooding: The Hackensack-Passaic watershed and Newark Bay. Adv. Water Resour. 110, 371–386. https://doi.org/10.1016/j.advwatres.2017.10.026

Salvadori, G., De Michele, C., Durante, F., 2011. On the return period and design in a multivariate framework. Hydrol. Earth Syst. Sci. 15, 3293–3305. https://doi.org/10.5194/hess-15-3293-2011

Salvadori, G., Durante, F., De Michele, C., Bernardi, M., Petrella, L., 2016. A multivariate copula-based framework for dealing with hazard scenarios and failure probabilities. Water Resour. Res. 52, 3701–3721. https://doi.org/https://doi.org/10.1002/2015WR017225

Santiago-Collazo, F.L., Bilskie, M. V., Hagen, S.C., 2019. A comprehensive review of compound inundation models in low-gradient coastal watersheds. Environ. Model. Softw. 119, 166–181. https://doi.org/10.1016/j.envsoft.2019.06.002

Scawthorn, C., Blais, N., Seligson, H., Tate, E., Mifflin, E., Thomas, W., Murphy, J., Jones, C., 2006. HAZUS-MH Flood Loss Estimation Methodology. I: Overview and Flood Hazard Characterization. Nat. Hazards Rev. 7, 60–71. https://doi.org/10.1061/(ASCE)1527-6988(2006)7:2(60)

Schepsmeier, U., Stoeber, J., Brechmann, E. C., G., B., Nagler, T., Erhardt, T., 2018.

VineCopula: Statistical inference of vine copulas.

Sebastian, A., Dupuits, E.J.C., Morales-Nápoles, O., 2017. Applying a Bayesian network based on Gaussian copulas to model the hydraulic boundary conditions for hurricane flood risk analysis in a coastal watershed. Coast. Eng. 125, 42–50. https://doi.org/10.1016/j.coastaleng.2017.03.008

Serafin, K.A., Ruggiero, P., Parker, K., Hill, D.F., 2019. What's streamflow got to do with it? A probabilistic simulation of the competing oceanographic and fluvial processes driving extreme along-river water levels. Nat. Hazards Earth Syst. Sci. 19, 1415–1431. https://doi.org/10.5194/nhess-19-1415-2019

Serinaldi, F., 2015. Dismissing return periods! Stoch. Environ. Res. Risk Assess. 29, 1179–1189. https://doi.org/10.1007/s00477-014-0916-1

Sklar, A., 1959. Fonctions de répartition à n dimensions et leurs marges. Publ. Inst. Stat. Univ. Paris 8, 229–231.

Smith, D.I., 1994. Flood damage estimation - a review of urban stage-damage curves and loss functions. Water SA 20, 231–238.

Sophocleous, M., 2002. Interactions between groundwater and surface water: The state of the science. Hydrogeol. J. 10, 52–67. https://doi.org/10.1007/s10040-001-0170-8

Streamline Technologies, 2016. ICPR4 Validation Report. Streamline Technol. Inc. Winter Springs, Florida.

Sukop, M.C., Rogers, M., Guannel, G., Infanti, J.M., Hagemann, K., 2018. High temporal resolution modeling of the impact of rain, tides, and sea level rise on water table flooding in the Arch Creek basin, Miami-Dade County Florida USA. Sci. Total Environ. 616–617, 1668–1688. https://doi.org/10.1016/j.scitotenv.2017.10.170

Sweet, W. V., Menendez, M., Genz, A., Obeysekera, J., Park, J., Marra, J.J., 2016. In tide's way: Southeast Florida's September 2015 sunny-day flood. Bull. Am. Meteorol. Soc. 97, S25–S30. https://doi.org/10.1175/BAMS-D-16-0117.1

Wahl, T., Jain, S., Bender, J., Meyers, S.D., Luther, M.E., 2015. Increasing risk of compound flooding from storm surge and rainfall for major US cities. Nat. Clim. Chang. 5, 1093–1097. https://doi.org/10.1038/nclimate2736

Ward, P.J., Couasnon, A., Eilander, D., Haigh, I.D., Hendry, A., Muis, S., Veldkamp, T.I.E., Winsemius, H.C., Wahl, T., 2018. Dependence between high sea-level and high river discharge increases flood hazard in global deltas and estuaries. Environ. Res. Lett. 13. https://doi.org/10.1088/1748-9326/aad400

Wdowinski, S., Bray, R., Kirtman, B.P., Wu, Z., 2016. Increasing flooding hazard in coastal communities due to rising sea level: Case study of Miami Beach, Florida. Ocean Coast. Manag. 126, 1–8. https://doi.org/10.1016/j.ocecoaman.2016.03.002

Woessner, W.W., 2000. Stream and Fluvial Plain Ground Water Interactions: Rescaling Hydrogeologic Thought. Groundwater 38, 423–429. https://doi.org/https://doi.org/10.1111/j.1745-6584.2000.tb00228.x

Yang, S., Tsai, F.T.C., 2020. Understanding impacts of groundwater dynamics on flooding and levees in Greater New Orleans. J. Hydrol. Reg. Stud. 32, 100740. https://doi.org/10.1016/j.ejrh.2020.100740

Zhang, K., 2011. Analysis of non-linear inundation from sea-level rise using LIDAR data: A case study for South Florida. Clim. Change 106, 537–565. https://doi.org/10.1007/s10584-010-9987-2

Zscheischler, J., Westra, S., Van Den Hurk, B.J.J.M., Seneviratne, S.I., Ward, P.J., Pitman, A., Aghakouchak, A., Bresch, D.N., Leonard, M., Wahl, T., Zhang, X., 2018. Future climate risk from compound events. Nat. Clim. Chang. 8, 469–477. https://doi.org/10.1038/s41558-018-0156-3

CHAPTER IV

Modelling the compound impacts of fluvial, coastal and groundwater floods with sea-level rise in North Miami using statistical and physically-based models

4 CHAPTER 4: MODELLING THE COMPOUND IMPACTS OF FLUVIAL, COASTAL AND GROUNDWATER FLOODS WITH SEA-LEVEL RISE IN NORTH MIAMI USING STATISTICAL AND PHYSICALLY-BASED MODELS

4.1 Abstract

Rising sea levels as well as the increase in compound flooding hazard scenarios due to climate change conditions are posing unprecedent socio-economic, demographic, structural and ecological challenges to coastal communities in Southeast Florida. Advancements in hydro-informatics and supercomputational power have improved our ability to understand the impacts caused by the interplay between pluvial, fluvial, and coastal flooding conditions at different scales. Nevertheless, this is not the case for groundwater mechanisms – which are a relevant driver in porous shallow water environments with the potential to cause widespread flooding across low-elevation areas – as the technical compatibility with hydrologic software and the sporadic frequency of these events have influenced their slow inclusion into the flood modeling framework. This research applies a loosely-coupled surface-subsurface numerical model (FLO-2D + MODFLOW-2005) to simulate complex hydrological processes by using different combinations of hydrological drivers under predefined water table thresholds and sea level rise (SLR) for future conditions in the Arch Creek Basin located in North Miami. Results demonstrate that compound flooding events are sensitive to changes in precipitation, surge levels and SLR projections, proving the variability of different scenarios. To support the findings, a flood depth-damage power function is used to quantify the economic harm of compound flooding scenarios to the building infrastructure. The identification of relevant/negligible flooding mechanisms and the influence of SLR projections to simulate compound flooding events sets the path to better adaptation and resilience strategies.

4.2 Introduction

The adverse impacts of anthropogenic climate change in sea-level rise (SLR) represent a matter of national security to most coastal regions worldwide (Williams, 2013). Urban developments located in low elevation coastal zones (LECZ) are particularly vulnerable to the effects of higher sea levels and extreme hydrometeorological events as the reduction of land, increased coastal flood risk and recurrent flooding compromise the population public health and safety, leading to large-scale migration, local gentrification, life disruption, and depreciation of assets (Bin et al., 2011; Dun, 2011; Keenan et al., 2018; McLeman and Hunter, 2011; Robinson et al., 2020).

The Southeast Florida peninsula - considered ground-zero for SLR due to its geographical location, low-lying elevation and highly porous limestone aquifer - (Compact, 2012) is subject to accelerated rising rates (5-13 mm/yr for the period 2006-2016) in respect to global mean seal-levels (≈3.4 mm/yr since 1992) (Wdowinski et al., 2016). Current SLR projections are expected to amplify future flood hazards in Miami-Dade County (MDC) including the variability in hydrological processes and extreme events, as well as the frequency and duration of nuisance flooding and shallow water tables (Obeysekera and Salas, 2016; Sweet et al., 2016).

MDC is already experiencing the cascading effects of climate change with a record of 39 high-tide flooding events in 2019 (Wdowinski, 2019), costliest and most active hurricane seasons in records (2017 and 2020) (NOAA, 2021), steady increase in higher water table anomalies since 2010 (SFWMD, 2021), continuous saltwater intrusion (Guha

and Panday, 2012; Obeysekera et al., 2011), and more frequent groundwater-induced flooding events (Compact, 2020; Peña et al. 2021; Sukop et al., 2018).

As a result, SLR will aggravate the likelihood of compound flooding events, defined as the co-occurrence of multiple flood drivers that individually are not necessarily extreme but in unison produce serious impacts (Bevacqua et al., 2017; Raymond et al., 2020; Seneviratne et al., 2012; Zscheischler et al., 2018). Despite acknowledging the influence of SLR projections in the region is beyond doubt, studies that assess their combination with extreme flooding scenarios are very limited (Obeysekera et al., 2019).

The aim of this study is to provide an outlook of compound flooding potential under SLR scenarios based on regional projections for the Arch Creek Basin located in North Miami. Based on the methodology by Jane et al. (2020) a multivariate statistical analysis is performed to simulate the joint occurrence of precipitation - storm tide water levels under predefined groundwater levels and regional SLR projections in a loosely-coupled 2D surface-subsurface modeling framework (FLO-2D and MODFLOW-2005). Understanding the exacerbated impacts of compound flooding events can provide helpful insights about the imminent challenges ahead. With most of the population living in areas barely above sea-level (1.2 meters or less), the identification of potential flood hotspots is pivotal for effective adaptation planning and resilience strategies.

4.3 Study Area

The Arch Creek Basin is an urbanized catchment in North Miami adjacent to the northeastern boundary of MDC along the coast of the Biscayne Bay (**Figure 4.1**). The study area is characterized by a high vulnerability to flooding due to its low-lying flat

topography, porous karst landscape, shallow water table, land use practices and the urbanization of flood zones, as most of the building infrastructure is located in elevations as high as 2 meters (Miami-Dade, 2016; Peña et al., 2021a). FEMA's severe repetitive loss (SRL) property database (FEMA, 2021) keeps a record of residential properties that have been affected by frequent flood losses over the years. Seventy-five properties have requested financial assistance since June 1995, in which 25 claims resulted from the aftermath of Tropical Storm Leslie (2-4 October 2000) and 18 from Tropical Storm Andrea (6-8 June 2013).

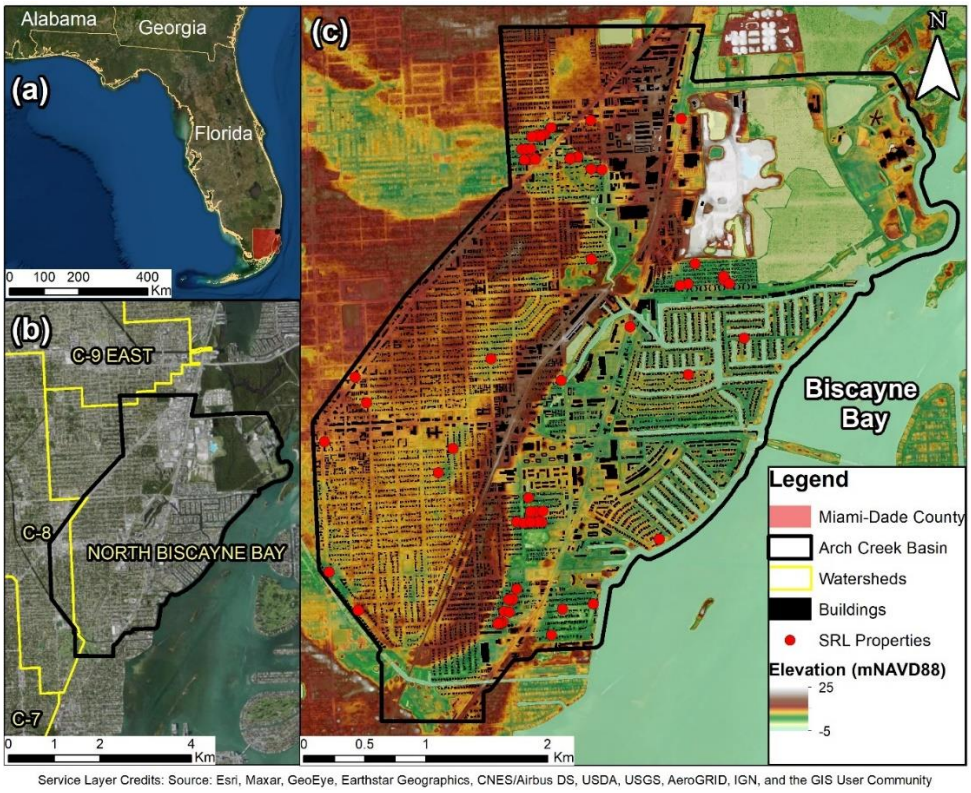

Figure 4.1. Area of research interest. (a) MDC (red) located in Southeast Florida, USA (b) geographic location of the Arch Creek Basin (black) within the North Biscayne Bay watershed, and (c) topographic elevation including the spatial distribution of buildings and FEMA's repetitive loss records.

4.4 Methods

4.4.1 Numerical Models

To simulate the interaction of surface hydraulics with groundwater flow, a loosely coupled modeling framework was selected. FLO-2D (O'Brien, 2011) is a physically-based volume conservation model suitable to perform two-dimensional hydrologic and hydraulic modeling for urban flood mapping, river overbank flooding, floodplain delineation, watershed processes, tsunami and hurricane surges, dam and levee breach, sediment transport, and flood damage assessment. The model is also capable to simulate groundwater flow when coupled with MODFLOW-2005. MODFLOW-2005 (Harbaugh, 2005) is a three-dimensional finite-difference groundwater model that simulates the movement of subsurface flow through aquifer layers. Readers are referred to Peña et al. (2021) for a detailed description of the numerical algorithms and the coupling development.

4.4.2 Model Configuration

The computational domain is composed by a 20 meters square-grid mesh interpolated from a high-resolution 2-meter LiDAR dataset (MDC). The boundary conditions include uniformly distributed precipitation throughout the FLO-2D domain and the coastal boundary along the Biscayne Bay for FLO-2D and MODFLOW-2005. The groundwater model is represented in a single aquifer layer based on the work by Hughes and White (2016) and Sukop et al. (2018). The water table behavior is represented on the western and southern perimeter to represent the stage of gauge station G-852 and Canal C-8 in MODFLOW-2005 respectively. The Green & Ampt infiltration method in FLO-2D is used to simulate the rainfall-runoff process, as well as the surface-subsurface flow

interaction that accounts for the infiltration volume that is transformed as recharge to MODFLOW-2005 or as emergence of the water table to the surface from MODFLOW-2005 back to FLO-2D. The infiltration parameters characterize the hydraulic conductivity, soil depth, porosity, capillary suction, and saturation levels. Building features (7827) were imported as impermeable individual elements that are free of flow volume.

4.4.3 Boundary Conditions

In an effort to extend the research of Peña et al. (2021b) we refer to 3.4.1 multivariate statistical analysis that applied a copula-based approach from a range of rainfall and tide gauge stations nearby the study site. The identification of bivariate extreme events was possible through the adoption of a two-sided conditional sampling approach (Wahl et al., 2015) to produce the overlap of the two quantile isolines for a 100-year design event. Sites S29_R and S28T exhibited the most extreme conditions from all possible combinations. In this study, an ensemble of three different combinations of rainfall and tide levels along the isoline corresponding to "surge only" (Event A), "most likely" (Event B) and "high rainfall" (Event C) patterns are selected to assess the effects of each scenario (**Figure 4.2**). Similarly, four conditional water table thresholds (NA, 1 meter, 2 meters, and 3 meters) were assigned to simulate their influence on the increasing risk of flooding. SLR projections, added to the coastal surge variable to account for the increase rate of sea levels, are presented in the next section.

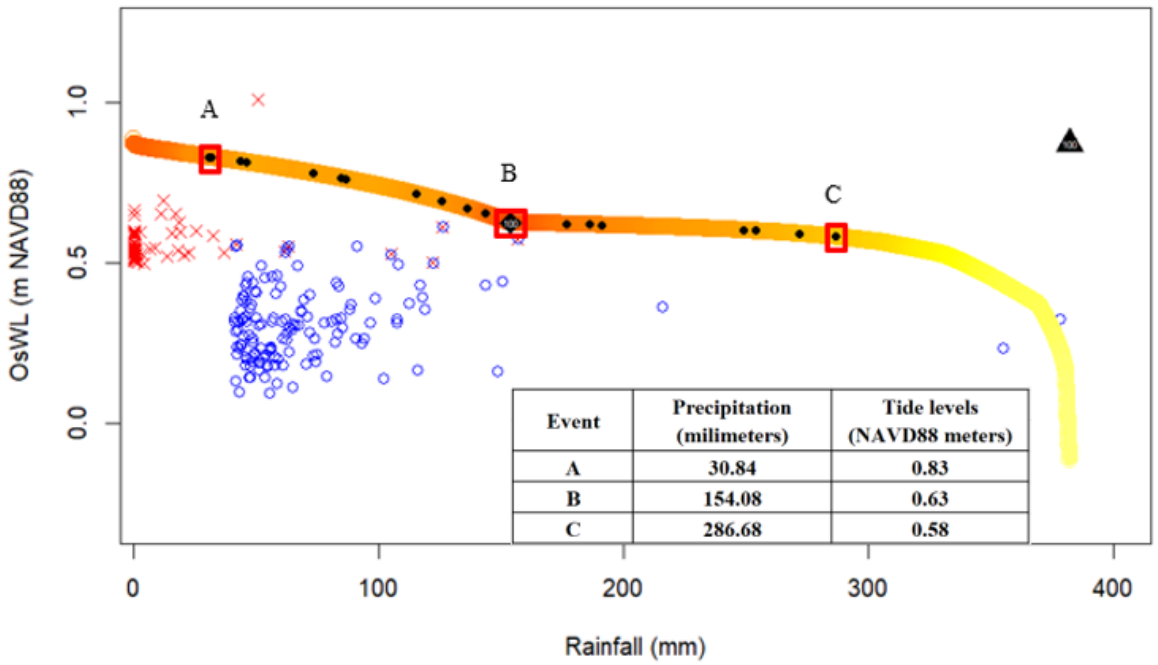

Figure 4.2. Quantile isoline for a 100-year return period between rainfall and Ocean-side Water Level at sites S29_R and S28_T. Selected events A-B-C (red square) from the ensemble sampling (black dots) were identified as input boundary conditions for the modeling framework.

4.4.4 Regional SLR Projections

Unified SLR projections were obtained from the most recent report by the Southeast Florida Regional Climate Change Compact's Sea Level Rise Ad Hoc Work Group (Compact). Updated on a quinquennial basis, the guideline document was developed from current global and national probabilistic projections of sea level rise adapted for the Southeast Florida region. The derived projections are referenced for selected future years in accordance with the Intergovernmental Panel on Climate Change (IPCC) AR5 RCP 8.5 scenario (IPCC, 2014), and National Oceanic and Atmospheric Administration (NOAA) using the Intermediate High, High, and Extreme curves (Sweet, 2017) (**Figure 4.3**). The projected boundaries are attributed to the Key West tide gauge mean sea level records

(NAVD88) to evaluate benefit-cost analyses on climate resilience projects and structural design frameworks for immediate and advanced adaptation planning strategies. This study covers the IPCC Median, NOAA Intermediate High, and NOAA High projections for years 2040, 2070, and 2120.

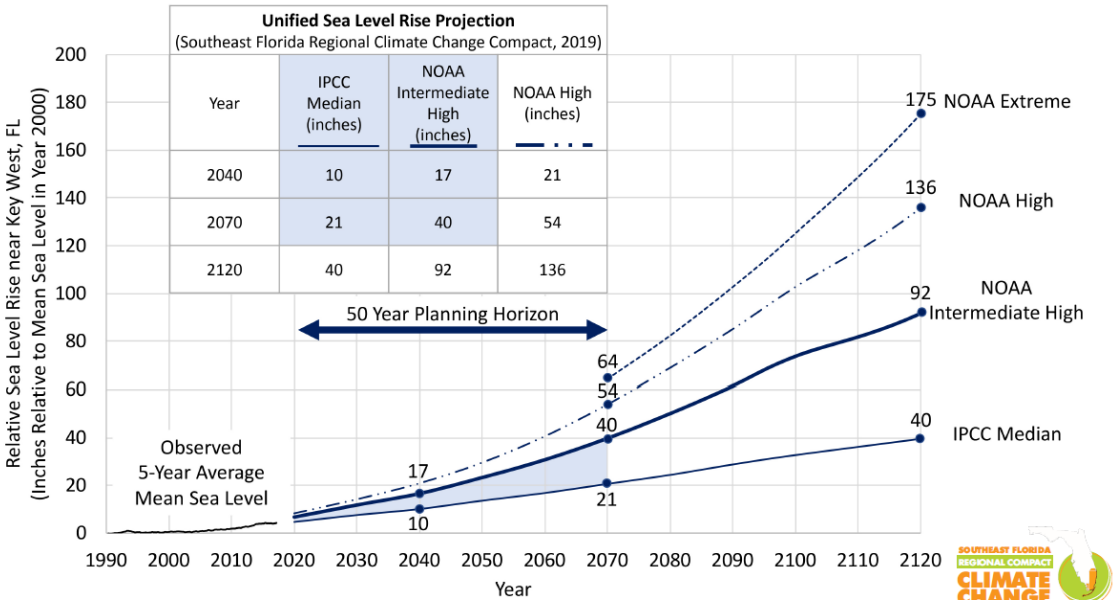

Figure 4.3. Regional SLR projections for Southeast Florida

4.5 Results and Discussion

The compound flooding potential of multiple hydrologic forcing variables with predefined water table levels and projected SLR scenarios for short, middle, and long-term horizons are presented from **Figure 4.4** – **Figure 4.12**. In addition, a global flood depth-damage curve (Huizinga et al., 2017) was applied to estimate the economic damage to building structures (**Table 4.1**). Results require careful examination to provide insights on how the flood drivers influence the inundation depth and extent over time.

Results show that "surge only" events for year 2040 (**Figure 4.4**) represent a low flood risk hazard scenario with a maximum water surface elevation of 1 meter in the canals and 0.25 meters across the urban domain. Interestingly, the NOAA High projection displays the impact of high tides at the coastline, covering the full extension of the Oleta Annex Park with flood depths up to 1.5 meters, while the flooding conditions are not as pronounced for "most likely" and "heavy rainfall" events (**Figure 4.5** and **Figure 4.6**). Although the emergence of the water table triggers widespread flooding throughout the Arch Creek Basin on all three projections resulting on a 21%, 17%, and 15% increase in flood extent under the worst water table level scenario (3 meters), the number of impacted buildings and potential economic damage is practically consistent with lower water table thresholds. Conversely, higher precipitation amounts exacerbate the compound flooding potential at the Basin, leading to an increase of inland flooding extent (24%, 21%, and 18%) and total damage (≈ 10%).

Figure 4.6 – **Figure 4.8** reveal notable evidence on the non-linear behavior of compound flooding dynamics under the influence of SLR for the year 2070. Predictions for the IPCC Median reveal that "surge only" and "most likely" events are similar in terms

of number and damage to buildings but differ in flood extension (≈ 10%), which is strictly related to the rise of the water table. On the other hand, heavy rainfall conditions led to a 9% increase in total damage becoming the worst scenario of all three events. While the pattern of number of damaged buildings and flooded area is also repeated in NOAA's projections, the total damage varies in each scenario. For the NOAA Intermediate High and High projections, the "only surge" event presents the highest damage ($42.68 million and $50.99 million) compared to "heavy rainfall" ($39.63 million and $49.18 million) and "most likely" events ($37.81 million and $47.89 million). Results suggest that this is due to the spatial distribution of the urban built environment, where the combined effects of storm surge and SLR outperformed the structural damage of "surge only" and "most likely" events by at least 42% compared to the IPCC Median projection. Similarly, topography plays a key role on preventing how far the surge waters are pushed inland. Coastal flooding is expected to have a direct influence on properties within a 2 km range of the Biscayne Bay, with flood depths of 1.5 meters on the Keystone Islands, Sans Souci Estates, and low-elevation neighborhoods near route US 1.

SLR projections for 2120 (**Figure 4.10** – **Figure 4.12**) display potentially catastrophic flood hazard across the vulnerable Arch Creek Basin, putting in permanent threat the livability of the coastal communities over regular flooding conditions. Similar to the 2070 scenario, NOAA Intermediate High shows that "surge only" event presents the most potential losses ($68.10 million) compared to the "heavy rainfall" ($66.60 million) and "design event" ($65.50 million). Conversely, the inundation extent is greater for "heavy rainfall" event (72%) while the flood extent is slightly higher compared to "most likely" (4%) and "surge only" (10%). The incorporation of the surface-subsurface water

interactions in the modeling framework reflects the impact of flooding from high water tables resulting in the progressive increase of inundation extent. The projected SLR scenario for the NOAA High curve (3.4544 meters) result in surge levels higher than 3 meters that practically reach the intersection of the railroad tracks and NE 125th Street, one of the elevated grounds in the study area (10 meters). In combination with the "only surge" scenario represent the worst compound scenario in terms of total damage ($99 million), in which all potential flood types (pluvial, fluvial, coastal and groundwater) interact at similar time scales. The water surface elevation exceeds the maximum capacity of the Arch Creek River and canals, resulting in fluvial flooding that exacerbate the urban flooding conditions on the west side of the domain.

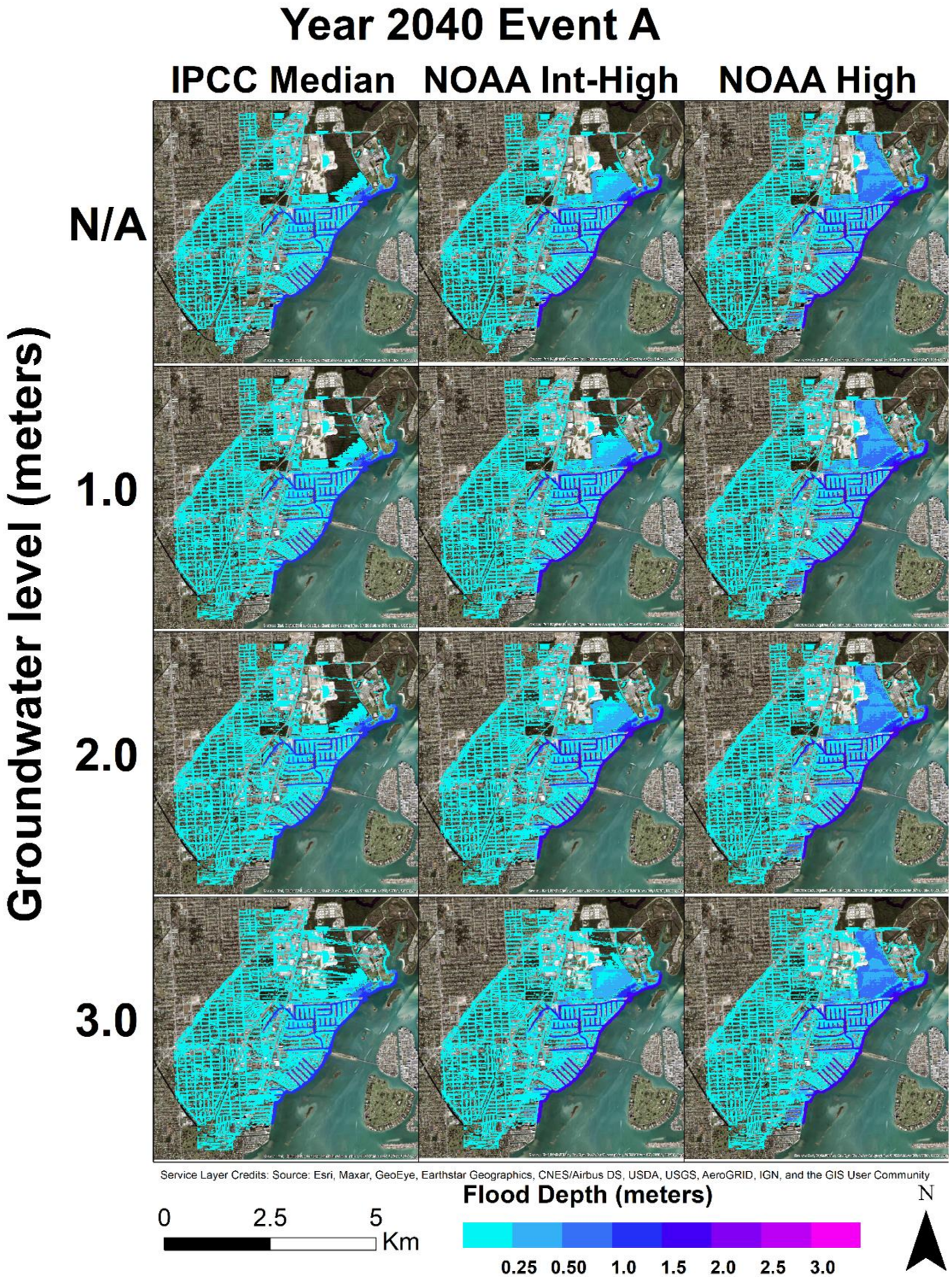

Figure 4.4. Flood map corresponding to "surge only" (Event A) under predefined water table levels and SLR scenarios for year 2040.

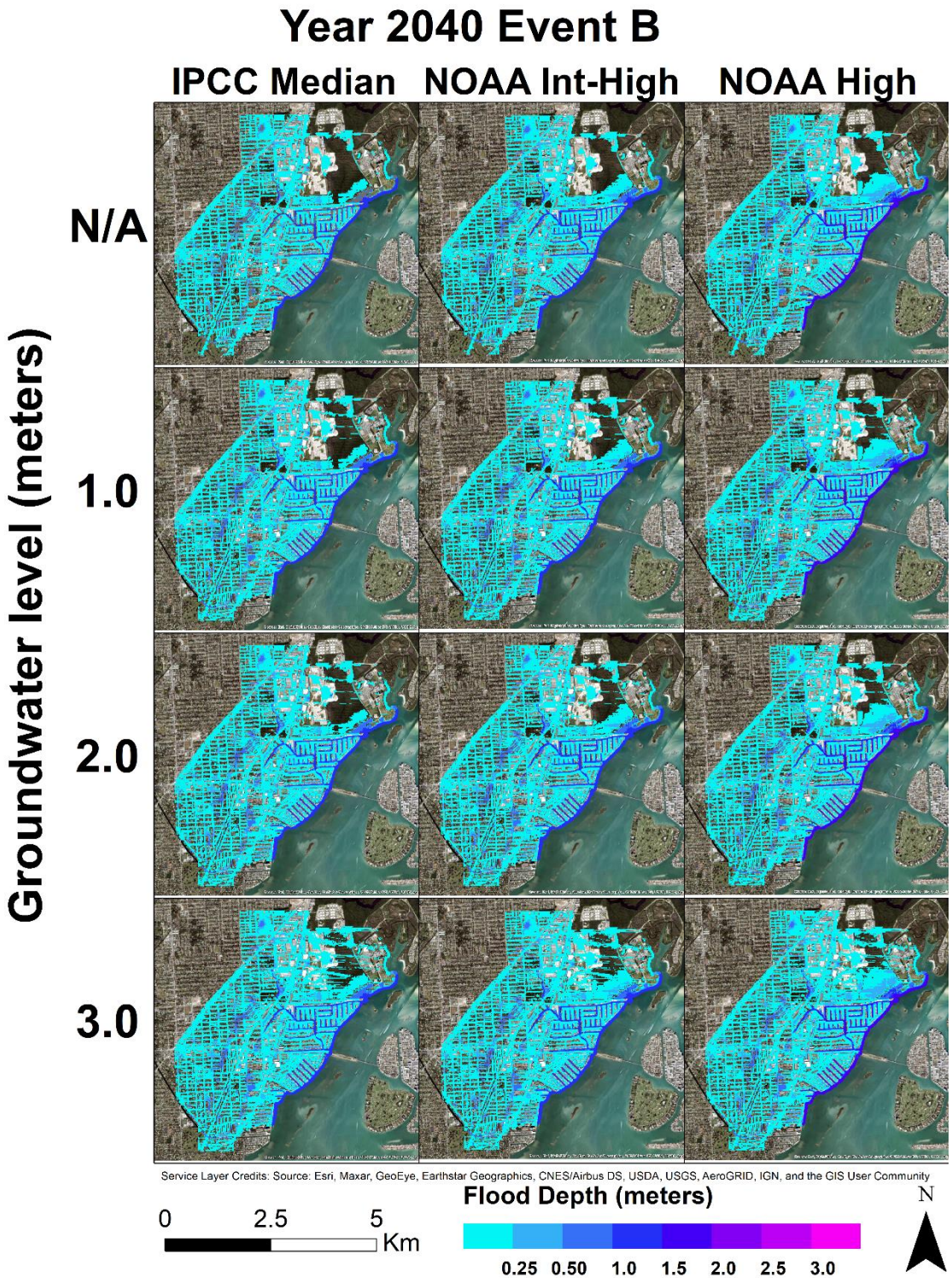

Figure 4.5. Flood map corresponding to "most likely" (Event B) under predefined water table levels and SLR scenarios for year 2040.

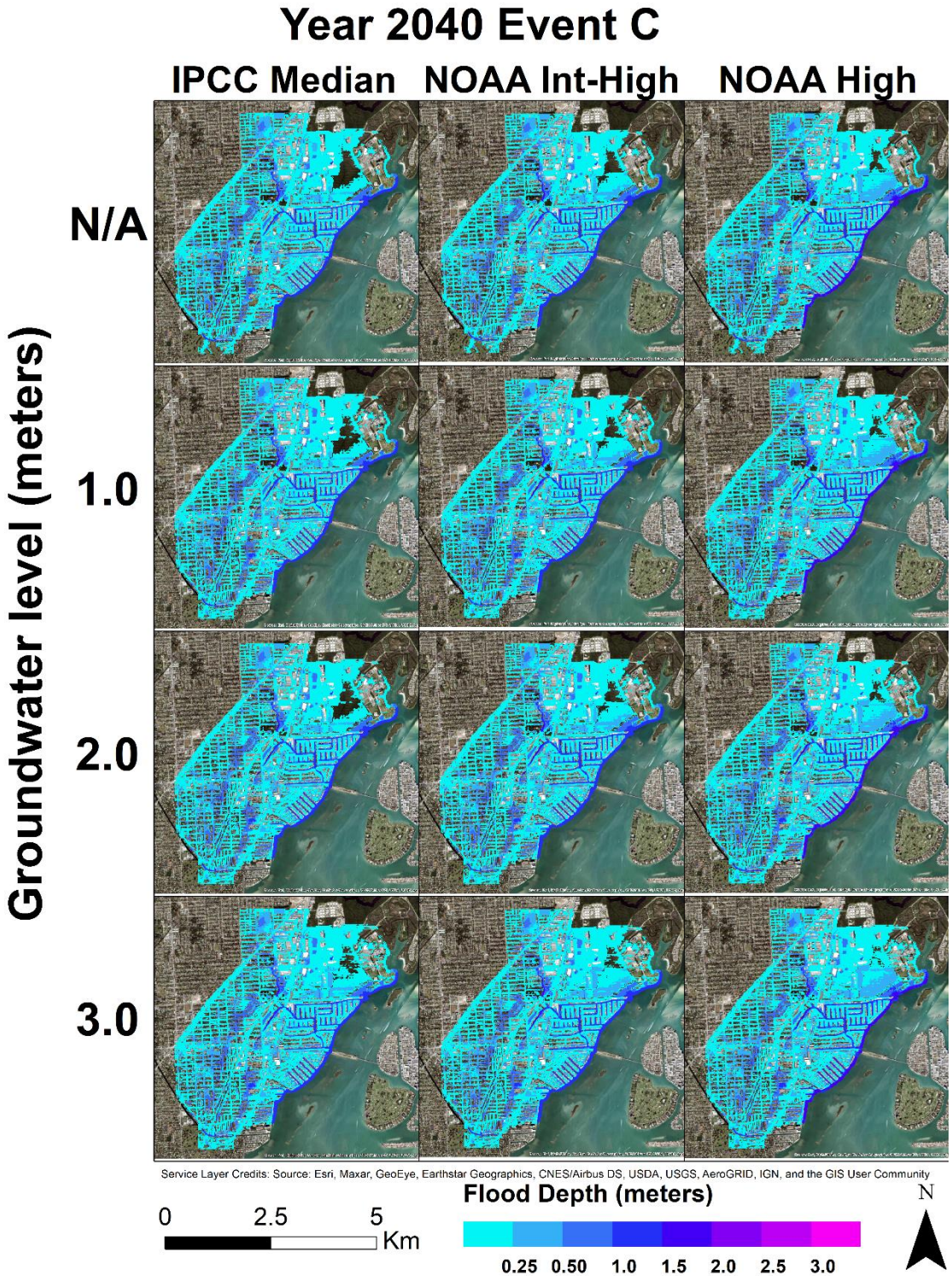

Figure 4.6. Flood map corresponding to "heavy rainfall" (Event C) under predefined water table levels and SLR scenarios for year 2040.

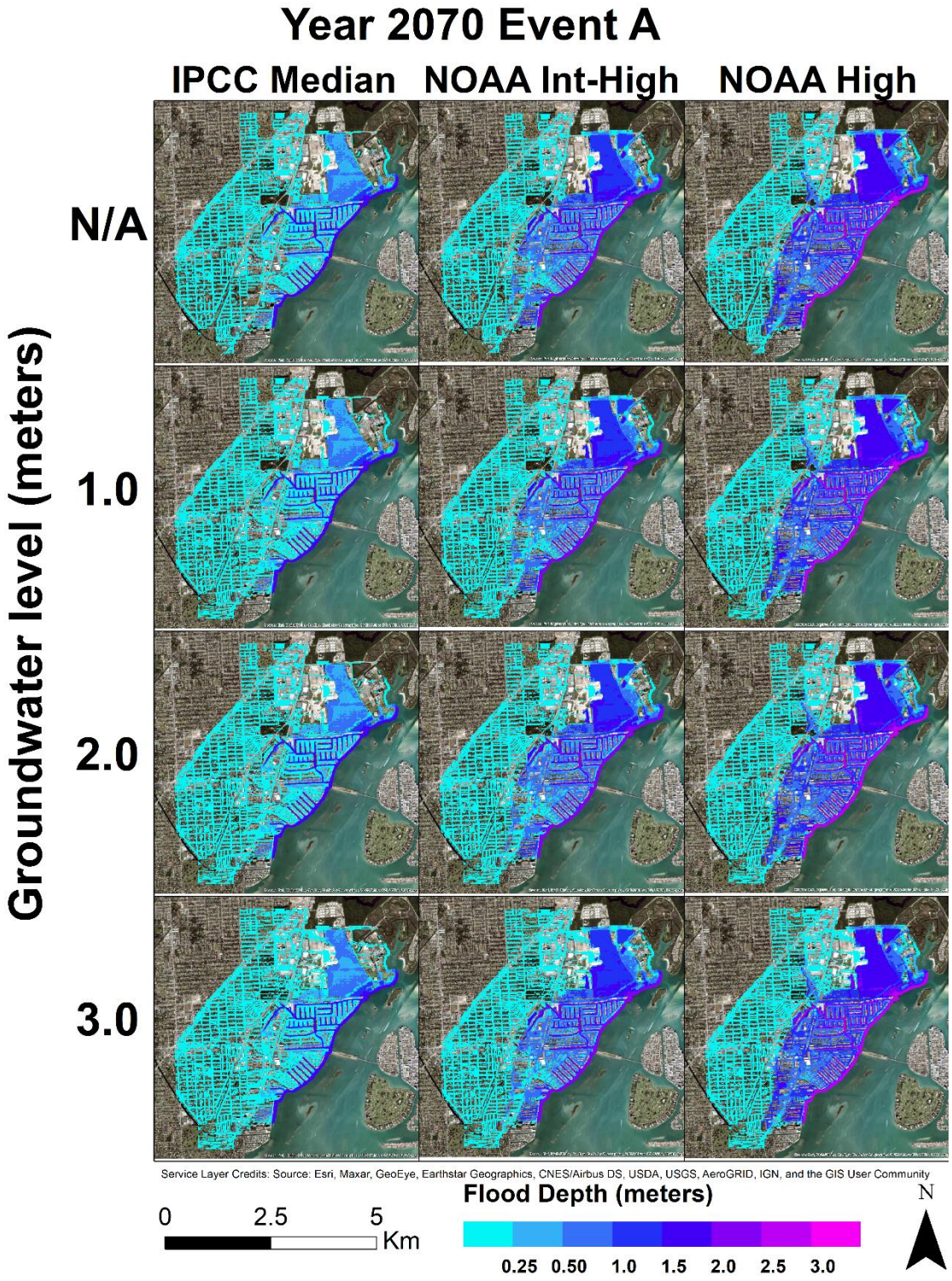

Figure 4.7. Flood map corresponding to "surge only" (Event A) under predefined water table levels and SLR scenarios for year 2070.

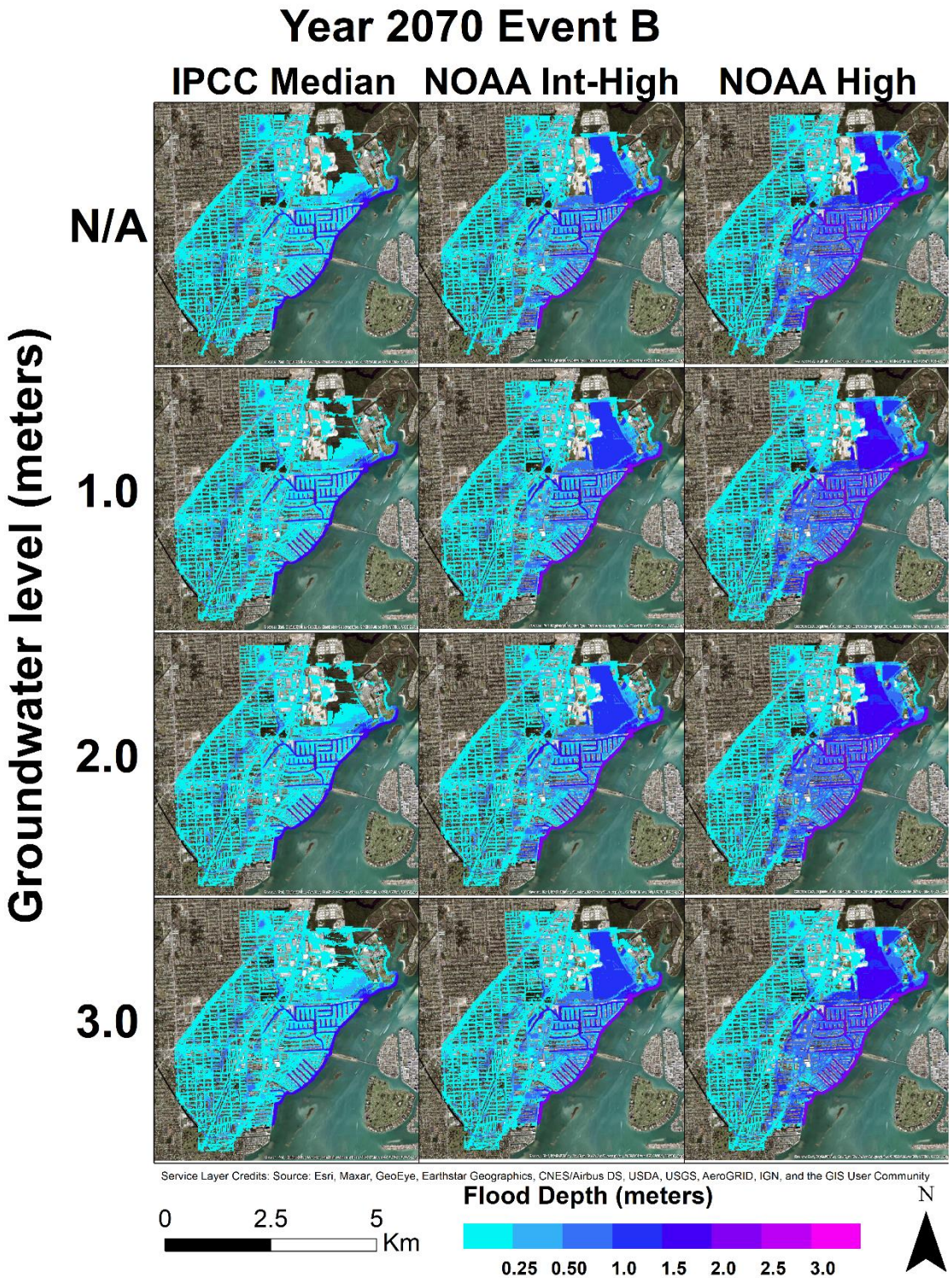

Figure 4.8. Flood map corresponding to "most likely" (Event B) under predefined water table levels and SLR scenarios for year 2070.

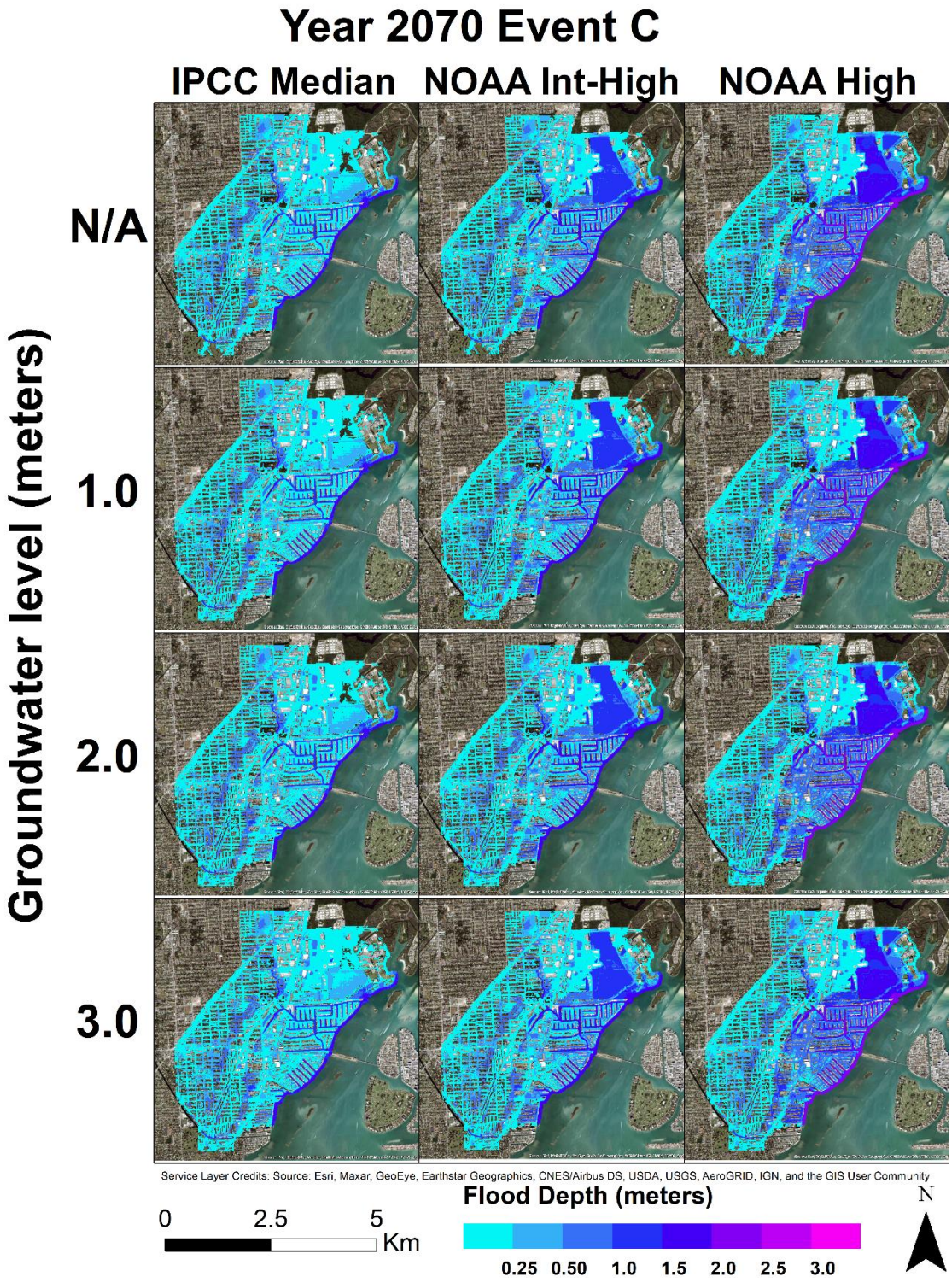

Figure 4.9. Flood map corresponding to "heavy rainfall" (Event C) under predefined water table levels and SLR scenarios for year 2070.

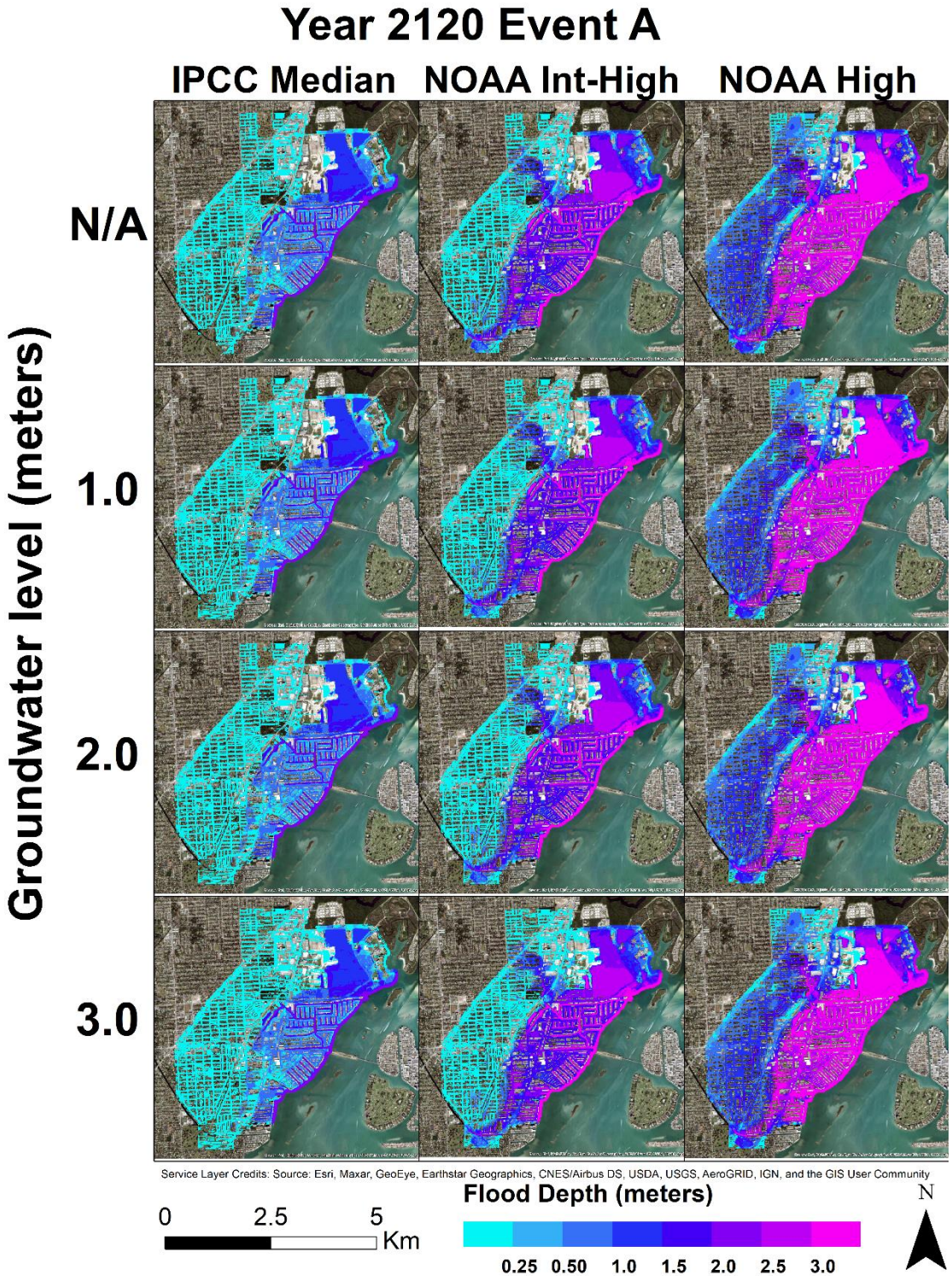

Figure 4.10. Flood map corresponding to "surge only" (Event A) under predefined water table levels and SLR scenarios for year 2120.

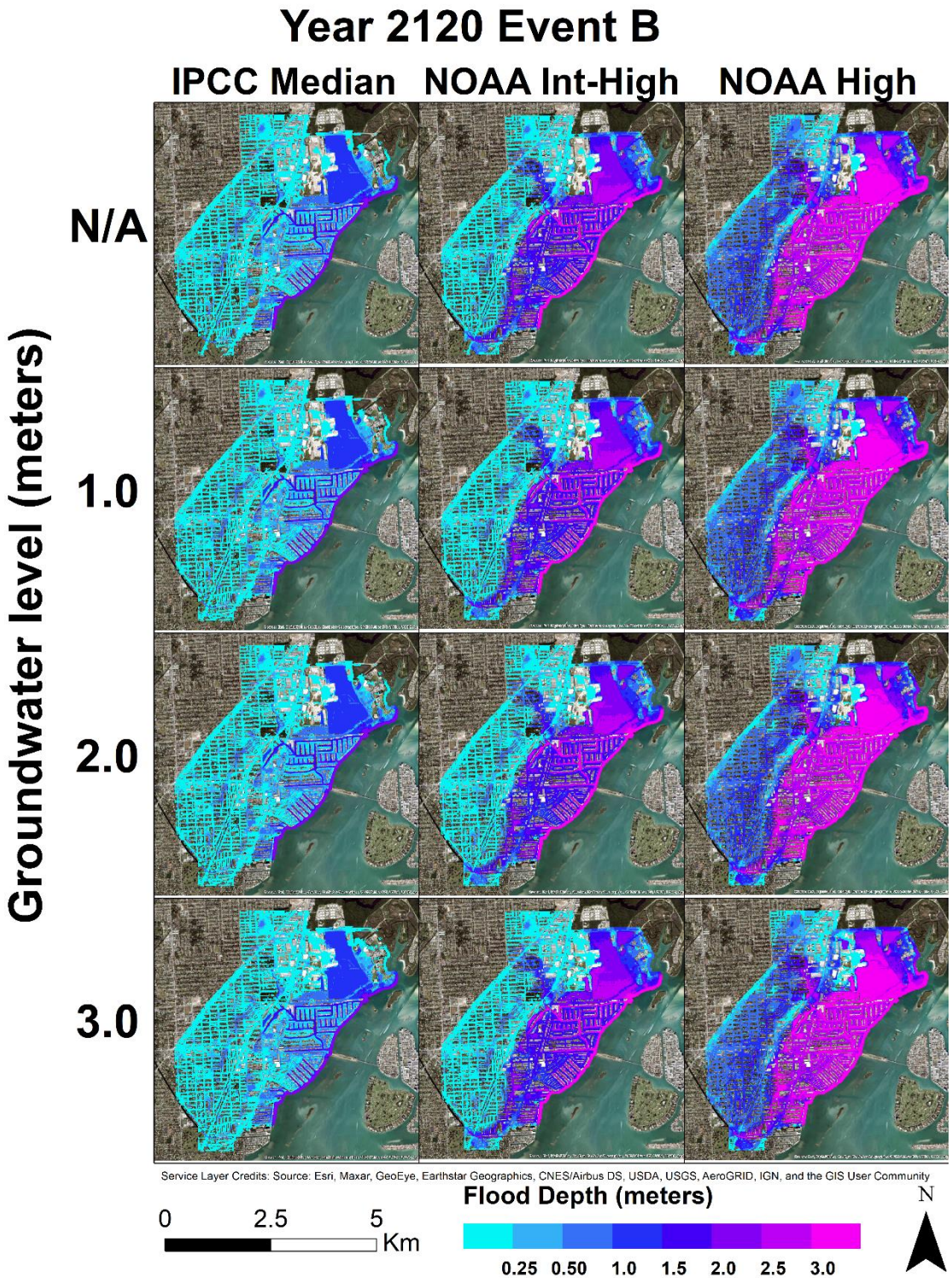

Figure 4.11. Flood map corresponding to "most likely" (Event B) under predefined water table levels and SLR scenarios for year 2120.

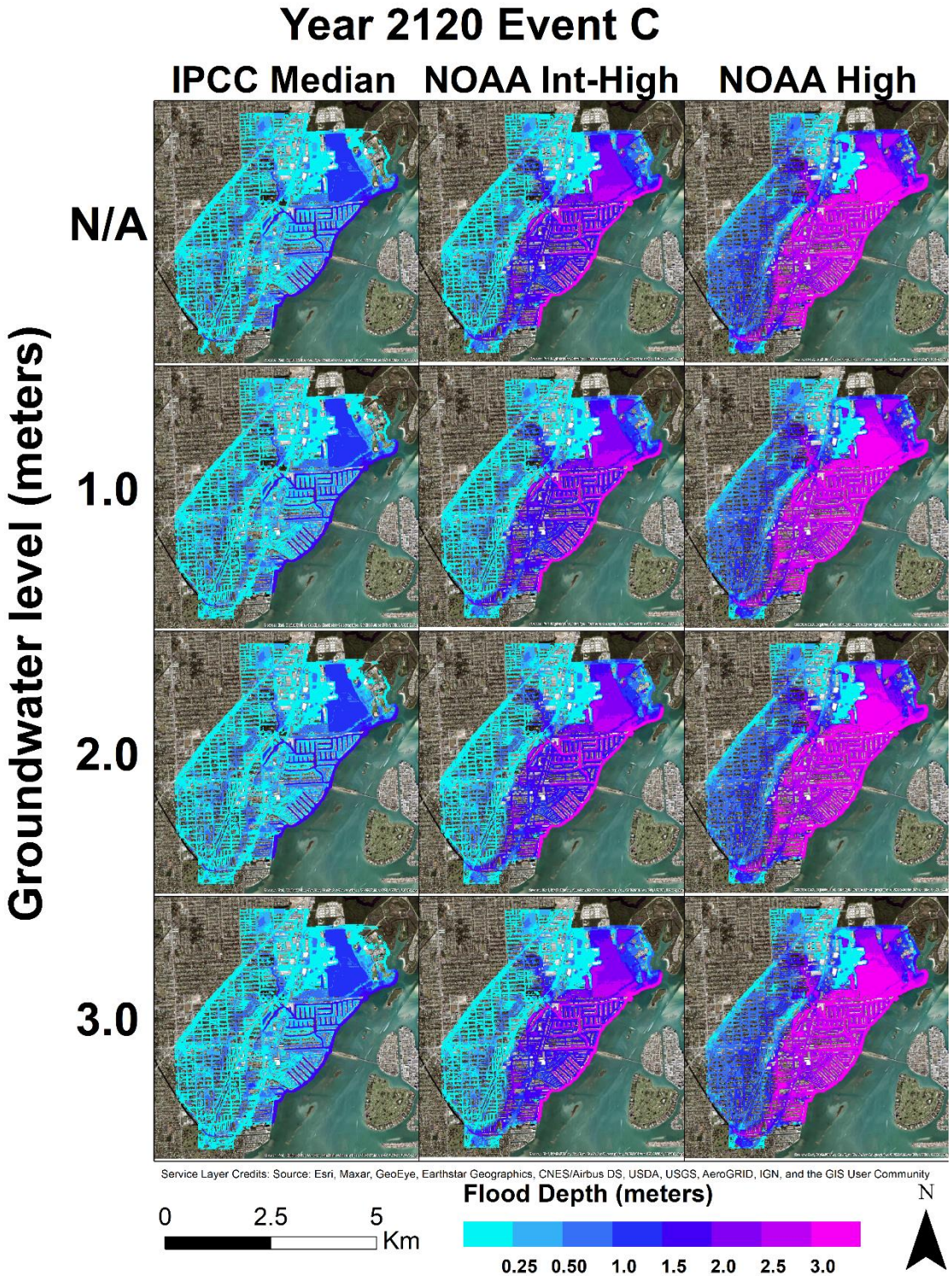

Figure 4.12. Flood map corresponding to "heavy rainfall" (Event C) under predefined water table levels and SLR scenarios for year 2120.

Table 4.1. Estimated compound flooding damage extent and potential from the interaction of precipitation, coastal surge, and predefined water table levels under SLR scenarios for the periods 2040, 2070 and 2120.

Year	Event	GW levels (meters)	IPCC Median			NOAA Intermediate High			NOAA High		
			# Buildings	% Flooded Area	Total Damage	# Buildings	% Flooded Area	Total Damage	# Buildings	% Flooded Area	Total Damage
2040	A	N/A	5885	45.73	$30.605	5885	48.49	$31.000	5886	51.33	$31.712
		1.0	5886	49.36	$30.609	5886	51.97	$31.011	5887	54.49	$31.719
		2.0	5886	50.11	$30.609	5886	52.65	$31.011	5887	55.11	$31.755
		3.0	5889	55.19	$30.622	5889	57.14	$31.023	5890	58.90	$31.774
	B	N/A	5926	56.09	$31.148	5926	57.11	$31.372	5926	58.27	$31.518
		1.0	5927	58.02	$31.268	5927	59.04	$31.492	5927	60.16	$31.638
		2.0	5927	58.66	$31.380	5927	59.62	$31.604	5927	60.71	$31.756
		3.0	5929	62.48	$31.398	5929	63.28	$31.623	5929	64.05	$31.779
	C	N/A	5940	64.29	$34.041	5940	65.25	$34.169	5940	65.94	$34.348
		1.0	5941	65.65	$34.201	5941	66.57	$34.349	5941	67.18	$34.465
		2.0	5941	66.06	$34.300	5941	66.96	$34.469	5941	67.57	$34.592
		3.0	5941	68.32	$34.400	5941	68.72	$34.577	5941	69.19	$34.693
2070	A	0.0	5886	51.33	$31.712	5885	57.25	$42.570	5893	59.63	$50.986
		1.0	5887	54.49	$31.719	5889	59.51	$42.676	5894	61.54	$50.998
		2.0	5887	55.11	$31.755	5889	60.00	$42.746	5894	61.91	$50.998
		3.0	5890	58.90	$31.774	5892	62.91	$42.758	5897	64.54	$51.002
	B	0.0	5926	58.27	$31.518	5927	63.78	$37.663	5928	66.15	$47.856
		1.0	5927	60.16	$31.638	5928	65.16	$37.772	5929	67.26	$47.878
		2.0	5927	60.71	$31.756	5928	65.55	$37.884	5929	67.53	$47.920
		3.0	5929	64.05	$31.779	5930	67.63	$37.924	5932	69.22	$47.944
	C	0.0	5940	65.94	$34.348	5940	68.45	$39.485	5942	70.02	$49.136
		1.0	5941	67.18	$34.465	5941	69.42	$39.567	5943	70.78	$49.170
		2.0	5941	67.57	$34.592	5941	69.72	$39.687	5943	70.98	$49.209
		3.0	5941	69.19	$34.693	5941	70.52	$39.777	5943	71.61	$49.230
2120	A	0.0	5885	57.25	$42.601	5906	65.21	$68.106	5975	70.23	$99.029
		1.0	5889	59.51	$42.676	5906	65.09	$68.125	5975	70.57	$99.024
		2.0	5889	60.00	$42.746	5906	65.37	$68.140	5975	70.66	$99.028
		3.0	5892	62.91	$42.758	5909	67.48	$68.150	5975	71.61	$99.038
	B	0.0	5927	63.78	$37.663	5937	68.83	$65.673	5976	70.94	$94.632
		1.0	5928	65.16	$37.772	5937	69.41	$65.695	5976	71.27	$94.645
		2.0	5928	65.55	$37.884	5937	69.60	$65.698	5976	71.40	$94.647
		3.0	5930	67.63	$37.924	5939	71.00	$65.722	5976	72.30	$94.650
	C	0.0	5940	68.45	$39.485	5949	72.08	$66.581	5978	73.02	$93.582
		1.0	5941	69.42	$39.567	5949	72.38	$66.586	5978	73.19	$93.582
		2.0	5941	69.72	$39.687	5949	72.49	$66.631	5978	73.26	$93.583
		3.0	5941	70.52	$39.777	5949	72.91	$66.638	5978	73.48	$93.590

4.6 Results and Discussion

Similar to Peña et al. (2021a, 2021b), a loosely coupled model for surface-subsurface water interactions was applied to simulate the compound flooding potential of different combinations of rainfall and coastal surge under predefined water table levels and projected SLR scenarios in a LECZ. The model demonstrates that there is a strong correlation between the rise of the water table and higher inundation extent at low-lying coastal and inland neighborhoods in the Arch Creek Basin. Although the economic impact of groundwater-induced flooding to buildings is marginal compared to flash, fluvial and coastal flooding, modeling the water table dynamics and SLR are crucial to improve the accuracy of local predictions for better regional water management planning.

The multivariate statistical analysis demonstrates that generalizations on ranking the severity of "only surge", "most likely" and "heavy rainfall" events should be avoided and must be analyzed independently to draw conclusions, as the response of complex interplay between flood drivers to SLR scenarios can amplify or reduce the compound flooding potential which can greatly underestimate flood risk. Thus, accounting compound inundation predictions with projected SLR can provide guidance on how authorities will address the threat of climate change. For instance, the incorporation of these scenarios into dynamic adaptive policy pathways and engineering standards may support climate resilience strategies in Southeast Florida and the Everglades coastal ecosystem over the next 20, 50, and 100 years.

Further research on incorporating the influence of extremes under nonstationarity conditions (Ghanbari et al., 2020; Obeysekera and Salas, 2016), as well as mesh optimization (Peña and Nardi, 2018) and local property datasets in the proposed coupled

framework may provide insights on refined distribution of flood dynamics in the urban terrain, potential cascading effects of future flood hazards on infrastructure and facilities and detailed quantification of flood metrics.

4.7 References

Bevacqua, E., Maraun, D., Hobæk Haff, I., Widmann, M., Vrac, M., 2017. Multivariate statistical modelling of compound events via pair-copula constructions: Analysis of floods in Ravenna (Italy). Hydrol. Earth Syst. Sci. 21, 2701–2723. https://doi.org/10.5194/hess-21-2701-2017

Bin, O., Poulter, B., Dumas, C.F., Whitehead, J.C., 2011. MEASURING THE IMPACT OF SEA-LEVEL RISE ON COASTAL REAL ESTATE: A HEDONIC PROPERTY MODEL APPROACH*. J. Reg. Sci. 51, 751–767. https://doi.org/https://doi.org/10.1111/j.1467-9787.2010.00706.x

Dun, O., 2011. Migration and Displacement Triggered by Floods in the Mekong Delta. Int. Migr. 49. https://doi.org/10.1111/j.1468-2435.2010.00646.x

FEMA, 2021. https://www.fema.gov/case-study/repetitive-flood-claims-program-benefits-city-and-homeowners [WWW Document].

Ghanbari, M., Arabi, M., Obeysekera, J., 2020. Chronic and Acute Coastal Flood Risks to Assets and Communities in Southeast Florida. J. Water Resour. Plan. Manag. 146, 04020049. https://doi.org/10.1061/(asce)wr.1943-5452.0001245

Guha, H., Panday, S., 2012. Impact of Sea Level Rise on Groundwater Salinity in a Coastal Community of South Florida. J. Am. Water Resour. Assoc. 48, 510–529. https://doi.org/10.1111/j.1752-1688.2011.00630.x

Harbaugh, A.W., 2005. MODFLOW-2005 : the U.S. Geological Survey modular ground-water model--the ground-water flow process, Techniques and Methods. https://doi.org/10.3133/tm6A16

Hughes, J.D., White, J.T., 2016. Hydrologic conditions in urban Miami-Dade County, Florida, and the effect of groundwater pumpage and increased sea level on canal leakage and regional groundwater flow. U.S. Geol. Surv. 175.

Huizinga, J., Moel, H. De, Szewczyk, W., 2017. Global flood depth-damage functions: Methodology and the database with guidelines, EUR 28552. ed. Publications Office of the European Union, Luxembourg. https://doi.org/10.2760/16510

Jane, R., Cadavid, L., Obeysekera, J., Wahl, T., 2020. Multivariate statistical modelling of the drivers of compound flood events in south Florida. Nat. Hazards Earth Syst. Sci. 20, 2681–2699. https://doi.org/10.5194/nhess-20-2681-2020

Keenan, J.M., Hill, T., Gumber, A., 2018. Climate gentrification: From theory to empiricism in Miami-Dade County, Florida. Environ. Res. Lett. 13. https://doi.org/10.1088/1748-9326/aabb32

McLeman, R.A., Hunter, L.M., 2011. Climate Change : Insights From Analogues. Wiley Interdiscip. Rev. Clim. Chang. 1, 450–461. https://doi.org/10.1002/wcc.51.Migration

Miami-Dade, 2016. Arch Creek Study Area, Miami-Dade County, Florida; Briefing Book for ULI Advisory Services Panel, May 22-27 2016.

NOAA, 2021. Storm events database [WWW Document]. URL https://www.ncdc.noaa.gov/stormevents/ (accessed 3.29.21).

O'Brien, J.S., 2011. FLO-2D Users Manual.

Obeysekera, J., Irizarry, M., Park, J., Barnes, J., Dessalegne, T., 2011. Climate change and its implications for water resources management in south Florida. Stoch. Environ. Res. Risk Assess. 25, 495–516. https://doi.org/10.1007/s00477-010-0418-8

Obeysekera, J., Salas, J.D., 2016. Frequency of Recurrent Extremes under Nonstationarity. J. Hydrol. Eng. 21, 04016005. https://doi.org/10.1061/(asce)he.1943-5584.0001339

Obeysekera, J., Sukop, M., Troxler, T., Irizarry, M., Rogers, M., 2019. Potential Implications of Sea-Level Rise and Changing Rainfall for Communities in Florida using Miami-Dade County as a Case Study. Miami FL.

Peña, F., Nardi, F., 2018. Floodplain terrain analysis for coarse resolution 2D flood modeling. Hydrology 5. https://doi.org/10.3390/hydrology5040052

Peña, F., Nardi, F., Melesse, A., Obeysekera, J., Castelli, F., Price, R.M., Crowl, T., Gonzalez-Ramirez, N., 2021a. Compound flood modelling framework for rainfall-groundwater interactions. Nat. Hazards Earth Syst. Sci. Discuss. 2021, 1–38. https://doi.org/10.5194/nhess-2021-259

Peña, F., Obeysekera, J., Jane, R., Nardi, F., Melesse, A., Price, R.M., Annis, A., 2021b. Investigating compound flooding in a low elevation coastal karst environment using multivariate statistical and 2D hydrodynamic modeling: A case study in the Arch Creek Basin, Miami-Dade County Florida USA. Weather Clim. Extrem.

Raymond, C., Horton, R.M., Zscheischler, J., Martius, O., AghaKouchak, A., Balch, J., Bowen, S.G., Camargo, S.J., Hess, J., Kornhuber, K., Oppenheimer, M., Ruane, A.C., Wahl, T., White, K., 2020. Understanding and managing connected extreme events. Nat. Clim. Chang. 10, 611–621. https://doi.org/10.1038/s41558-020-0790-4

Robinson, C., Dilkina, B., Moreno-Cruz, J., 2020. Modeling migration patterns in the USA under sea level rise. PLoS One 15, 1–15.

https://doi.org/10.1371/journal.pone.0227436

Seneviratne, S., Nicholls, N., Easterling, D., Goodess, C., Kanae, S., Kossin, J., Luo, Y., Marengo, J., Mcinnes, K., Rahimi, M., Reichstein, M., Sorteberg, A., Vera, C., Zhang, X., 2012. in Managing the Risks of Extreme Events and Disasters to Advance Climate Change Adaptation: A Special Report of Working Groups I and II of the Intergovernmental Panel on Climate Change (eds Field, C. B. et al.).

SFWMD, 2021. DBHYDRO [WWW Document]. URL http://my.sfwmd.gov/dbhydroplsql/show_dbkey_info.main_menu (accessed 1.1.21).

Southeast Florida Regional Climate Change Compact Sea Level Rise Work Group (Compact), 2020. A document prepared for the Southeast Florida Regional Climate Change Compact Climate Leadership Committee.

Southeast Florida Regional Climate Change Compact Sea Level Rise Work Group Compact Inundation Mapping and Vulnerability Assessment Work Group, 2012. Analysis of the Vulnerability of Southeast Florida to Sea Level Rise.

Sukop, M.C., Rogers, M., Guannel, G., Infanti, J.M., Hagemann, K., 2018. High temporal resolution modeling of the impact of rain, tides, and sea level rise on water table flooding in the Arch Creek basin, Miami-Dade County Florida USA. Sci. Total Environ. 616–617, 1668–1688. https://doi.org/10.1016/j.scitotenv.2017.10.170

Sweet, W. V., Menendez, M., Genz, A., Obeysekera, J., Park, J., Marra, J.J., 2016. In tide's way: Southeast Florida's September 2015 sunny-day flood. Bull. Am. Meteorol. Soc. 97, S25–S30. https://doi.org/10.1175/BAMS-D-16-0117.1

Wahl, T., Jain, S., Bender, J., Meyers, S.D., Luther, M.E., 2015. Increasing risk of compound flooding from storm surge and rainfall for major US cities. Nat. Clim. Chang. 5, 1093–1097. https://doi.org/10.1038/nclimate2736

Wdowinski, S., 2019. Coherent saptio-temporal variations in the rate of sea level rise along the US Atlantic and Gulf coasts, in: AGU Fall Meeting Abstracts. pp. OS21A-07.

Wdowinski, S., Bray, R., Kirtman, B.P., Wu, Z., 2016. Increasing flooding hazard in coastal communities due to rising sea level: Case study of Miami Beach, Florida. Ocean Coast. Manag. 126, 1–8. https://doi.org/10.1016/j.ocecoaman.2016.03.002

Williams, S.J., 2013. Sea-Level Rise Implications for Coastal Regions. J. Coast. Res. 184–196. https://doi.org/10.2112/SI63-015.1

Zscheischler, J., Westra, S., Van Den Hurk, B.J.J.M., Seneviratne, S.I., Ward, P.J., Pitman, A., Aghakouchak, A., Bresch, D.N., Leonard, M., Wahl, T., Zhang, X., 2018. Future climate risk from compound events. Nat. Clim. Chang. 8, 469–477. https://doi.org/10.1038/s41558-018-0156-3

CHAPTER V

General Conclusions

5 CHAPTER 5: GENERAL CONCLUSIONS

In this final section, the main research outcomes, future work, and recommendations are presented. Section 5.1 outlines the transition of CF studies from a traditional univariate perspective to a more comprehensive multivariate approach. Section 5.2 highlights the main statistical and model findings that contribute to advancements in the field. Section 5.3 underlines limitations and some recommendations to foster similar CF research.

5.1 Overview

In recent years, city-scale hydraulic models have taken advantage of advances in availability and quality of altimetry, hydrologic, ocean, and groundwater data, as well as from breakthroughs in computer processing capability of higher resolution scales (Bates et al., 2018; Meesuk et al., 2015) leading to a shift from single to integrated approaches. Traditionally, flood hazard modeling was restricted to simulate single flood processes (Apel et al., 2016), creating significant simplifications of the urbanized coastal systems (i.e., neglecting overbank channel flows, storm surge, or water table dynamics), which underestimate the extent, depth, and severity of the flooded areas and velocities.

Nowadays, the quantification of flood hazard, in particular the use of joint-probability statistics, have been used to assess the dependency probabilities of two or more flood drivers, including precipitation, river discharge, coastal surge, water table levels, and sea-level rise (Hsu et al., 2000; Chen et al., 2010; Fan et al., 2009; Yu et al., 2019). A growing number of loosely coupled hydrodynamic models have simulated multivariate interactions of flood drivers to capture the interactions between rainfall-runoff and storm surge by linking time-variant boundary conditions of flood hydrographs and water surface

elevations, as are more reliable to produce more comprehensive flood risk assessments based on physical processes.

However, the combination of stochastic and 2D hydrodynamic models remains hardly available, and groundwater flood hazard is entirely a neglected component in most environments. The main goal of this dissertation is to use 2D hydrodynamic model as a reference model to simulate extreme CF conditions under present and future scenarios in an urbanized karst LECZ environment highly vulnerable to flooding.

5.2 Research Outcomes

This work investigates the relevance of considering multiple drivers governing flood risk when a combination of compound events shall be considered. A review study of relevant scientific literature was performed identifying several fluvial, pluvial and coastal CF studies using statistical or deterministic approaches. A knowledge gap was explicitly identified considering the groundwater component that still misses a consolidated modeling framework, especially for LECZ, where storm surge, surface runoff, and groundwater flood drivers (individually or in combination) have the potential to create devastating flooding conditions.

The Arch Creek Basin in North Miami is used as a pilot study site to study CF conditions. Prior anthropogenic action, the Arch Creek River acted as a transition flow corridor that connected the flow originated in the Everglades, moved throughout the wetland ecosystem (today MDC) and discharged into the Biscayne Bay. The geographical location and meteorological conditions of Florida's Southeastern coast make it vulnerable to hurricanes and extreme rainfall events, specifically during the wet season with annual precipitation totals of ≈1500 mm (60 in). Rapid urban development and canal construction

in the 1940's considerably modified the catchment hydrology. At these initial stages, the lack of flood regulation standards determined a permanent threat of pluvial and groundwater flood risk in neighborhoods below 1.5 NAVD elevation.

The storm drain infrastructure, composed of a hybrid system of drainage wells and French wells, is designed to redirect the stormwater runoff to the ground or outfall discharges.

Positioned above a highly porous and permeable carbonate aquifer, the Arch Creek is subject to swift fluctuations in water table dynamics due to precipitation and sea-level rise. The rise above normal levels impacts the storm drain system capacity and increases flood hazard in low surface elevation areas. Although high tide flooding is becoming a recurrent issue in the MDC, the Arch Creek Basin perched on the mainland Biscayne Bayfront is not directly affected by storm surge since it is protected by the Oceanfront Islands Surfside, North Beach, and Bay Harbor. The Keystone Island and Sans Souci canals also act as 'buffer' zones that mitigate the impact of waves and flooding extents inland, resulting in localized flooding from the overbank flow.

Three research questions are posed, and the research work aimed to address them by employing proper methods. A coupling mechanism was tested to achieve spatial, temporal, and mathematical compatibility between FLO-2D and MODFLOW-2005. FLO-2D acts as the base model for a linked compound inundation model to consider hydrologic, ocean, and groundwater boundary conditions. A 25-year storm event was used to calibrate the coupled model. Despite limitations in obtaining VGI flooding imagery during the peak flood event, the model was validated using official insurance claims that experienced repetitive flood damage. Results corroborate the value of producing more comprehensive

flood hazard mapping considering multiple flood drivers, particularly how surface flooding is influenced by high water tables that can exacerbate floodwater depth and areal extent. Multivariate probability analyses were carried on characterizing historical rainfall, tides, and groundwater patterns from gauging stations near the study area. Bivariate and trivariate approaches were implemented to determine the level of dependency between flooding mechanisms, and designed events derived from single joint isolines were obtained for specific return periods. The statistical output was subsequently used as boundary conditions for the coupled flood model to make more accurate predictions on compound flooding events. Ultimately, SLR projections from the Southeast Florida Regional Climate Change Compact were incorporated to use these scenarios for regional water management planning.

The ability to couple surface and subsurface water interactions is scientifically relevant to professionals in hydroinformatics since it sets the path to improve the understanding, prediction, and response time of water table recharge and dynamics in the aquifer to precipitation. The contributions of this research are substantial and go beyond the numerical simulation scope, as it supports numerous fields and real applications including flood management, urban planning and design, flood mapping and zoning, DRR, flood insurance policies and policy making.

5.3 Limitations and Future Developments

Opportunities and limitations encountered in this work are presented. Scientists and scholars passionate about CF hazards can use the following section as guidance to further knowledge in the field by addressing research gaps and questions within the proposed modeling framework.

The competitive advantage of coupling FLO-2D and MODFLOW-2005 to simulate the combined interplay of pluvial, fluvial, coastal and groundwater flooding drivers at similar spatiotemporal scales represents an innovation in the field compared to the other physically-based hydraulic models that have numerical limitations in coupling these processes. This work opens new horizons on the development of CF models from a holistic perspective.

While Miami's hydrogeomorphology is one of the most complex globally, the compounding effects of flood drivers may respond differently in diverse geographic settings. Therefore, further research should consider the proposed modeling framework to assess the CF risk in different geographical regions prone to multiple flood drivers, specifically in areas that have access to post-event flooding maps in the form of remote sensing products or VGI data for calibration and validation purposes.

The quality and accuracy of flood hazard mapping in urban areas are strictly related to the model spatial resolution considering that the vertical datum and built-up environment influence flow propagation dynamics. A 20-meters grid resolution was selected to balance the computational demands of both numerical algorithms with a certain level of precision without compromising the quality of the simulation. However, the investigation of higher resolution and coarser mesh size in CF studies might yield insights into the estimation of inundated areas and time performance at different scales.

Further research should also consider the role of storm drain systems and stormwater pump stations in CF under different return periods. The response and interaction of drainage infrastructure are critical to alleviating the impact, duration, and potential damage

of flooding scenarios. Therefore, we recognize the need to include more details of the urban environment to evaluate the extent and the effect of their contribution.

Similarly, the ability to simulate rising groundwater levels and SLR will be of great interest to the MDC working group on the impact of flooded septic systems from an ecological and public health perspective, providing a clearer view on the spread of septic tank effluent and contamination hotspots.

The broader impact and potential societal benefit of this research can be in the form of modeling potential mitigation scenarios based on current and extreme CF events. Conventional structural solutions are not an option anymore to prevent flooding in coastal cities; therefore, innovative nature-based solutions, such as the restoration of natural systems in vulnerable areas as 'flood parks,' historic creeks, or sloughs, should be considered to increase the hydraulic capacity of the system, and restore the ecological function of the area. Similarly, transforming vulnerable sites into hybrid green-recreation spaces could serve as valuable flood defenses to reduce flood vulnerability. A feasibility analysis of these potential solutions can be assessed by simulating CF scenarios.

Ultimately, this research is a small piece of multidisciplinary work that analyzes the ripple effects of flooding in a wide range of fields (such as socio-economic costs, urban and ecological degradation, and health) and can set the basis for prevention, protection, accommodation, and even retreat/relocation policies.

A. Appendix

Investigating compound flooding in a low elevation coastal karst environment using multivariate statistical and 2D hydrodynamic modeling: A case study in the Arch Creek Basin, Miami-Dade County Florida USA

This section is dedicated to relevant background information regarding the multivariate statistical analysis. The section is structured to introduce the bivariate procedure from the time series analysis (11.1) to the fitting copula distributions (1A.2.5) as the production of isolines for design events is presented in 3.5.1.

1.1 Time Series Analysis

The time-based characteristics of selected rainfall (NEXRAD, S27_R, and S29_R), tides (Virginia Key, S28_T, S27_T), and groundwater (G-852 and S-18) records (Table 3.1) are presented in Figure A.1 to describe the variability and oscillation of observations. The analysis is carried on from the first measure on record to November 30, 2020, with most gauge stations within a radius of 10 km of Arch Creek (except Virginia Key ≈ 20 km). Despite their proximity, gauge measurements are sensitive to the local weather conditions, geographical location, and local environment, recording unique measurements that are not necessarily in the same range of values to nearby gauging stations.

For instance, NEXRAD data provide a clear overview of the rainfall patterns in the study area. Individual peaks in the time series are identified as extreme rainfall events during hurricane season, with the heaviest daily rainfalls recorded in 2002, 2009, and 2013. S29_R records are similar to NEXRAD except for two higher precipitation peaks exceeding 300 mm in a day. S27_R behavior is also comparable to other stations with an unusual event in June 2020 exceeding 600 mm, compared to 36 mm based on the NEXRAD measurement in the study area.

Regarding the tides and OsWL series, S27_T and S28T are statistically homogeneous over time due to the shorter distance from discharge in the Biscayne Bay, the proximity between stations (1km), and geographical location as the structures are protected by the

Miami Beach shoreline. On the other hand, Virginia Key’s tide levels are considerably higher because the station faces the Atlantic Ocean. Tropical storms and the moon's gravitational pool are responsible for the sudden peaks in coastal water levels, with Hurricane Irma producing the all-time record in the Arch Creek Basin.

The interpretation of groundwater time series is a complex task due to the number of factors (i.e., hydrogeologic properties, antecedent soil moisture conditions, or water table levels) that influence groundwater dynamics' response to rainfall processes. Although G-852 and S-18 present similar maximum and minimum values, G-852 records higher water table levels because of its proximity to Biscayne Bay.

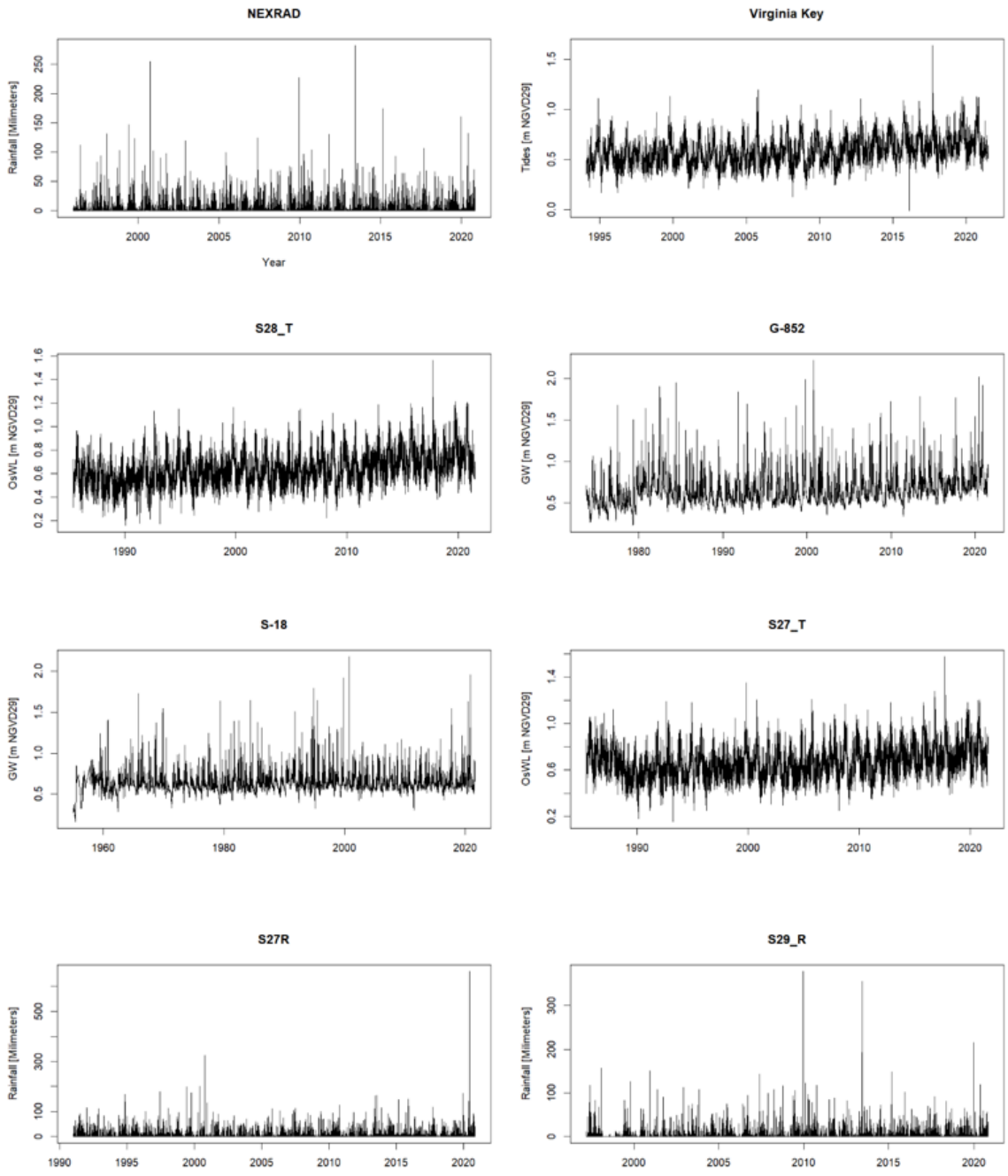

Figure A.1. Time series data records of selected gauge stations

1.2 Bivariate analysis

A.2.1 Marginal and Joint Distributions

The bivariate time series analysis is presented in Figure A.2 – Figure A.**4**. The black dots represent an event that consists of a pair of variable measurements taken on the same day. Results illustrate a concentration of low magnitude-high frequency events close to the axis compared to the scarce distribution of high-impact extreme events.

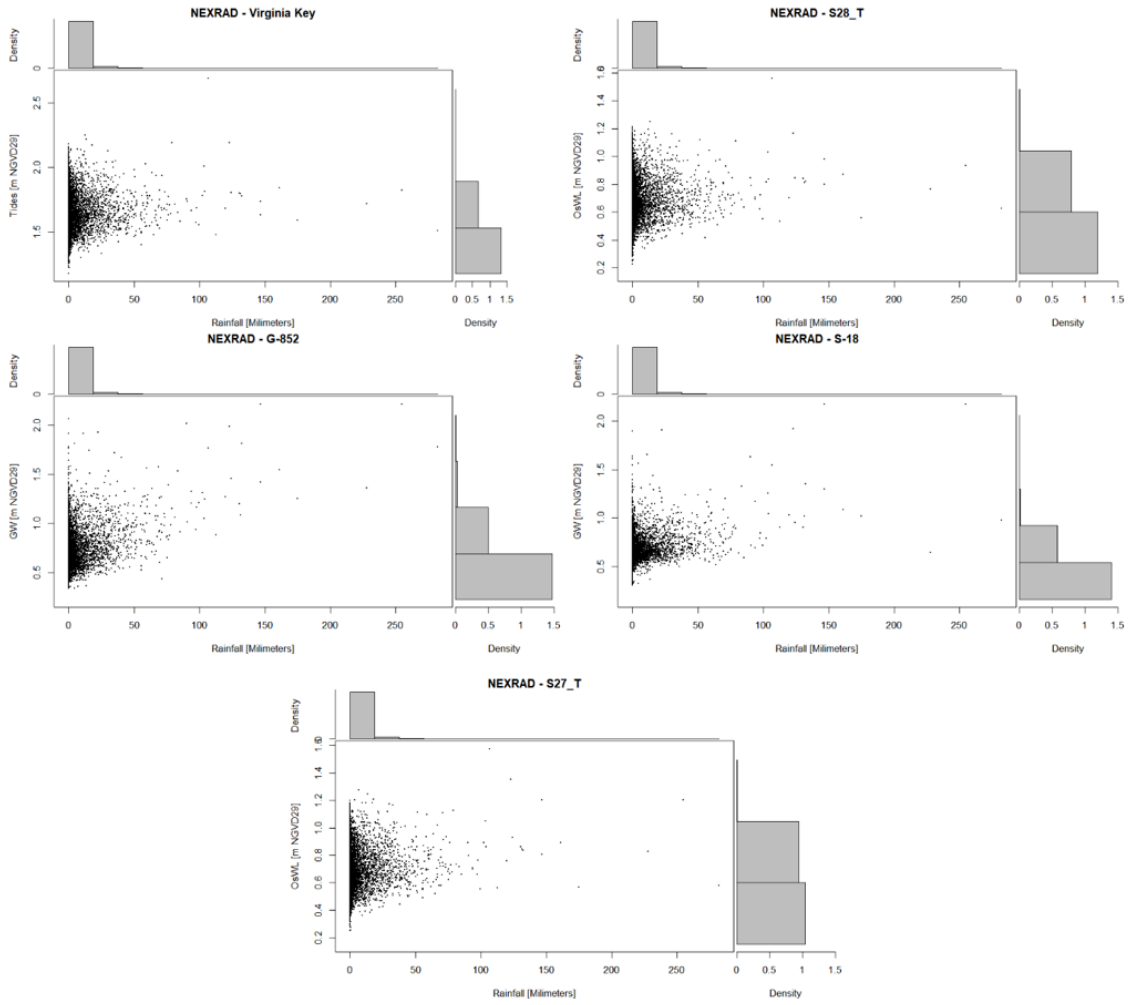

Figure A.2. Marginal and joint distributions of flood drivers at the Arch Creek Basin using NEXRAD grid data as rainfall reference condition

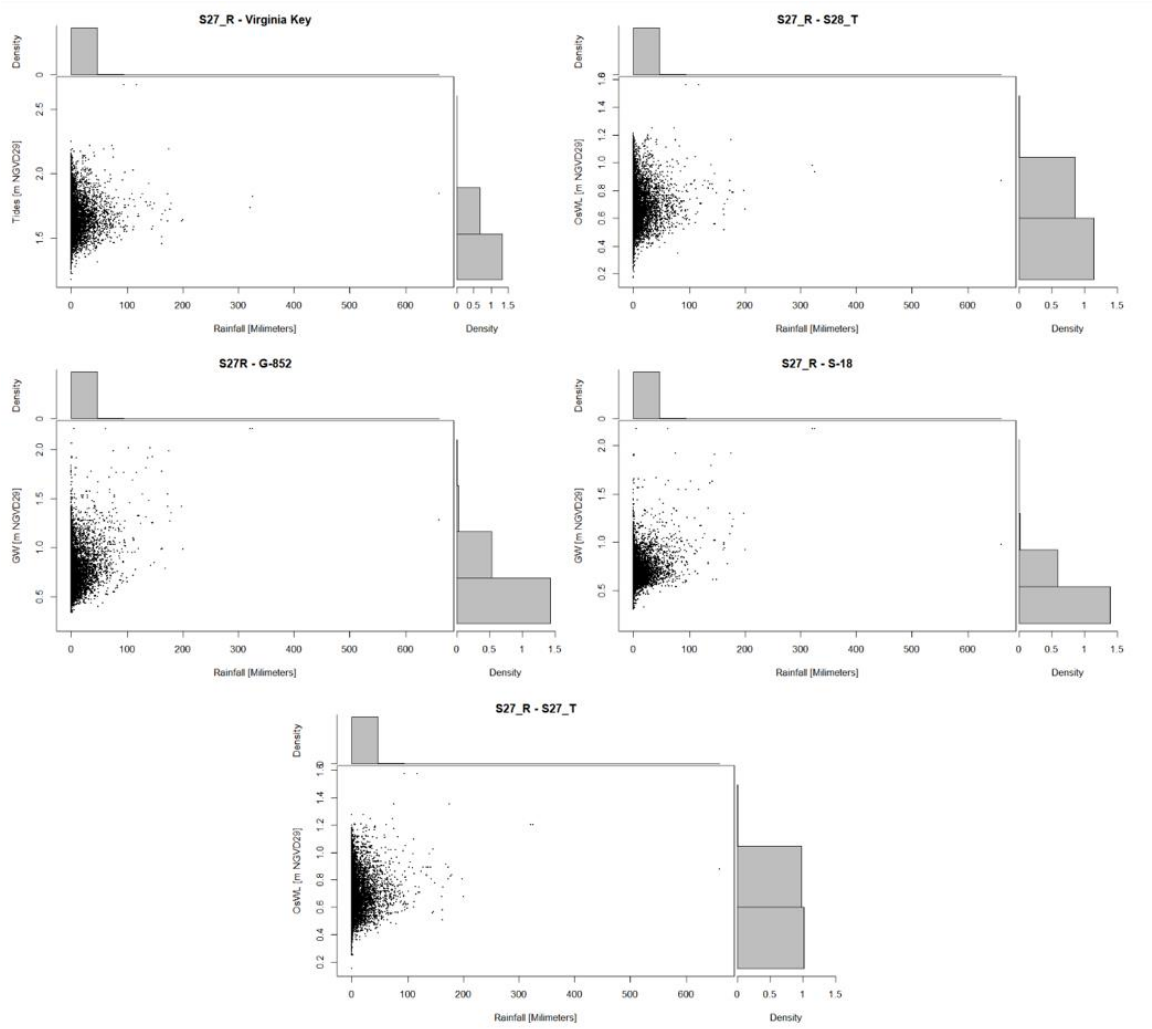

Figure A.3. Marginal and joint distributions of flood drivers at the Arch Creek Basin using S27_R data as rainfall reference condition

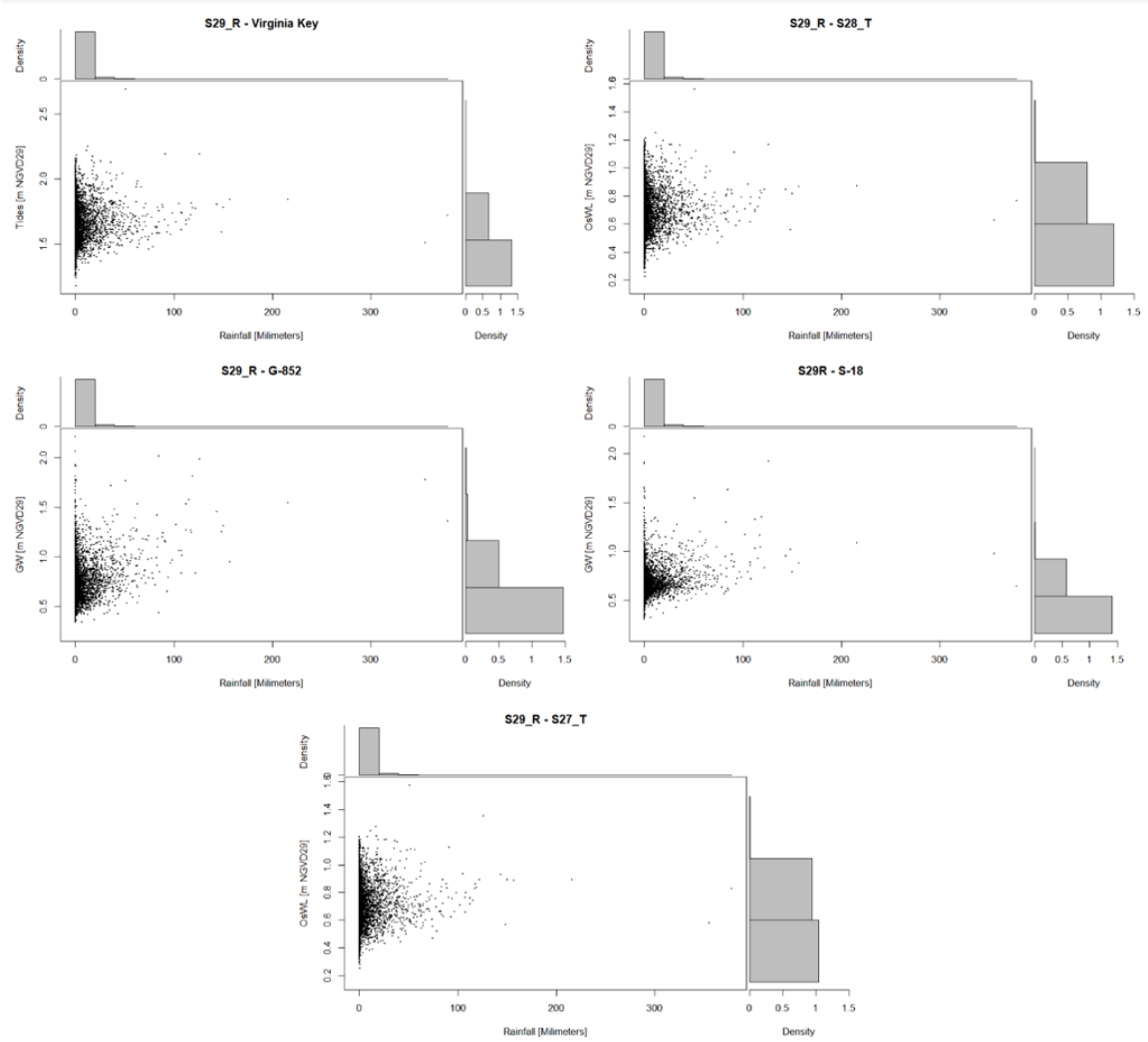

Figure A.4. Marginal and joint distributions of flood drivers at the Arch Creek Basin using S29_R data as rainfall reference condition

A.2.2 Declustering

The identification of events that exceed the separation criteria is presented in Figure A.5. The green line denotes the declustering threshold of 95%, events below the threshold are represented in black, and the cluster maxima of extreme events is given in red.

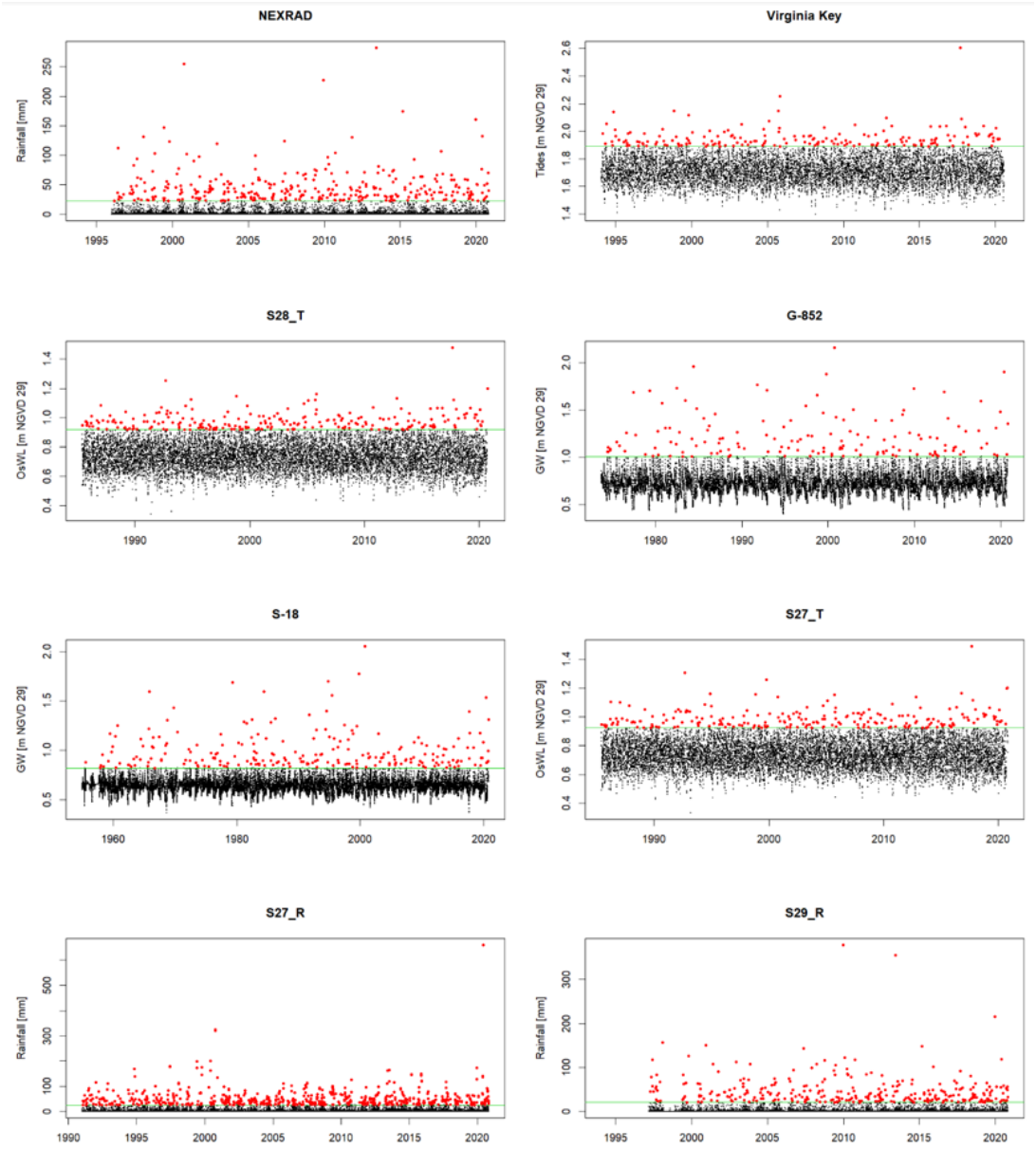

Figure A.5. Scattered plot of daily rainfall, tides and groundwater data against time. The unbroken green line is the threshold separation criterion and red dots the declustered timeseries above the threshold.

A.2.3 Best Fitting Copula

The best-fitting copula selection for conditional samples at specific thresholds is presented in **Figure A.6** – **Figure A.8**. For a pair of variables, two conditional samples are drawn by pairing the declustered excesses of one (conditioned variable) with co-occurrences of the other series (non-conditioned variable) and repeating the procedure with the variables reversed. The left graphs display the Kendall Tau correlation coefficient over a range of thresholds at 95 to 99 percentiles for each conditional sample. The best fitting of 40 copula families for the two conditional samples is given in the plot. The numbers provide the conditional sample size, and the filled circles denote whether the correlation between the variables is significant. On the right, the copula family for each conditional sample at the selected threshold is assigned to an object.

It should be emphasized that the procedure to select the appropriate threshold is not straightforward and is subject to interpretation, which can lead ultimately to variations in results.

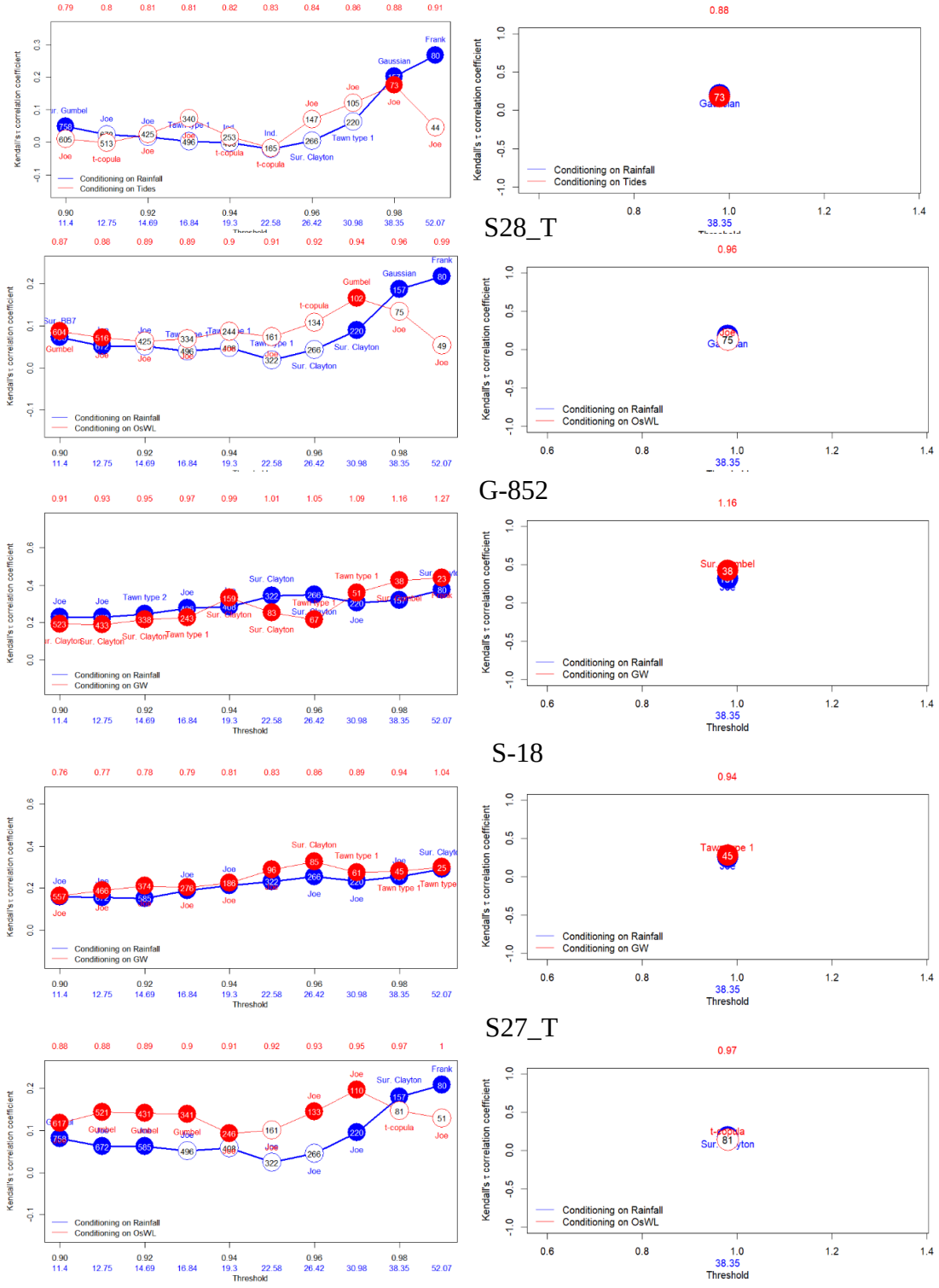

Figure A.6. Selection of best fitting copula based on the conditional samples at specific thresholds using NEXRAD grid data as rainfall reference condition

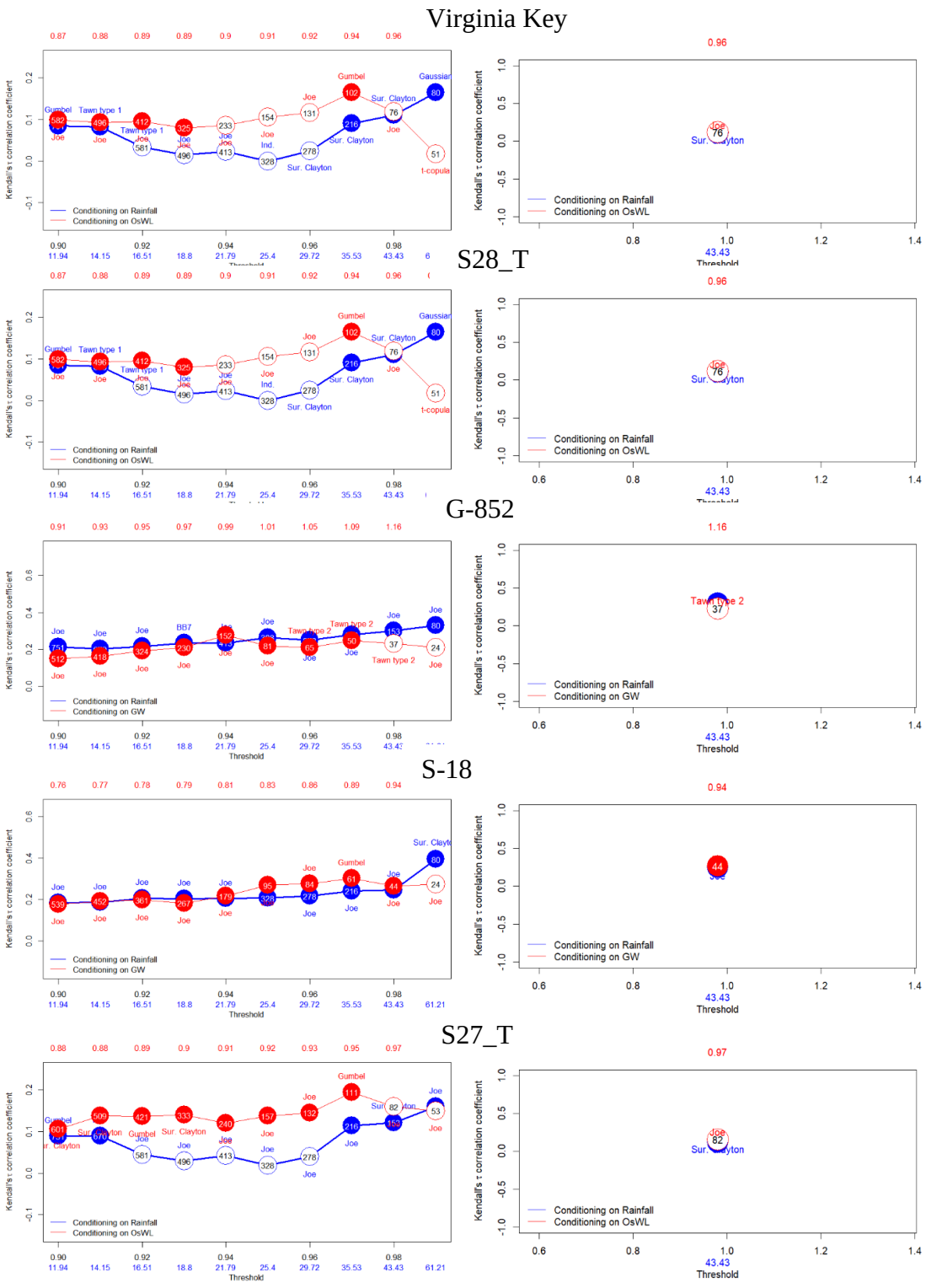

Figure A.7. Selection of best fitting copula based on the conditional samples at specific thresholds using S27_R data as rainfall reference condition

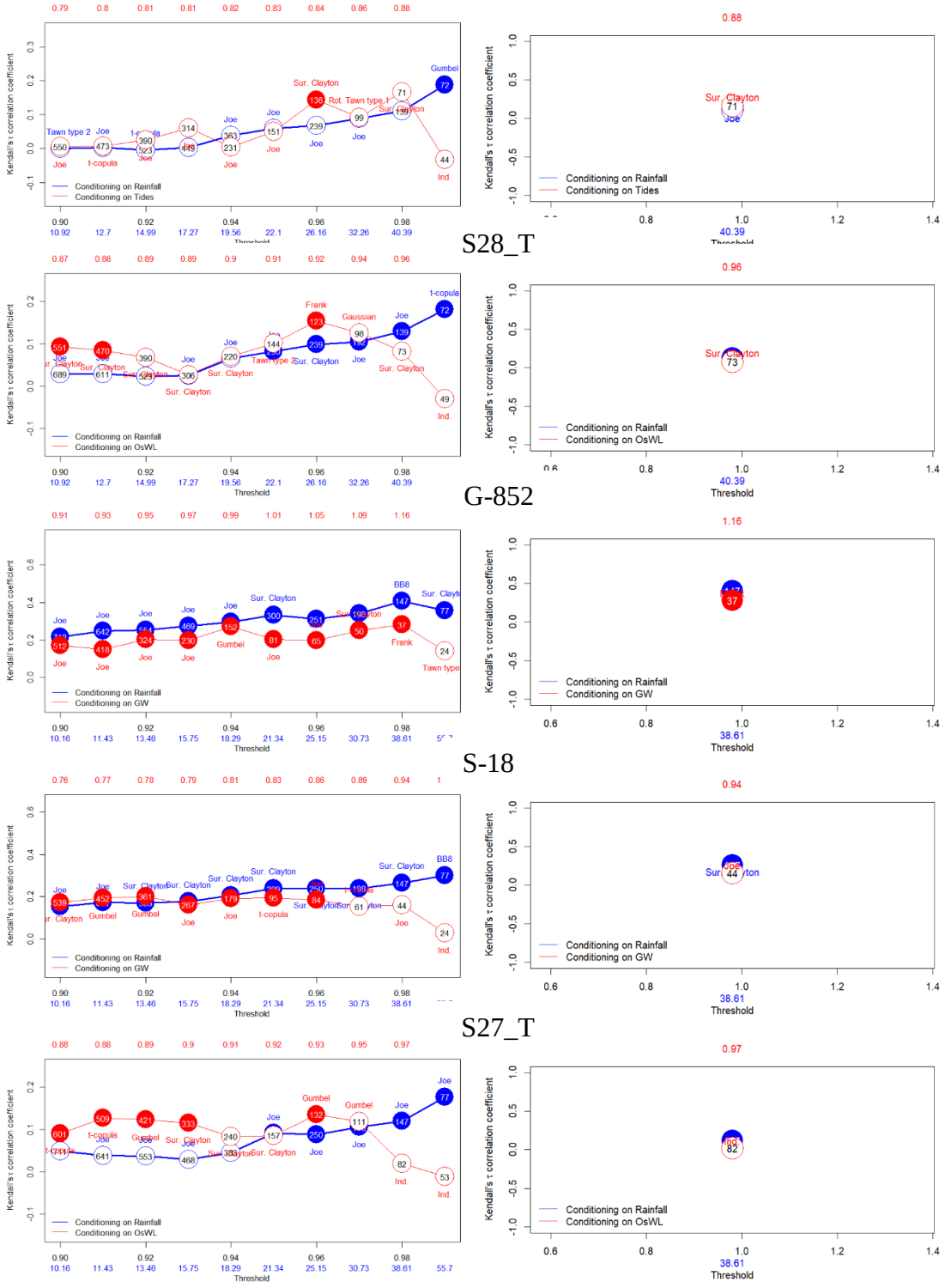

Figure A.8. Selection of best fitting copula based on the conditional samples at specific thresholds using S29_R data as rainfall reference condition

A.2.4 Fitting GPD to the conditioned variable

The purpose of the GPD is to find the marginals for the conditioned variable in each of the two conditioned samples. Four diagnostic plots are presented in **Figure A.9** – **Figure A.11**. Probability and quantile plots (top) illustrate empirical values, with the straight blue line indicating a perfect fit between the data and the GPD. Considering that the results of both plots lie close to the straight line, it is a good indication that the GPD fits the conditioned variables. The density plot (bottom left) displays the GPD blue curve superimposed over the density histogram providing a good fit. In the return level plot (bottom right), the black line represents the GPD, and the blue lines are the 95% confidence intervals. The selected thresholds are de facto acceptable considering that the empirical observations lie within the upper or lower bounds and the straight GPD line with only a few exceptions.

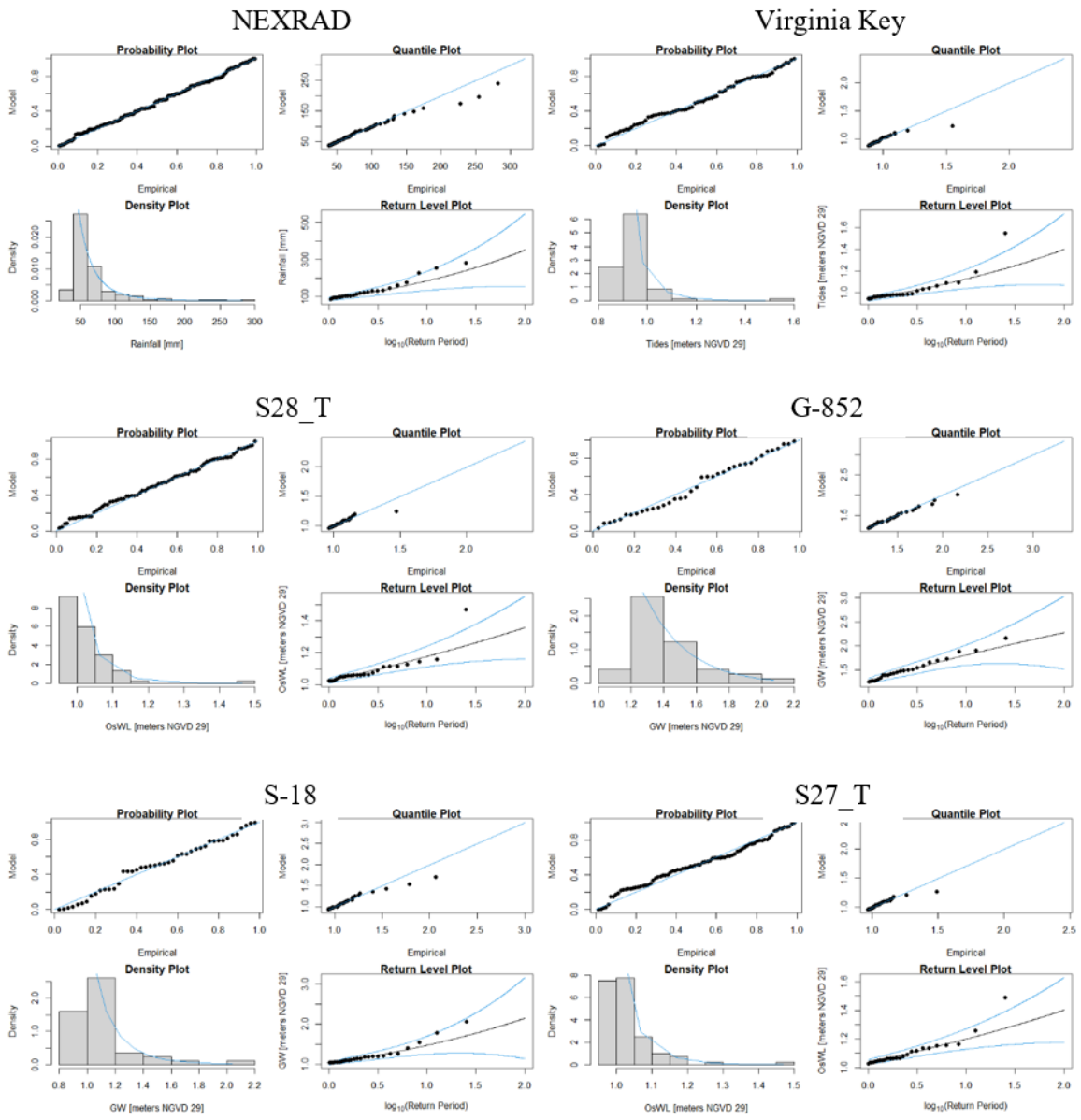

Figure A.9. Fitting General Pareto Distribution to the non-conditioned variable using NEXRAD grid data as rainfall reference condition

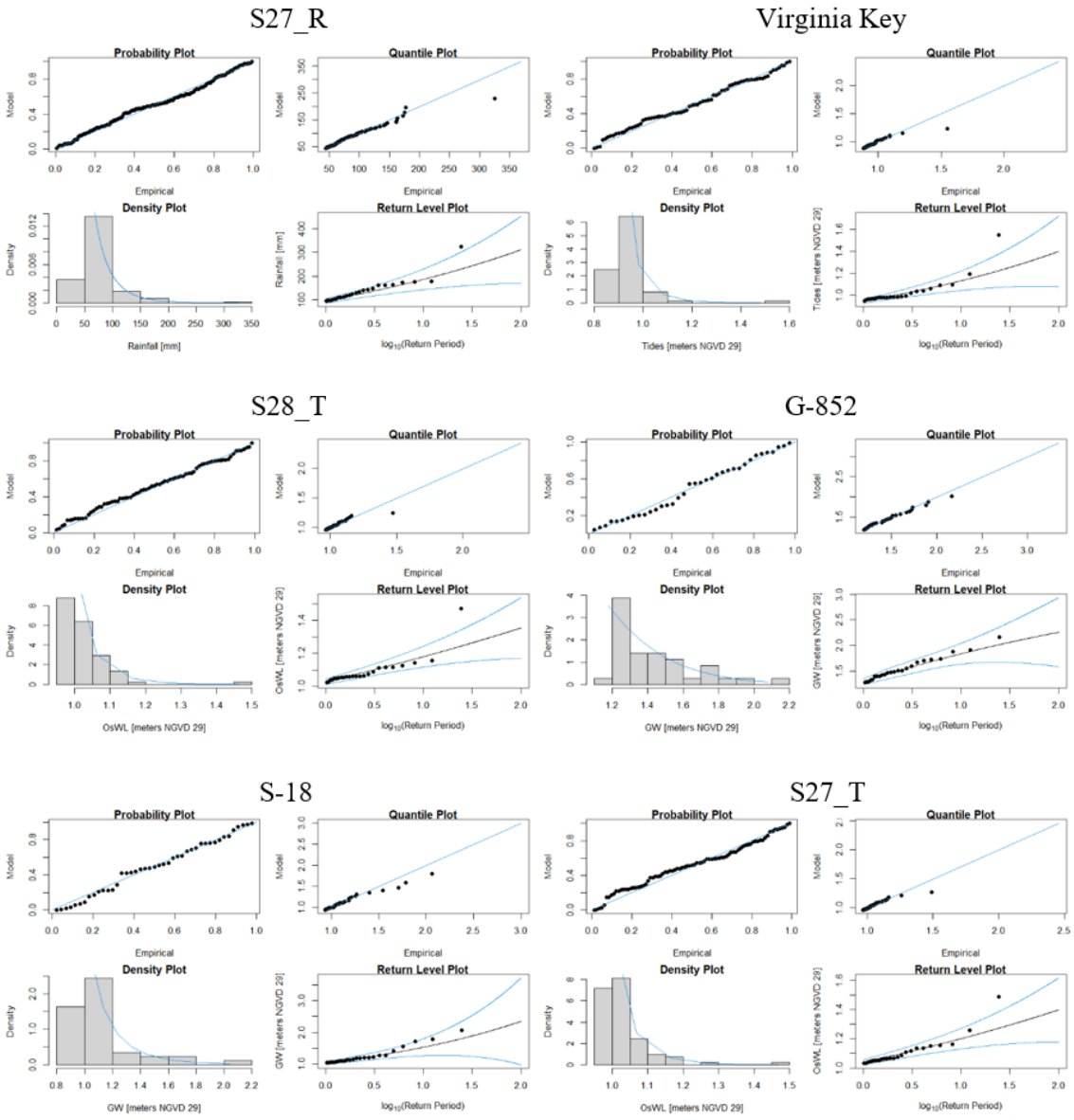

Figure A.10. Fitting General Pareto Distribution to the non-conditioned variable using S27_R data as rainfall reference condition

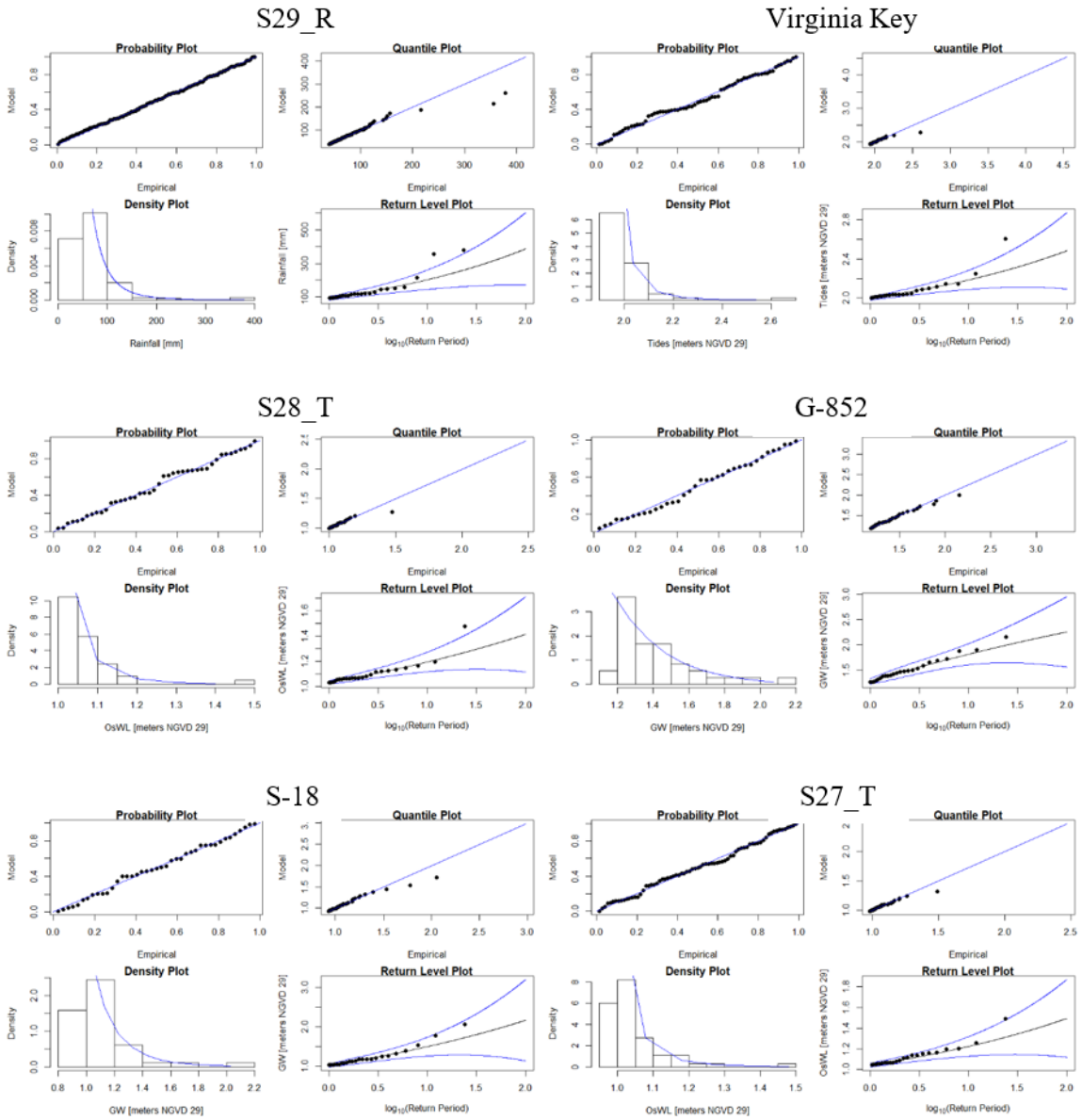

Figure A.11. Fitting General Pareto Distribution to the non-conditioned variable using S29_R data as rainfall reference condition

A.2.5 Fitting distributions to the non-conditioned variable

The goodness of fit of two non-extreme marginal distributions for unbonded variables based on the Akaike Information Criterion (AIC) is presented in two panes with three plots each (**Figure A.12** – **Figure A.14**). On the left pane, the upper plot depicts the AIC of the two fitted distributions, the Gaussian ("Gaus") and the Logistic ("Logis"). The AIC measures the distance between the model and reality, penalizing the number of distribution parameters to balance fit and complexity. The middle plot presents the PDFs of the fitted densities superimposed on the histogram of the data, and the lower plot displays the CDFs of the fitted distributions overlaid on a plot of the empirical CDF. The distribution yielding the lowest AIC corresponds to the best fitting unbounded distribution. The right pane displays only the best fitting distribution with the Logistic is almost always more suitable than the Gaussian.

Similarly, the goodness of fit is assessed to a series of non-extreme value marginal distributions for bounded and unbounded variables according to the AIC (**Figure A.15** – **Figure A.17**). Seven distributions are proposed to find a suitable parametric distribution: Birnbaum-Saunders (BS), exponential (Exp), gamma (Gam), lognormal (LogN), truncated normal (TNorm), Tweedie (Twe), and Weibull (Weib). The distributions are compared, and the best fit is chosen based on the lowest AIC, with the BS distribution almost always being the most suitable parametric distribution.

a

b

c

d

e

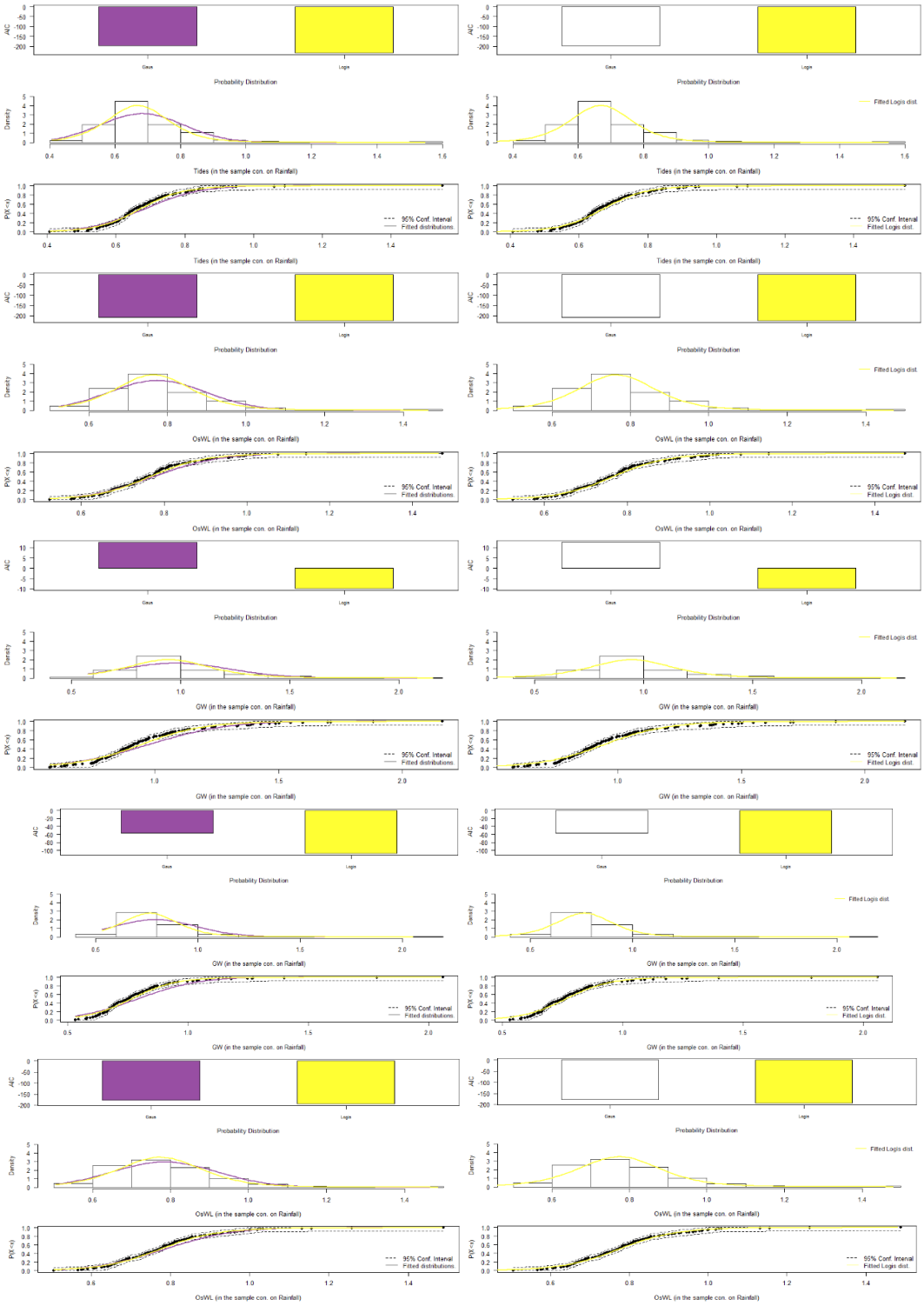

Figure A.12. Fitting distributions to the non-conditioned variable using NEXRAD grid data as rainfall reference condition for: (a) Virginia Key; (b) S28_T; (c) G-852; (d) S-18; (e) S27_T

a

b

c

d

e

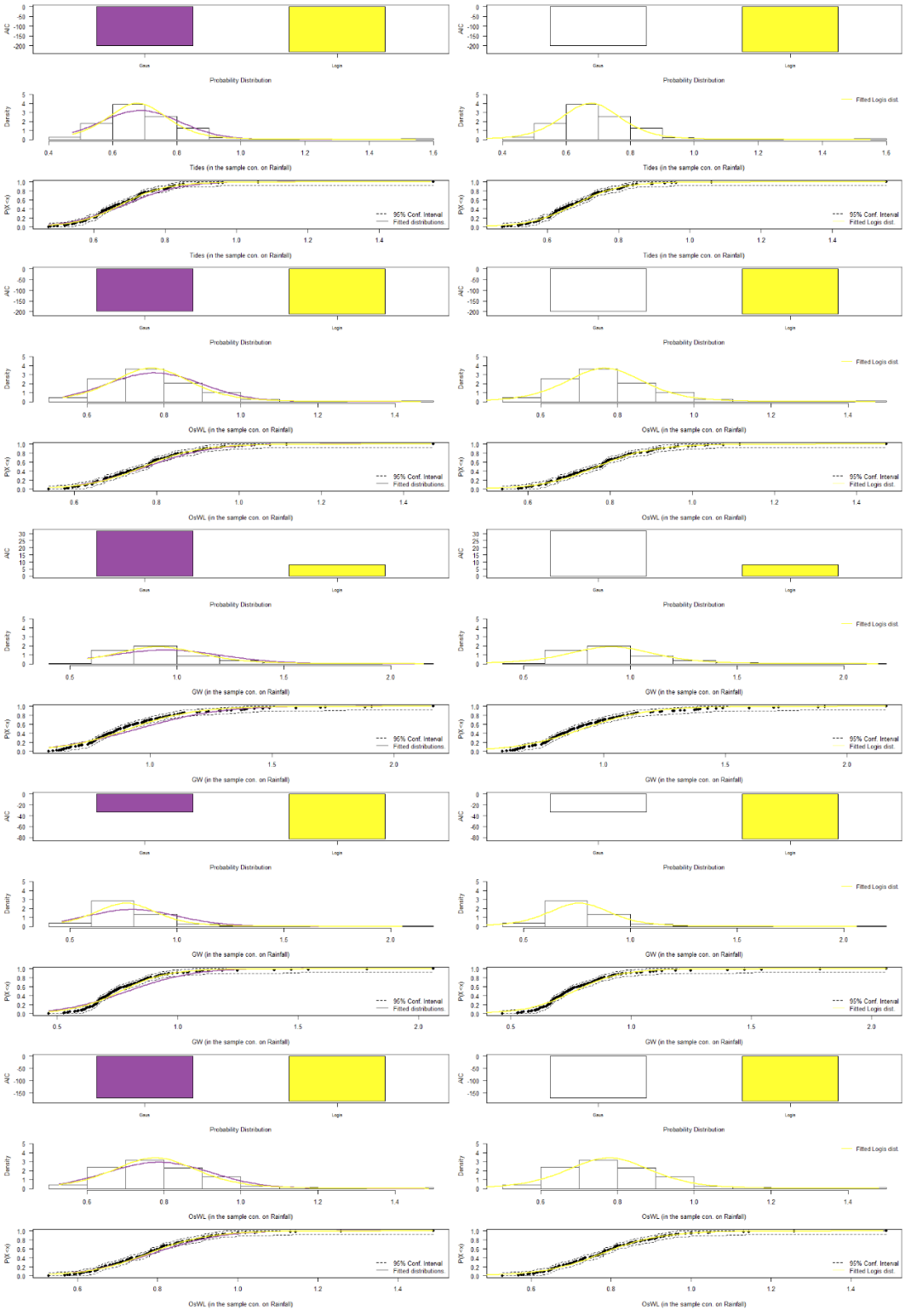

Figure A.13. Fitting distributions to the non-conditioned variable using S27_R data as rainfall reference condition for: (a) Virginia Key; (b) S28_T; (c) G-852; (d) S-18; (e) S27_T

a

b

c

d

e

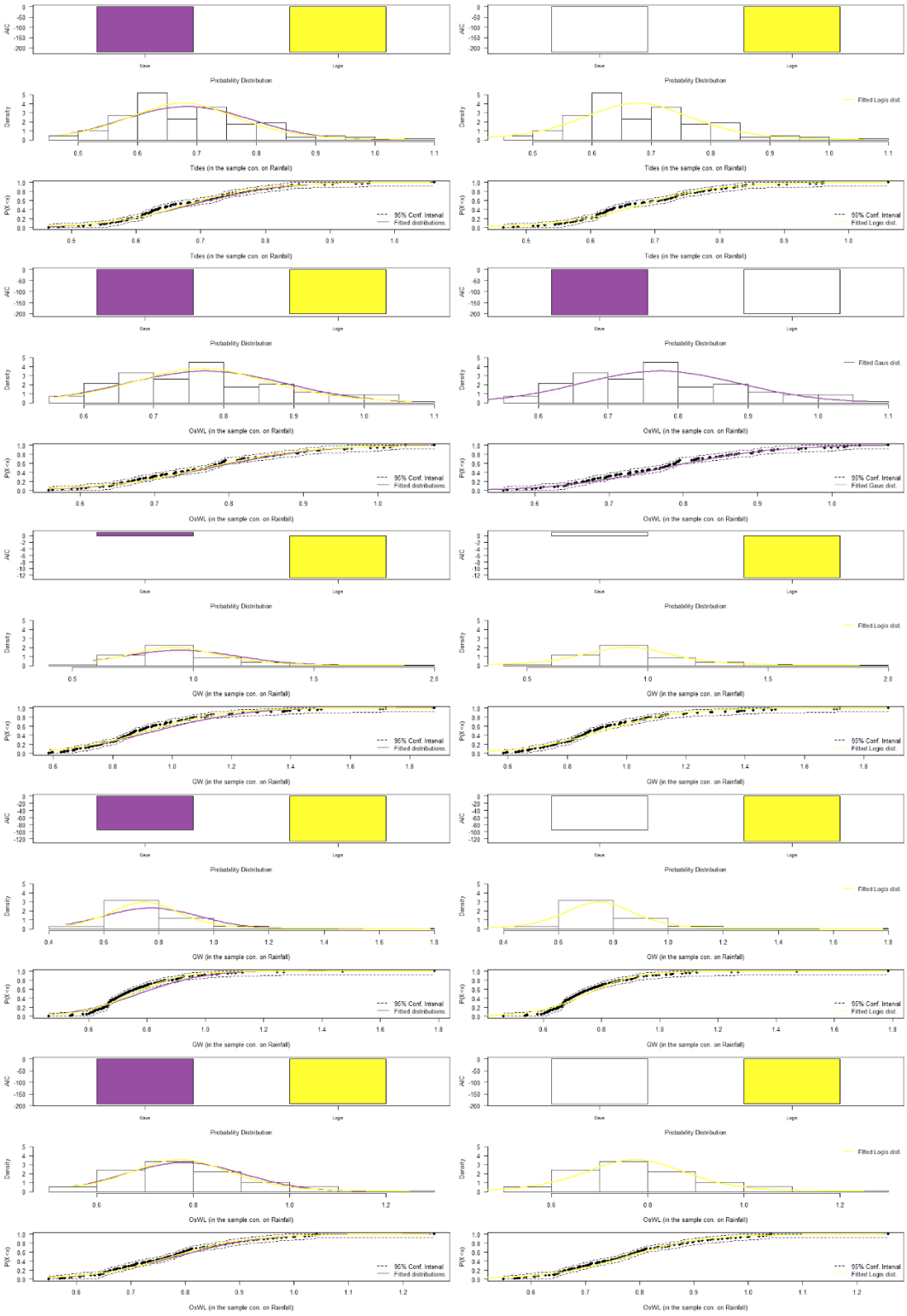

Figure A.14. Fitting distribution to the non-conditioned variable using S29_R data as rainfall reference condition for: (a) Virginia Key; (b) S28_T; (c) G-852; (d) S-18; (e) S27_T

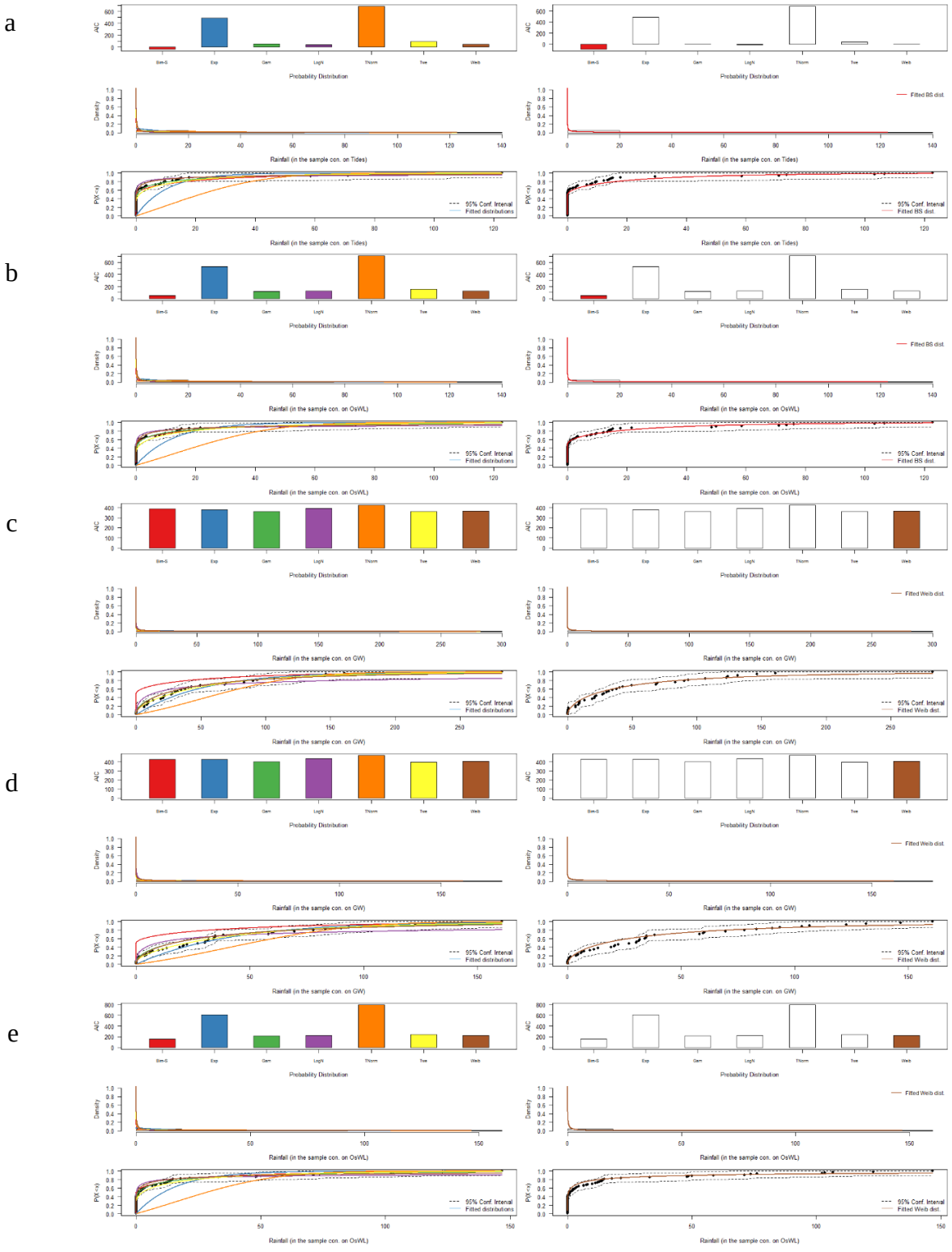

Figure A.15. Fitting distribution for bounded and unbounded non-conditioned variables using NEXRAD grid data as rainfall reference condition for: (a) Virginia Key; (b) S28_T; (c) G-852; (d) S-18; (e) S27_T

a

b

c

d

e

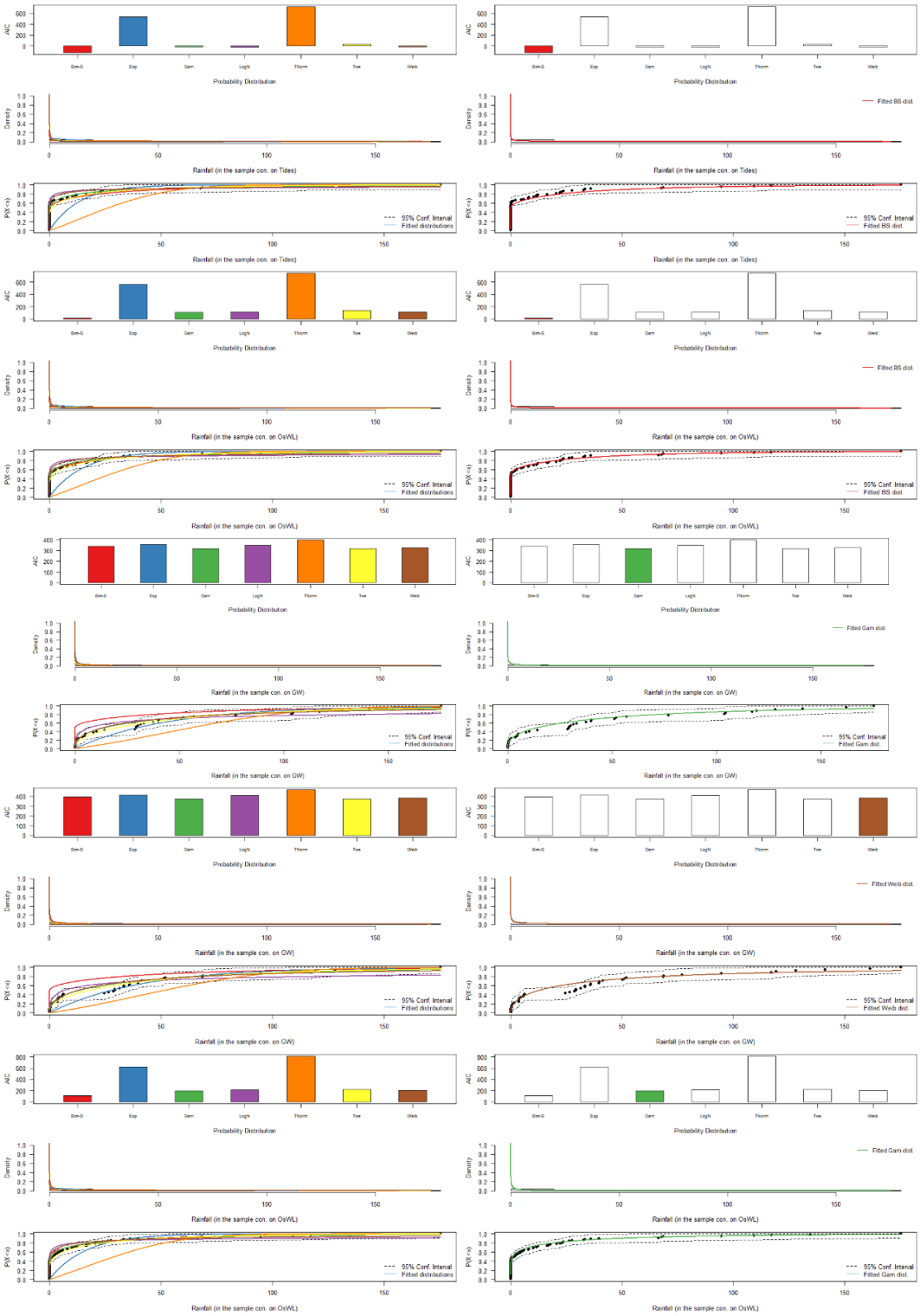

Figure A.16. Fitting distribution for bounded and unbounded non-conditioned variables using S27_R as rainfall reference condition for: (a) Virginia Key; (b) S28_T; (c) G-852; (d) S-18; (e) S27_T

a

b

c

d

e

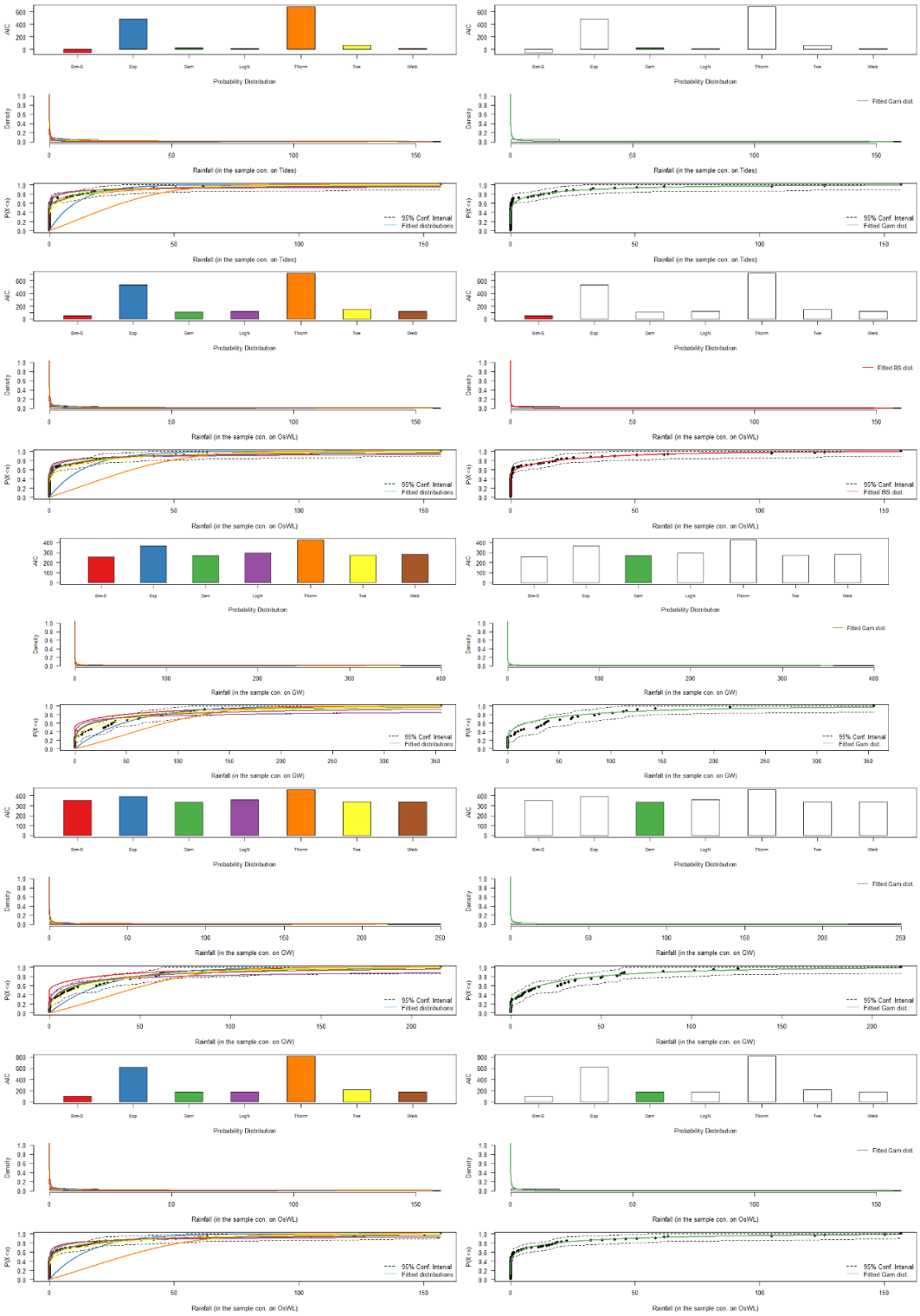

Figure A.17. Fitting distribution for bounded and unbounded non-conditioned variables using S29_R as rainfall reference condition for: (a) Virginia Key; (b) S28_T; (c) G-852; (d) S-18; (e) S27_T

VITA

FRANCISCO FEBRONIO PEÑA GUERRA

1989	Born: Monterrey, México
2006-2007	Mardela Middle & Highschool Mardela Springs, MD
2007-2013	B.S., Civil Engineering Universidad Autónoma de Nuevo León Monterrey, México
2011-2012	B.S., Thesis in Urbanism and Urban Renewal Institut National des Sciences Appliquées (INSA) Lyon, France
2015	Internship at Housing and Land Management Unit United Nations Economic Commissions of Europe Geneva, Switzerland
2016-2021	Research Associate Water Resources Research and Documentation Center Perugia, Italy
2019-2021	Research Associate Sea Level Solutions Center (SLSC) Miami, FL
2020	M.S., Environmental Studies Florida International University Miami, FL
2020-2021	Dual Doctoral Candidate University of Florence and Florida International University Florence, Italy and Miami, Florida
2019 – present	Student Delegate UNESCO Chair on Sustainable Water Security

PUBLICATIONS AND PRESENTATIONS

Peña, F.; Obeysekera, J.; Jane, R.; Nardi, F.; Melesse, A.; Price, R., Annis, A., 2021. Modelling the compound impacts of fluvial, coastal and groundwater floods with sea-level rise in North Miami using statistical and physically-based models (Work under progress)

Peña, F.; Obeysekera, J.; Jane, R.; Nardi, F.; Melesse, A., Castelli, F., 2021. Investigating compound flooding in a low elevation coastal karst environment using multivariate statistical and 2D hydrodynamic modelling: A case study in the Arch Creek Basin, Miami-Dade County Florida USA (Work under progress)

Peña, F.; Nardi, F.; Melesse, A.; Obeysekera, J.; Castelli, F.; Price, R.; Crowl, T.; Gonzalez-Ramirez, N., 2021. Compound flood modelling framework for rainfall and groundwater interactions. *Nat. Hazards Earth Syst. Sci. Discuss.* 2021, 1-38, https://doi.org/10.5194/nhess-2021-259

Peña, F., Nardi, F., Melesse, A., Obeysekera, J., 2021. Assessing geomorphic floodplain models for large scale coarse resolution 2D flood modelling in data scarce regions. *Geomorphology* 107841. https://doi.org/10.1016/j.geomorph.2021.107841

Peña, F., Nardi, F., Obeysekera, J., & Melesse, A., "Integrating compound flood conditions through 2D hydraulic modeling for simulating flood risk processes in North Miami". *American Geophysical Union Annual Meeting 2020*. San Francisco, California (virtual). 7-11 December 2020. Poster presentation.

Peña, F., Obeysekera, J., Nardi, F., Castelli, F., & Melesse, A. Building flood resilience through integrated 2D flood modeling: The case study of Arch Creek Basin. *11th Annual Southeast Florida Regional Climate Leadership Summit 2019* – Key West, Florida. 3-5 December 2019. Poster presentation.

Peña, F., Freni, G., Nardi, F., Castelli, F., & Melesse, A., "Innovative 1D-2D urban flood models for effective water risk management. The case study of Palermo, Italy". *ESRI Italy Conference* – Rome, Italy. 10-11 April 2019. Oral presentation.

Annis, A. Nardi, F., Peña Guerra, F. F. & Castelli, F., "Large scale inundation simulations integrating Floodplain terrain and 2D hydraulic modelling with remote sensing and crowdsourced data". *American Geophysical Union Fall Meeting* – Washington, USA. December 2018. Poster presentation.

Peña, F., Nardi, F., 2018. Floodplain terrain analysis for coarse resolution 2D flood modeling. *Hydrology* 5. https://doi.org/10.3390/hydrology5040052

Pena, F. & Nardi, F., "Fluvial geometry data processing for large scale 2D flood modelling". *XXXVI Convegno Nazionale di Idraulica e Costruzioni Idrauliche* – Ancona, Italy. 12-14 September 2018. Oral presentation.

Pena, F. & Nardi, F., “Global web-risk mapping: Data driven storytelling for DRR”. *Geoscience and Information Technology* – Sarzana, Italy. 11 June 2018. Oral presentation.

Peña, F. & Nardi, F., “DTM floodplain morphology processing for large scale 2D modelling”. *Hydrology Days 2018* – Rome, Italy. 18 May 2018. Oral presentation.

Padua D.; Calzati V., 2018. *Percorsi di innovazione e sviluppo locale: Il caso PMI umbre e Made in Italy*. Chapter 5- Analisi geospaziale su variabili produttivo-turistiche.

Peña, F. & Nardi, F., “Integrating geomorphic and 2D hydraulic algorithms within GIS urban ecosystem models for large scale physically based flood modelling and mapping”. *PhD Days 2017* – Turin, Italy. 28 June 2017. Oral presentation.

UN Habitat, 2016. Habitat III Regional Report for the UNECE Region